Thermal Field Mapping Technique for Friction Stir Process

by

Sakthivael Kandaswaamy

A dissertation submitted to the Graduate Faculty of
Auburn University
in partial fulfillment of the
requirements for the Degree of
Doctor of Philosophy

Auburn, Alabama
Dec 18, 2009

Approved by

Lewis N. Payton, Chair, Associate Research Professor of Mechanical Engineering
Robert E. Thomas, Professor of Industrial and Systems Engineering
Robert L. Jackson, Associate Professor of Mechanical Engineering

Abstract

Friction Stir Welding is a solid state "green" welding method developed by The Welding Institute (UK). An internal thermal mapping instrument has been developed which allows for symmetrical mapping of the thermal fields developed by a Friction Stir Welding tool as it passes through the material being welded. This symmetrical mapping conclusively documents statistically the asymmetrical nature of the heat sources within the friction stir welding process. The various models in the literature are compared against these results. A model developed by the authors using classic metal cutting theory predicts the observed thermal fields. A successful predictive model will facilitate tool optimization and welding schedules, while optimizing the mechanical properties of the weld.

Acknowledgments

First of all, I would like to thank my mentor and my advisor Dr.Lewis Payton, for rendering tremendous support, not only in this project but throughout my course, academically and morally, without whom, completion of my course work and the project would not have been possible. Dr.Payton's support also includes funding for this project.

I would also like to thank my committee members, Dr.Robert Thomas and Dr.Robert Jackson for their guidance in this project and Dr. Saeed Maghsoodloo, for his guidance and support with the statistical tools involved with this project. I extend my thanks to Dr. W. A. Foster, for his valuable suggestions as an outside reader.

I am thankful to Mr. David Branscomb for helping me with the Lab view programming part of the project.

Last but not the least; I would like to show my gratitude to my parents, my sister, my brother-in-law and my friends for their support and love.

Table of Contents

List of Tables

List of Figures

I. INTRODUCTION

Friction Stir Welding (FSW) is a relatively new industrial process that was invented at The Welding Institute (TWI, United Kingdom) and patented in 1992 under research funded in part by the National Aeronautics and Space Administration (NASA). It is considered to be a "solid state" welding process since the base material never melts. Often quoted advantages of the process include good strength and ductility along with minimization of residual stress and distortion. It produces superior weld products in difficult-to-weld materials without producing any toxic fumes or solid waste that must be controlled as hazardous waste. Noise pollution in the work place is greatly reduced. The process is robust and environmentally friendly. Operators may be quickly trained in a few hours to produce highly repeatable, highly desirable weld structures.

Although there have been several flow models and heat source models proposed in the refereed literature of Friction Stir Welding, there is a shortage of real world thermal data against which to validate the proposed models. This is largely due to the contained nature of the actual Friction Stir Welding process. The heat sources of deformation are located within the base metal being welded and underneath the rotating tool shoulder. As such, surface pyrometry measures are ineffective.   The limited amount of thermal data in the reported literature is usually coincidental to the primary goal of the experimental design and non-symmetrical.

An internal thermal mapping protocol/device has been developed which allows for symmetrical mapping of the thermal fields developed by the tool as it passes through the material being welded. This symmetrical mapping clearly documents the asymmetrical nature of the heat sources within the friction stir welding process. One side of the pin is always without fail hotter than the other, with similar results for the two sides of the shoulder.

The system developed at Auburn University with NASA MSFC funding uses a shouldered pin tool as detailed in Figure 1 below. Each tool has a shoulder whose rotation against the substrate generates most of the heat required for welding. The pin on the tool is plunged into the substrate and helps stir the metal in the solid state. The pin tool is made to rotate and is slowly plunged into a weld joint with constant pressure until the shoulder contacts the work surface. The pin-tool is then made to traverse the joint affecting a weld as it travels.
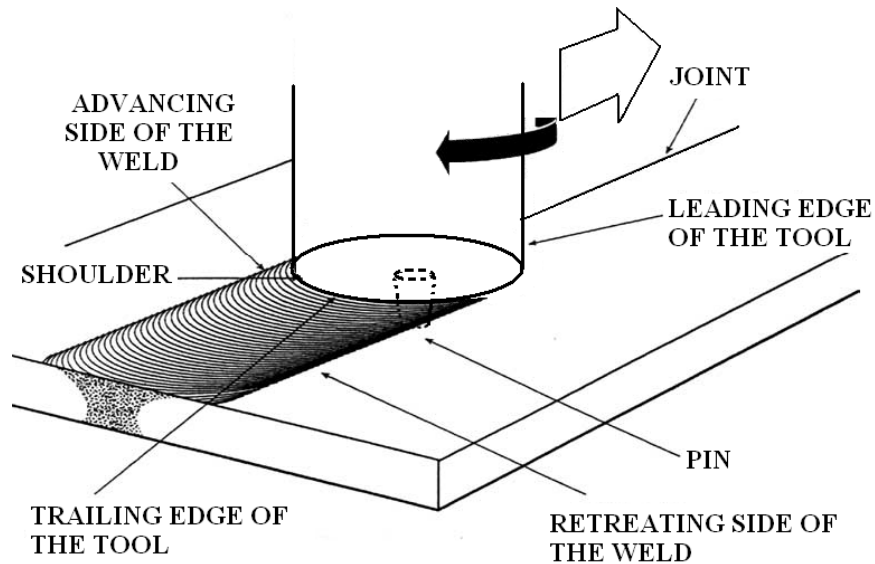
Figure 1: Schematic of Tool and Material Process

II. SCOPE AND OBJECTIVES

This experiment was conducted to gain a better understanding of the thermal fields surrounding a Friction Stir Welding tool as it passes through a material being welded together by the passage of the tool. A detailed symmetrical observation of these thermal fields is essential in order to understand the thermodynamically driven recrystallization of the material behind the tool after it has passed.

The objectives of the experiment included:

(1) A comprehensive review of the available Friction Stir literature to include:

 a. Previous thermal measurements.

 b. Previous thermal models.

(2) A comprehensive review metal cutting literature which applies to rotating tools.

(3) Build an instrument capable of accomplishing the following goals:

 a. Rapid exchange and setup of samples.

 b. Use commercially available metal geometries to hold down cost.

 c. Validate statistical repeatability and statistical sensitivity.

 d. Achieve a statistical sampling power of 90% with 7 replicates.

(4) Utilize analysis of variance to design an experiment with the equipment.

(5) Compare resulting data to previous models.

(6) Demonstrate the use of multi-physics software to simulate the most promising model from the literature, comparing it to the real world data obtained.

III. LITERATURE REVIEW OF THERMAL MEASUREMENTS IN FSW

This chapter presents a comprehensive overview of the thermal aspects of the Friction Stir Welding (FSW) process. The basic process and nomenclature commonly found in the literature is reviewed and illustrated. This is followed by a detailed description of the thermal zones and nomenclature associated with the Friction Stir Welding process and dynamic recrystallization. A detailed review of thermal observations will then be presented. This will include those observations which make no attempt at modeling the results and those observations made by researchers attempting to model the temperatures they observed during experiments. The survey will conclude with a brief review of the efforts of classical metal cutting to predict temperatures in the geometrically similar process of slot milling.

Basic Review of the Friction Stir Welding Process

In order to visualize the fundamentals of the process, consider Figure 2. The two materials to be welded are placed in contact via either an overlapping or, in this case, a butt joint fashion. A broad tool with a narrower pin on the end is fabricated. The tool is then inserted while rotating at a high speed into the material until the wider "shoulder" of the tool makes contact with the material being welded. At this point, the tool begins a traverse of the weld seam, deforming the material in its passage, leaving behind a formed weld. The material does not melt during this solid-state deformation. Personnel with shop experience will recognize similarities with a type of end-milling referred to as slot-milling. For the travel direction depicted in Figure 2, the left hand side of the weld is referred to as the advancing side of the tool and the right hand side is referred to as the retreating side of the tool. Classic milling theory

refers to the advancing side as the side undergoing "up-milling" and the retreating side as undergoing "down-milling". Figure 3 details a flatter 2D aspect of the process which illustrates several important features.
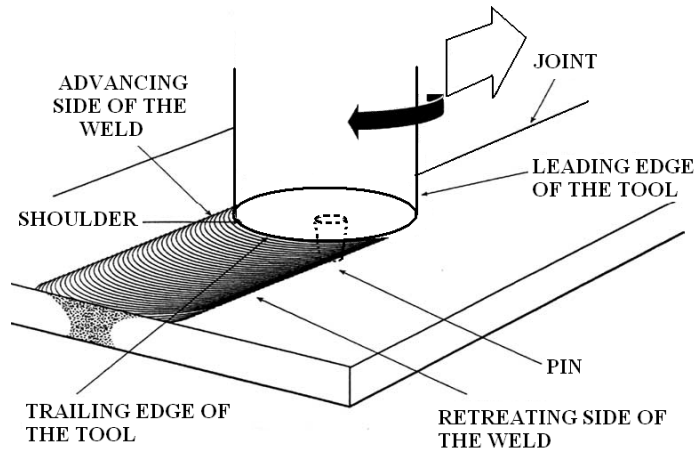
Figure 2: Isometric nomeclature and geometry of FSW
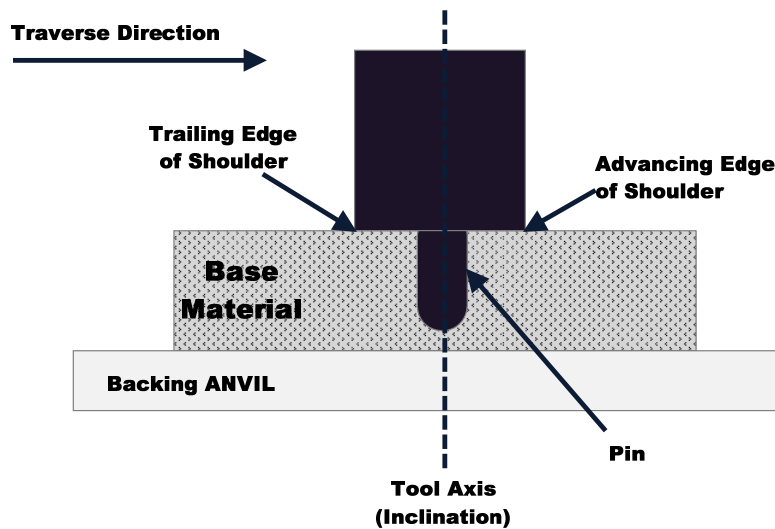
Figure 3: Side view of FSW geometry with nomenclature

The base material illustrated in Figure 3 will always be contained from above by the shoulder of the passing tool and from below by the relatively immobile backing plate which is commonly

referred to as the "anvil". The leading edge is commonly referred to as the advancing edge and the back side is referred to as the trailing edge. Pin tools may be smooth as illustrated in Figure 3, threaded or geometrically shaped in any number of ways. It is also common to "incline" the axis of the tool so that there is a height difference between the advancing versus retreating edge of the tool. The tool in Figure 3 would thus be said to have an inclination angle of 0 degrees.

Dynamic Recrystallization and Temperature

FSW could be considered as a hot working process instead of a welding process. As the tool passes through the material (Figure 4), material flows around the tool without melting. This leaves a distinct, asymmetrical nugget within the material as shown below.
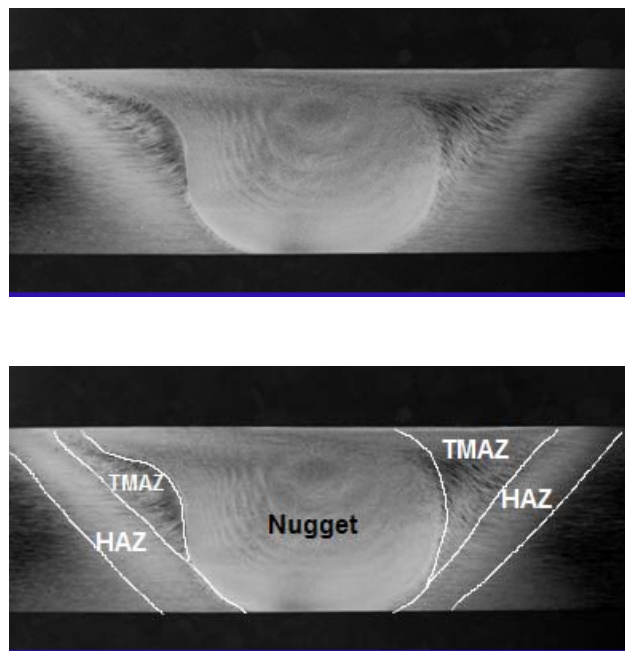
Figure 4: Cross section of typical friction stir weld. Top photo shows weld cross section without markup. Lower photo is same photo marked up to show temperature zones.

This process involves a large amount of deformation at high strain rates. Such deformation leads to a change in the grain structure of the material in the deformed region.

The weld usually consists of four distinct regions. They are the base metal, the refined weld nugget, the Thermo Mechanically Affected Zone (TMAZ) and the Heat Affected Zone (HAZ). Figure 4 depicts all of these zones. The base metal zone is left unmarked since it surrounds all the other zones. The base metal zone does not experience either the heat or the deformation. Its microstructure and mechanical properties are never affected by these. The HAZ comes next to the base metal zone. This region is affected by the heat generated but not by the plastic deformation. The TMAZ zone experiences both plastic deformation and heat generated during welding. Due to this the microstructure of the region is altered. It usually has elongated and recovered grain structures [1] with different mechanical properties from the parent base metal(s) being welded together. The weld nugget refers to the core of the weld zone where recrystallization occurs due to severe thermo-mechanical effect and is comprised of extremely fine grains [2]. This leads to a general strengthening of mechanical properties in most welds.

According to Jata [3] the weld nugget, whose extent is comparable to the size of the pin, comprises of equiaxed, fine and dynamically recrystallized grains. When the size of these grains was compared to the size of the grains in the parent metal, it was found that the recrystallized nugget grains are smaller than that of the parent metal.

Jata compared his micro structural analysis study of FSW with the micro-structural analysis study of hot forging. He concluded that the dynamic recrystallization in FSW had the same dependence as that of the dynamic recrystallization of hot forging process.

Jata's study was based on research by Murr [4]. Murr also stated that the grain size in the weld nugget was smaller than that of the parent metal. He noted that grain size was smaller near the weld bottom. Murr detailed a significant difference in the grain size of welded region and the parent metal in both aluminum alloy (AA) 6061 and aluminum alloy (AA) 1100. He suggested

that the dynamic recrystallization is the principal feature of friction stir weld development. He gave out a relation for the grain growth occurring, in the form,

$$D^2 - D_0^2 = kt \tag{1}$$

Where D_0 - Initial recrystallized grain size

D - Residual FSW grain size

And k is given by an equation in the form of,

$$k = A\exp(-\frac{Q}{RT}) \tag{2}$$

Where A -constant,

Q - Appropriate energy for the grain growth

R - Gas constant

T - Absolute temperature characterizing the grain growth over time, t.

Murr [5], has presented a diagrammatic system to better explain the approach of dynamic recrystallization in FSW as shown in the below figure. The process starts with the clockwise rotation of the head pin stirring metal A into B.
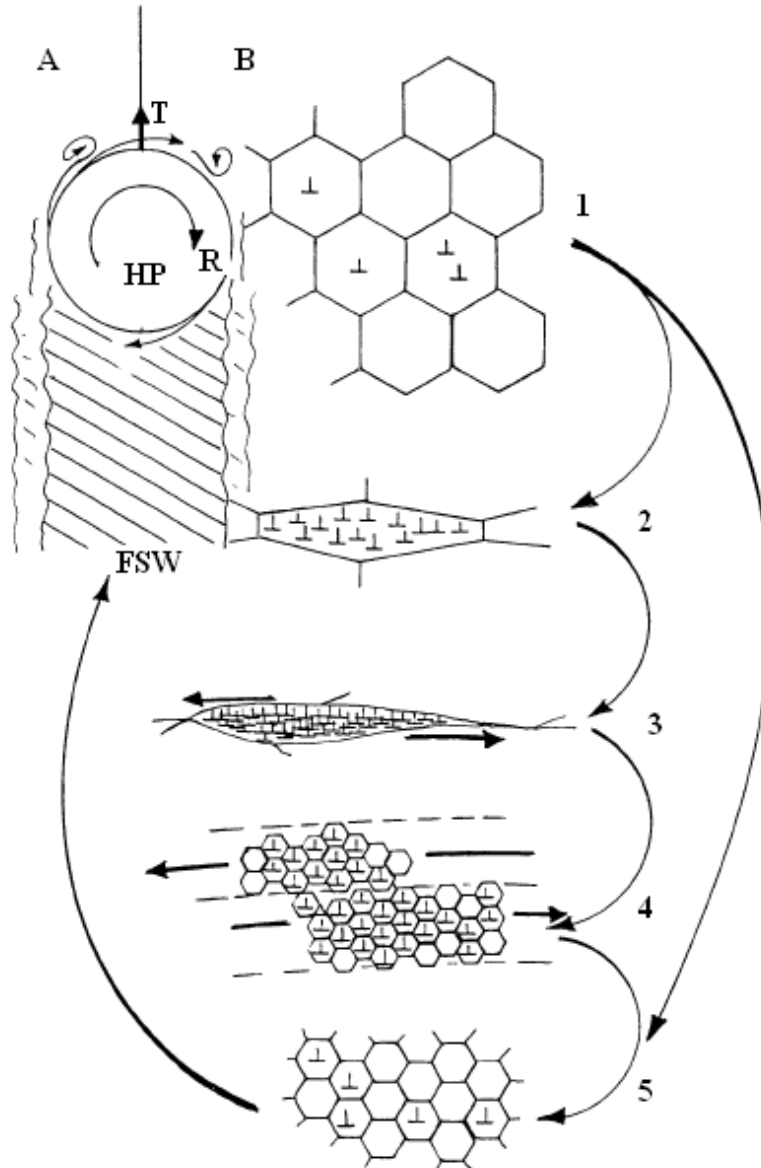
Figure 5: Murr's diagram illustrating dynamic recrystallization and grain growth associated with the FSW process.

Murr's approach to dynamic recrystallization has 5 steps.

Step 1 shows the original microstructure of the base metal in which dislocations are denoted by symbol "⊥".

Step 2 shows the deformed grain as a result of increase in dislocation density.

Step 3 is the result of more dislocations and more distorted making the grains saturated

Step 4 shows the nucleation of new stress free recrystallized grains which occurred due to the stored energy.

Steps through 1-4 would be repeated continuously for further plastic deformation of recrystallized grains.

Step 5 shows the recrystallized grains which are subjected to certain amount of grain growth. This is a result of the frictional heat generation during the FSW process. The amount of heat determines the amount of grain growth.

James [6] hypothesizes a relation between the defect formation in FSW and the grains structures obtained. He classified the known defects of FSW to include a lack of penetration, voids and root defects, also called as kissing bonds. James hypothesized a region in the advancing side where chaotic flow occurs. There is a location above and below this region where the flow tends to be in the opposite direction, thus creating a vortex which leads to the development of voids. The voids developed might be a source for the crack formation. He also states that larger planar facets are the possibility for larger cracks and higher crack growth rate.

One thing is common in all discussions: effects of temperature upon grain recovery and defect generation/presence. It is therefore important to be able to predict the temperatures around the rotating tool. A review of temperature studies is indicated. There are two main types of thermal observation in the literature. Type one are those temperature observations conducted randomly in conjunction with an experiment whose objective lies elsewhere. The type two temperature observations were typically conducted by modelers attempting to predict temperatures so that they can simulate weld properties. There is a small subset of this group whose goal is to design better tools based upon classic metal cutting theory. This chapter will

review the temperature observations and the temperature models, followed with a review of classic milling theory as it might apply to FSW.

Temperature Measurement, Attempts to Model Temperature Fields:

Various researchers have documented thermal results as part of their overall report. Most of the experiments were carried out by recording temperatures only on one side of the weld. Few experiments captured the temperature on both sides of the weld. All the researchers who had recorded temperatures on both sides of the weld had an asymmetric placement of thermocouples except Xu, who had thermocouples placed on both sides of the weld symmetrically. Interestingly, all the researchers has treated FSW as a process with symmetrical temperature field in their models. This chapter covers the experiment done by various researchers and their models in the following order.

- Experiments capturing temperature on one side of the weld.

- Experiments capturing temperature on both sides of the weld asymmetrically.

- Experiments capturing temperature on both sides of the weld symmetrically.

Experiments capturing temperature on one side of the weld:

W.Tang, X.Guo, J.C.McClure, L.E.Murr, and A.Nunes [7] had a series of thermocouples placed in the holes made on the under-side of their 6061-T6 aluminum samples. The thermocouples were placed at one quarter, one half and three quarters of the plate thickness respectively and were at different distances from the weld seam, mainly between 5 mm to 15 mm from the weld seam. They recorded a maximum of 420 Celsius from a thermocouple kept at 5 mm from the weld seam. The diameter of the shoulder was twice as much as the pin. The rotational speed of the tool ranged from 400 to 1200 RPM, with a traverse speed of 2 mm per second.

Chen and Kovacevic [8] in 2003 made an attempt to study the thermal history and thermo-mechanical process of FSW using aluminum alloy 6061 T6. They measured the temperature with eight thermal couples embedded in the plate on the retreating side.
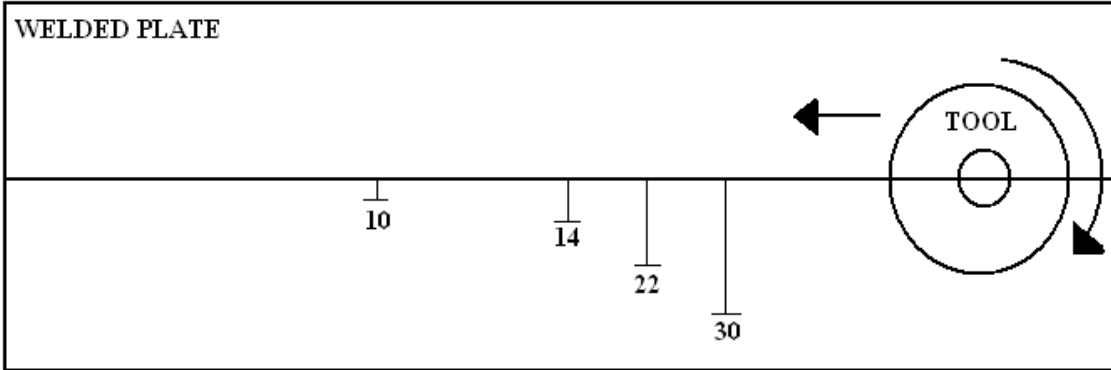
Figure 6: C.M. Chen and R. Kovacevic's thermocouple positions. Dimensions in mm.

Four were located 1.6 mm below the top surface and four were located 1.6 mm from the bottom surface, with a distance of 10 mm, 14 mm, 22 mm and 30 mm respectively to the weld centre-line. The tool was made of AISI A2 steel with 24 mm shoulder diameter and 6 mm pin diameter and the weld was traversed at 140 mm per minute at 500 RPM. ANSYS was the finite element tool used for the simulation of the process. The source of heat was assumed to be the friction between the work piece and the tool, considering both the shoulder and the pin.

Heat source due to friction between tool and the work piece was given by,

$$q = \frac{2}{3}\pi\omega\mu(t)p(t)(R^3 - r^3) \tag{3}$$

Where, μ -coefficient of friction.

ω- Angular velocity

R,r - Radius of the shoulder and pin

The thermal and mechanical solutions were coupled in the model to increase the accuracy of the temperature gradient obtained.
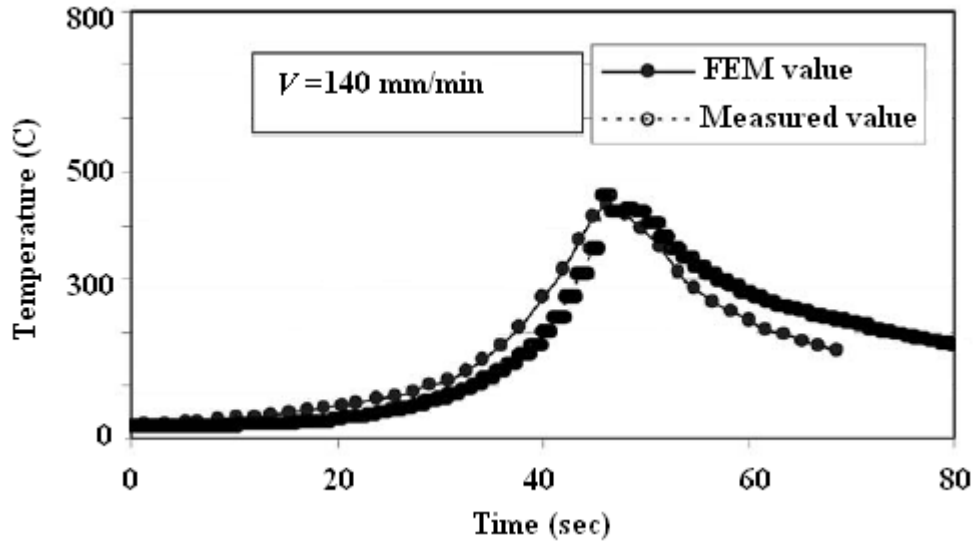
Figure 7: Comparison of Simulated and measured results of Chen.

The modeling solution was compared with the actual thermocouple measurements, and the peak

temperature obtained from simulation was around 450C.   According to the result obtained, the

maximum temperature was obtained just beyond the shoulder edge in both the longitudinal and

lateral directions.

Chao [9], in 2003, formulated the heat transfer problem into a steady state boundary value

problem for the tool, and a transient boundary value problem for the work piece. According to

Chao, the heat generated due to the friction between the tool and the work piece, is a result of the

sum of the heat lost to the backing plate, heat lost from the surface of the work piece to the

environment and the heat content in the work piece, neglecting the radiation. Chao claimed that

the model, which does not consider the heat generated due to the plastic deformation of the

material, is a reasonable approach for the study.

13
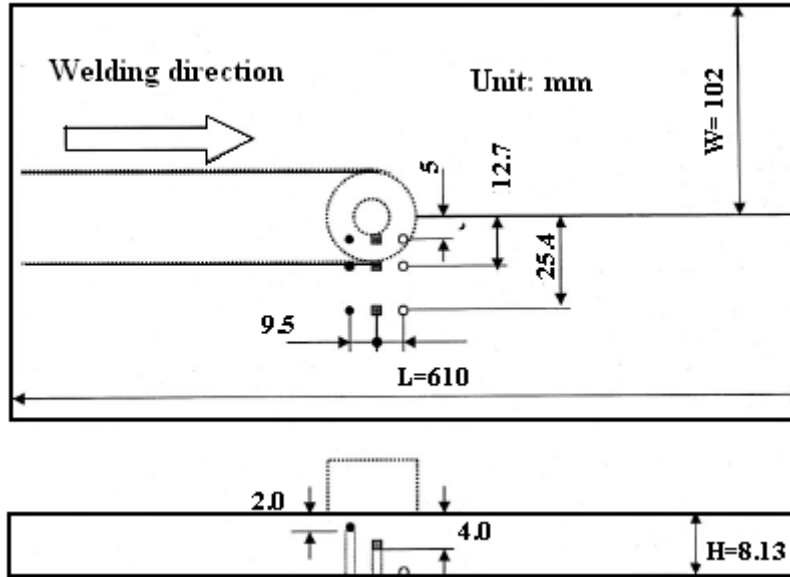
Figure 8: Yuh J.Chao, X.Qi and W.Tang's Thermocouple Positions.

They conducted experiments with 3 sets of thermocouples placed at 3 different positions.

Position 1 was below the shoulder. Position 2 was below the pin and the Position 3 was near the

base point. First set was placed 5 mm from the center of the tool and the second 12.7 and the

third set 25.4 mm from the center of the tool. They measured 440 Celsius for the shoulder and

425 Celsius for the pin as their peak temperature. The welding simulation code WELDSIM was

used for the study. Only half of the work piece was simulated as Chao state that the other half is

symmetrical to the simulated half. Since the model does not consider the heat generated due to

the plastic deformation, larger heat conduction coefficient was used to compensate this.

The heat equation used was given as,

$$q = \frac{3Q_3 r}{2\pi r_0^3} \text{ For } r \le r_0 \tag{4}$$

Where r_0 - Outside radius of the shoulder.
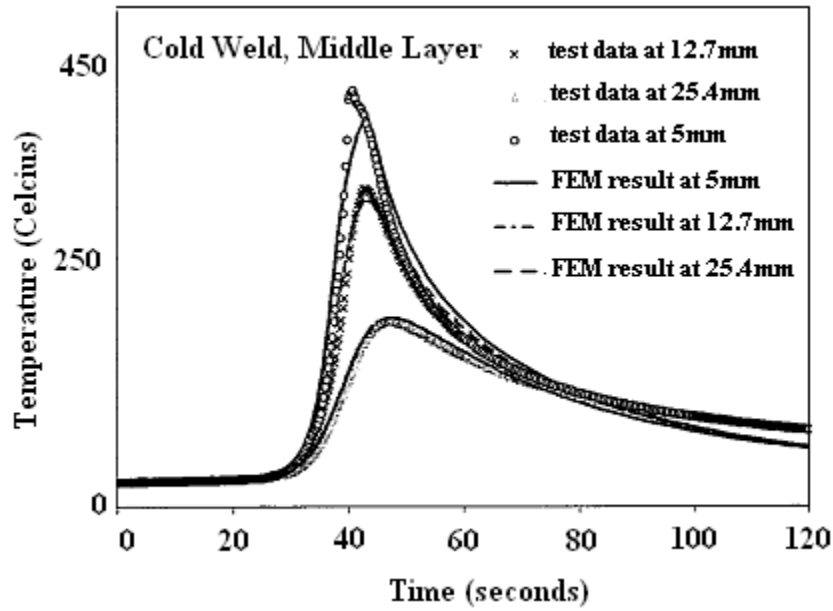
*Figure 9***:** Comparison between Chao's modeled and recorded temperature

The peak temperature of 420 Celsius was predicted at a region underneath the shoulder at about 5 mm from the weld line.

Khandkar [10], in 2003, proposed a three dimensional thermal model to study the thermal mapping during the process. Temperature measurements were carried out in aluminum alloy 6061. A tool with 25 mm shoulder diameter, 10 mm pin diameter and 8 mm pin length was used. The experiment was carried out at 390 RPM with a traverse speed of 142 mm/min. The thermocouples were placed at different distances from the weld line. This model considered the backing plate and the heat lost to it. The heat input in this experiment, was given, assuming a uniform shear stress at the work piece-tool interface. Also the heat input was correlated with the torque that was measured experimentally.

Heat input equation at the interface was given as,

$$q_{interface} = q_{tot} \times \frac{Generated\tau}{Total\tau} \qquad (5)$$

Where τ - Torque

$q_{\text{int}erface}$ - Heat input at an interface

q_{tot} - Total heat input.

The torque at the shoulder interface was found by,

$$M_{shoulder} = \int_{r1}^{r0} (\tau r)(2\pi r)dr \tag{6}$$

The torque at the pin bottom was given by,

$$M_{pinbottom} = \int_{0}^{r1} (\tau r)(2\pi r)dr \tag{7}$$

The torque at the vertical pin surface was given by,

$$M_{pinsurface} = (\tau r_1)2\pi r_1 h \tag{8}$$

Where, r - Radial distance from the tool center

r_0 - Radius of the shoulder

r_1 - Radius of the pin

τ - Assumed shear stress

A peak temperature of around 460 Celsius was obtained as a result of the simulation at the interface of the tool and the work piece. The limitation of this experiment was the uncertainty of thermal contact conductance. Khandkar also claims that the model developed was unique in the way the friction coefficient was back calculated.

A moving tool approach was adopted by Song [11] in 2003. For the experimental setup, they had two sets of thermocouples in their FSW experiment with AL 6061 T6 plate. Each set had 4 thermocouples and were placed at 8, 12, 16 and 25 mm from the weld line. The first set was 2 mm from the top surface of the plate and the second set at 8 mm from the top surface and

16

recorded a peak of around 580 Celsius (850 kelvin). The tool had a 50 mm shoulder diameter and 12 mm pin diameter. They used 344 RPM, 637 RPM and 914 RPM at 1.59 and 3.18 mm/sec.
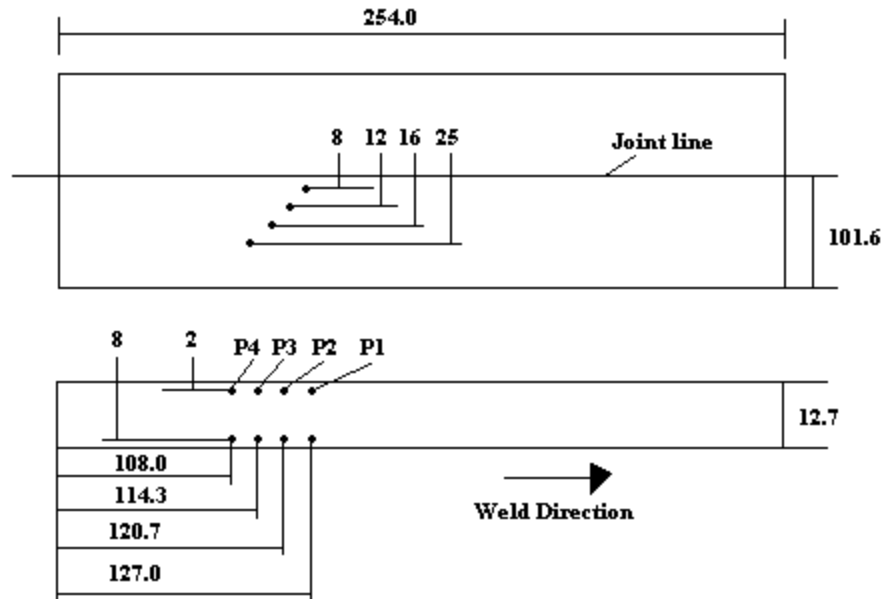
ALL DIMENSIONS ARE IN MM

Figure 10: M Song and R Kovacevic's thermocouple positions.

He developed a thermal model of the process in a moving coordinate. This reduced the difficulty of modeling the moving tool. The model had two sources of heat. One is the heat from the shoulder and the other from the pin.

The heat generated by the shoulder was given as,

$$q = 2\pi\mu F_n R_i n \qquad\qquad (9)$$

Where μ - Friction coefficient

F_n - Downward force

R_i - Distance from the calculated point to the axis of the tool

n - Rotational speed of the tool.

17

The heat input from the pin was the sum of the heat generated by the shearing action of the pin, heat generated by the friction of the bottom surface of the pin and the heat generated by the friction of the vertical surface of the pin.

The heat generated due to pin was given as,

$$q = 2\pi r_p hkY \frac{V_m}{\sqrt{3}} + \frac{2\mu k Y \pi r_p hV_{rp}}{\sqrt{3(1+\mu^2)}} + \frac{4F_p \mu V_m \cos\theta}{\pi} \tag{10}$$

Where, $\theta = 90^0 - \lambda - \tan^{-1}(\mu)$

$$V_m = \frac{\sin\lambda}{\sin(180^0 - \theta - \lambda)} v_p$$

$$V_{rp} = \frac{\sin\theta}{\sin(180^0 - \theta - \lambda)} v_p$$

$$v_p = r_p \omega$$

λ -Helix angle of the thread

μ -Friction coefficient

Y - Average shear stress

Song claims that the simulated temperature is very accurate and the model developed could be easily applied to model the coupled heat transfer process in both the tool and the work piece. The simulated temperature results were compared with the real experimental data. Song also states that the maximum temperature obtained beneath the tool shoulder would be close to the melting temperature of the work piece.
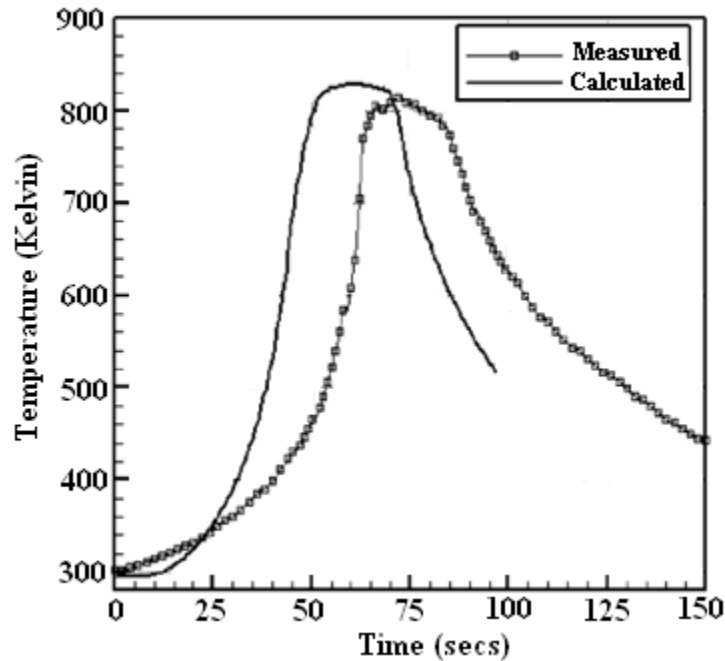
Figure 11: Comparison of Song's Simulated and the Experimental results.

Experiments capturing temperature on both sides of the weld asymmetrically:

McClure [12], in 1998, developed a friction stir welding model with a moving point heat source . He used AL 6061 for their FSW experiment and captured the temperature field on both sides of the weld. They had thermocouples inserted through holes drilled at the bottom of the piece. The holes were randomly placed and were not symmetrical to the weld line. The pin tool used was High Carbon steel with 19 mm (0.75 inch) shoulder diameter and 5.46 mm (0.215 inch) pin length. The weld was done at 400 RPM at 2 mm/sec.
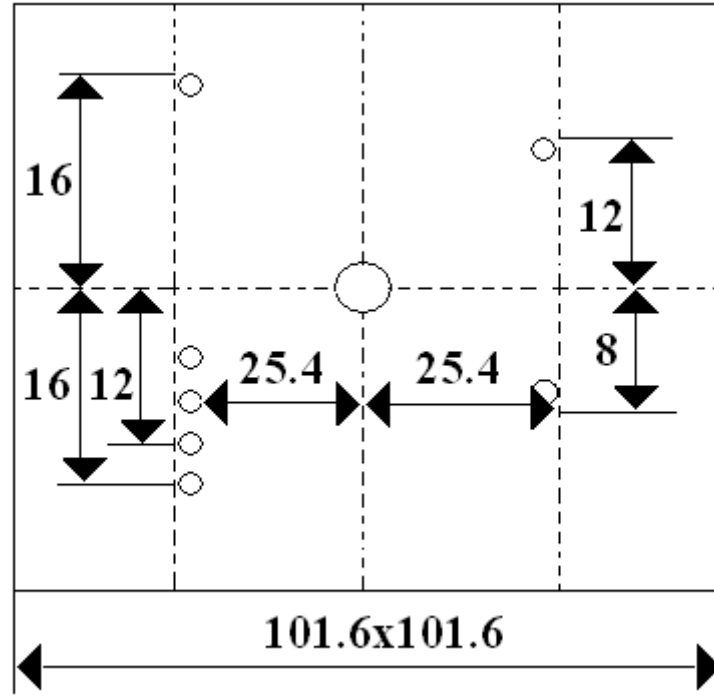
ALL DIMENSIONS IN MM

Figure 12: J.C. McClure's thermocouple positions

To model the process, McClure considered the fact that the shoulder was the major heat source in the process. This was concluded from the macro view of the experimental weld which clearly indicated that the heat affected zone (HAZ) was equal to the diameter of the shoulder and the observation of the temperature gradient through the work piece thickness which was indicated by the boundary between the work piece base metal and the HAZ.

The heat generation equation used was,

$$q = 2\pi\mu P\omega\xi^2 d\xi d\alpha \qquad (11)$$

Where , μ - Friction coeffiecient

ω- Spindle rotation speed

P - Downward pressure.

The downward pressure was given as,

$$P = \frac{F}{\pi(R_2^2 - R_1^2)} \qquad (12)$$

Where, R_2, R_1 - Radii of the shoulder and the pin.

This equation shows that downward pressure changes with varying radius, which in turn, varies the heat generated according to the diameter of the tool. The maximum temperature obtained in the model was around 420 Celsius and McClure claims that the results obtained were similar to that of the experimental results.

Unlike McClure, Dong considered the heat generated by pin due to the plastic deformation of the material. Dong, Lu and Hong [13] in 2001, made an attempt to study the coupled friction heat, plastic flow slip zone development and the three dimensional heat flow in Friction stir welding using a numerical model. According to Coulomb friction law which was assumed to apply to the heat generation, shear work was completely transformed into a point wise heat generation along the interface of the tool and the work piece. The coupled friction heat generation equation was given as,

$$q = 2\pi\omega r^2 \mu(T) p(T, s) \qquad (13)$$

Where, ω - Angular velocity

$p(T, s)$ -Pressure distribution along the interface s

r - Radius of the tool

μ -Friction coefficient.

The equation for heat generated due to plastic deformation at a given time and material point was given as,

$$q = \eta s_{ij} i_{ij}$$ (14)

Where, η - Measurement of the fraction of the plastic work converted to heat flux.

s_{ij} -deviatoric stress

i_{ij} - Incremental plastic strain rate.

Conditions related to finite deformation thermoplasticity were considered for this project. With the results obtained, Dong found that the coupled thermomechanical friction heating was responsible for the heat in the upper region, and the plastic work induced heat was responsible for the heat in the lower region of the weld. They also suggested that the pin geometry and the pin height have more influence on the heat generated, and a high temperature zone would be created below the bottom of the pin having a temperature of about 300 Celsius.

Though Dong was able to include the plastic deformation of material in his model, he did not model a moving tool. Khandkar [14], in 2001, used a finite element analysis to develop a 3D thermal model of the process. The model captures the heat generated due to the moving tool and also the convective and diffusive heat transfer caused due to the plastic deformation of the material. In the model, the heat generated in the process was due to the friction between the shoulder and the work piece, and also the friction between the pin and the work piece.

Heat generated by the shoulder was given by,

$$q = \frac{2\mu FNr}{r^2_{shoulder} - r^2_{pin}}$$ (15)

Where, μ - Friction coefficient

F - Downward force

N -Tool rotational speed

r - Distance from the center of the tool

Heat generated due to the pin was given as,

$$q = k \frac{2\mu F N r}{r_{shoulder}^2 - r_{pin}^2} \qquad (16)$$

Where k - constant and was assumed to be 3%.

Since the heat was assumed to be generated only by the friction between the tool and the work piece, Khandkar has used the same equation, for both the shoulder and the pin, except for an addition of a constant for the pin equation. The maximum temperature obtained in the model was around 500 Celsius.

T.J. Lienert, W.L. Stellwag.Jr and L.R.Lehman[15], measured the temperature of AA 6082-T6 with two thermocouples on top of the piece, one on the advancing and the other on the retreating side of the weld at 6.35 mm (1/8 inch) from the edge of the weld. The tool used was made of H13 tool steel with 19 mm (3/4 inch) shoulder diameter. They measured a peak of 360 degree Celsius in both the thermocouples at eleven inches per minute at 1250 RPM. This system failed to detect the temperature difference between the advancing and retreating side. The reason could be because the thermocouples were placed above the workpiece and away from the weld.

S. G. Lambrakos, R. W. Fonda, J. O. Milewski [16], and J. E. Mitchell also had thermocouples placed asymmetrically on both sides of the weld. They had 5 thermocouples placed in the holes drilled from the bottom side of 6.35 mm thick AL 6061-T6. Actual placement of the thermocouples was assumed to be at a depth of 3.8 mm from the top surface of the plate. They had one thermocouple at the weld center and all others around the tool on both advancing and retreating side of the tool, but the placement of the thermocouples were not symmetric to the weld line. The tool used was made of H13 tool steel with 25.4 mm shoulder diameter and 5.72 long pin with 6.35 mm diameter.
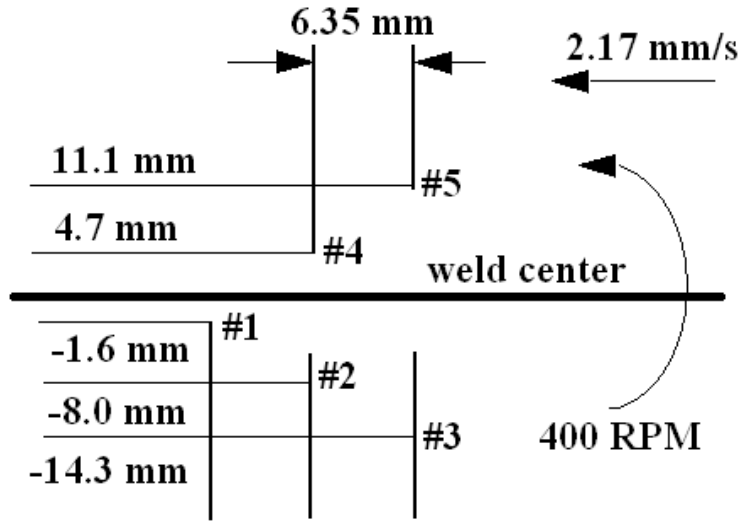
*Figure 13***:** S. G. Lambrakos's thermocouple positions.

The tool had a 6 degree lead angle. The weld was done at 2.17 mm per second at 400 RPM. The model was constructed considering only the HAZ. An arbitrary value was assigned to each element of the cylindrical surface corresponding to the pin of the tool where the heat is generated. This arbitrary value was scaled relative to the surface elements corresponding to the base of the tool shoulder and the base of the pin according to their radial distance to that of the arbitrarily scaled cylindrical surfaces.
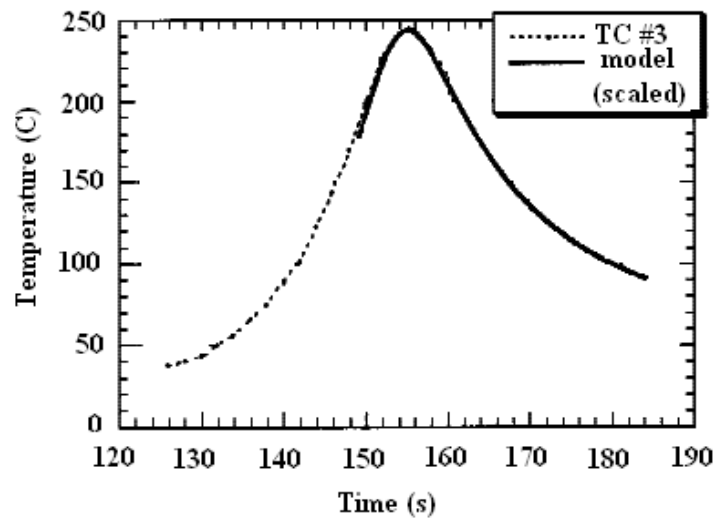
Figure 14: S. G. Lambrakos's comparison between simulated and recorded temperature.

Experiments capturing temperature on both sides of the weld symmetrically:

Interestingly, Xu had thermocouples symmetrical to the weld line. Junde Xu, Suhas P.Vaze, Robert J.Ritter, Kevin J.Colligan, Joseph R.Pickens[17], recorded temperatures in aluminum magnesium alloy 5083-H116 plate. They used an infrared camera and thermocouples to measure the temperature at different points of the workpiece.
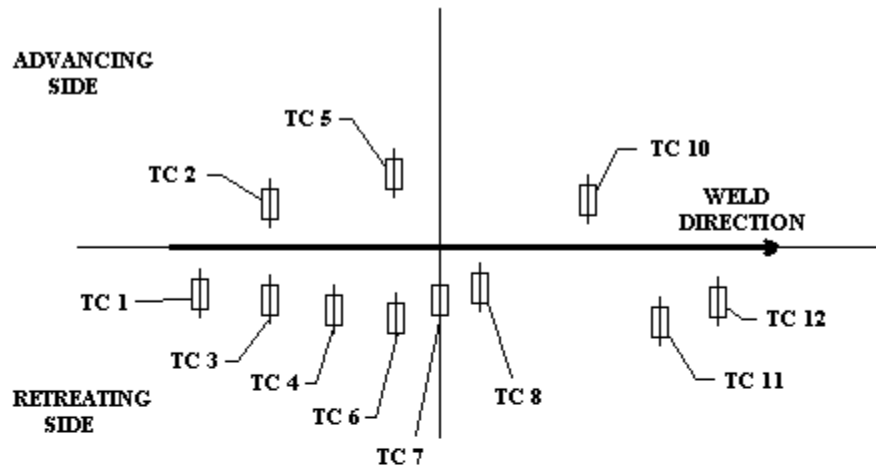
Thermocouple	Distance to Centerline (in)	Depth from the Bottom (in)
1.00	0.24	0.25
2.00	0.27	0.50
3.00	0.27	0.50
4.00	0.45	0.50
5.00	0.70	0.50
6.00	0.70	0.50
7.00	0.30	0.75
8.00	0.24	0.25
10.00	0.27	0.50
11.00	0.70	0.50
12.00	0.30	0.75

Figure 15: Junde Xu's thermocouple positions.

They had thermocouples placed randomly in the work piece, but had two pairs of thermocouples on the advancing and retreating sides of the weld at equal distances from the weld center. Xu did not document any difference in temperature between the advancing and the retreating side

thermocouples even though the thermocouples were placed in such a way that they fall directly under the shoulders used. The tool material was MP159, with 9 mm (0.35 inches) pin diameter and 25 mm (0.996 inches) pin length. The tool rotation speed was 250 RPM at traversing speed varying between 100 to 177 mm per minute (4 to 7 inches). The maximum temperature recorded was around 537 Celsius (1000 F). Xu's model was derived from Chao's model.

Temperature recording was also done when two dissimilar metals were welded together. W H Jiang and R Kovacevic utilized FSW to join two dissimilar metals, 6061-T6 aluminum (Al) alloy and AISI 1018 steel. The tool used was H13 tool steel with 25 mm shoulder diameter and 5.5 mm pin diameter. The traverse speed was 140 mm per minute at 914 RPM. Temperature was measured during the process near the nugget using K-type thermocouples. The thermocouples were placed at the center thickness of the sheets about 5 mm and 2 mm from the original interface between the two sheets in the Al alloy side and the steel side respectively and measured around 490 Celsius for aluminum and 620 Celsius for steel.

Ulysse[18] in 2002, used a different approach for his model. He solved conductive - convective steady state equation to get the temperature distribution equation for the model. Ulysse used a three-dimensional visco-plastic modeling technique to model the Friction stir process.

The equation used was given as,

$$\rho c_p u \nabla \theta = \nabla(k \nabla \theta) + Q \tag{17}$$

Where ρ -density

c_p -Specific heat

k -Conductivity

u -Velocity vector
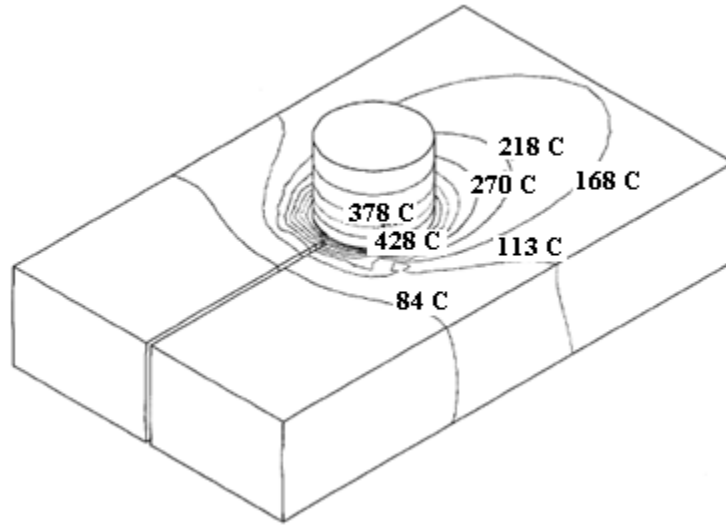
Figure 16: Temperature distribution of Ulysse's simulated model

The peak temperature obtained was in the range of 400 Celsius below the shoulder. The obtained results were compared with the measured values.
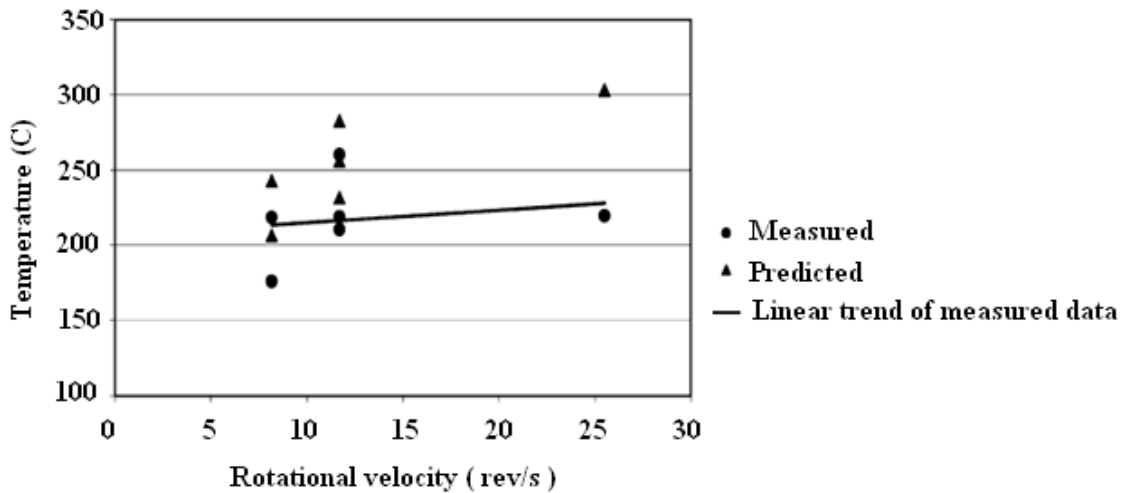
Figure 17: Comparison of Predicted and the measured values of Ulysse's model.

The behavior of the metal for a wide range of strain-rate is discussed to be the reason for the predicted values being greater that the measured values.

Chang [19] in 2003 developed a numerical heat flow model for the process and used a thermo-elastic-plastic finite analysis tool to simulate the process and examine the thermal

behavior. The model had an assumption that the heat was generated in two ways. One was due to the friction between the tool and the work piece. The other was due to the plastic deformation at stir zone in the rotating pin zone.

The heat equation was assumed to be,

$$q = \frac{4}{3}\pi^2 \mu PNR^3 \tag{18}$$

Where, μ - Friction coefficient

P - Pressure distribution

N - Rotation speed

R - Surface radius.

The analysis of heat distribution characteristics of the process was done using the two dimensional unstationary heat conduction theories. Temperature distribution in different segments of the weld were obtained as the result of the simulation. The stir zone had a maximum temperature of 530 Celsius, the thermo-mechanically affected zone had a temperature ranging from 480-500 Celsius and the heat affected zone had a temperature ranging from 450-480 Celsius. For the experiment, Chang used aluminum alloy 6061-T6, 300 mm in length, 300 mm in width and 4 mm in thickness. The experiments were carried out with different speeds varying from 87 mm/min to 567 mm/min at 1600 RPM.

Lawrjaniec [20], in 2003, used two different numerical heat sources for the modeling of the process. They were a 2D superficial source developed with SYSWELD and a 3D axi-symmetrical source developed with MARC, where, MARC and SYSWELD are finite element codes. According to him, there are three heat generation regions during the process and it includes the shoulder contact region, pin contact region and the region where material shears. The equation for heat generated was given by,

$$q = \frac{4}{3}\pi^2 \mu \omega P \sum^{n} (R_i^3 - R_{i-1}^3)$$ (19)

Where, μ - friction coefficient

ω - Rotational speed

P - Vertical pressure

R_i - Shoulder radius

He states that the shoulder radius was responsible for the heat generated and the maximum temperature was obtained at the periphery. He also claims, there is a need to calibrate the 2D and the 3D source is to maximize the accuracy of the results obtained, since some of the parameters in the equation including the friction coefficient and the tool vertical pressure were difficult to obtain. The results obtained were checked against the recorded temperature results using thermocouples and infrared cameras.

The results obtained by the 2D superficial source were not symmetrical to the weld line as the retreating side was hotter than the advancing side with a maximum temperature of about 360 Celsius whereas the results obtained by the 3D source gave a symmetrical temperature field.

Liu[21] in 2004 attempted to study thermal and heat transfer phenomenon in Friction stir welding. Aluminum alloy 6061-T6 was used for this experiment. Heat generation during the process was considered to be from the friction between the tool and the workpiece and from the plastic deformation of the metal due to the stirring action of the pin. According to Liu, there were several issues that were not addressed by previous researchers. Those issues include the relative contribution of the heat generated at the interface of tool and the workpiece, the heat contributed by the plastic deformation of the material due to the stirring action, the heat conducted by the backing plate. WELDSIM, the welding simulation code was used to model the heat transfer

phenomenon. Liu's model was based on Chao's study [22],[9],[23] that 5% of the total energy generated during the process was conducted by the machine tool. Liu also states that the pin accounts for considerable amount of heat generated. According to him, a full length pin of about 24.3 mm accounts for 28% of heat generated and a short length pin of about 6.7 mm accounts for 6.7% of total heat generated in the workpiece.
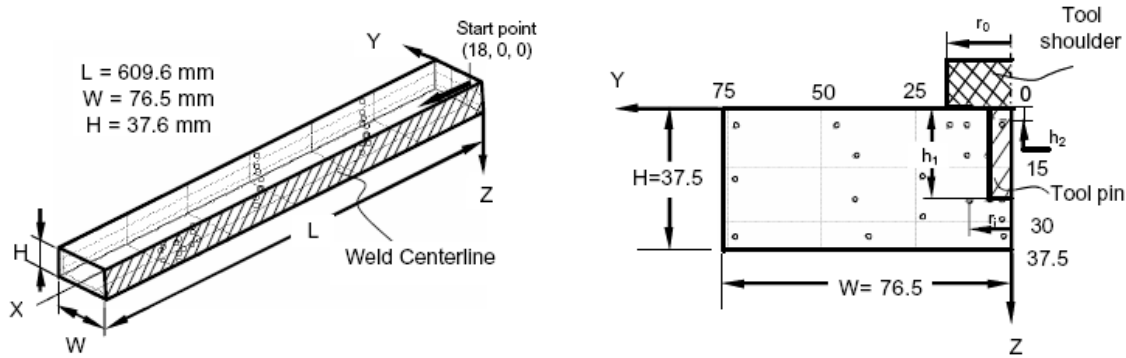
Figure 18: Liu's thermocouple placements.

The experiments were carried out in aluminum 6061-T6 at 350 RPM with a traverse speed of 2.5 mm/sec. 31 thermocouples were placed symmetrically on both sides of the weld line.
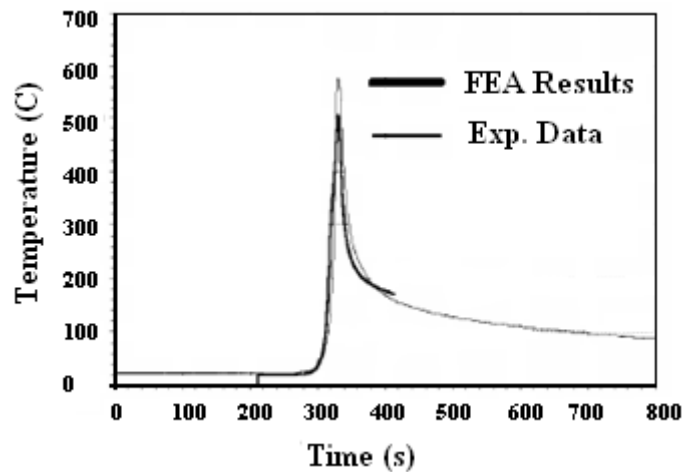
Figure 19: Comparison of the predicted and experimental results of Liu.

He concluded saying that the maximum temperature, close to the melting temperature, occurs at the top surface of the workpiece near the weld line. The maximum temperatures obtained by

simulation and by the experiment were around 500 Celsius and 580 Celsius respectively at the top surface of the work piece.

Schmidt [24] in 2004 developed an analytical model for heat generation in friction stir welding. The experiment was carried out in 2024 T3 alloy at 400 RPM and 120 mm/min traverse rate.
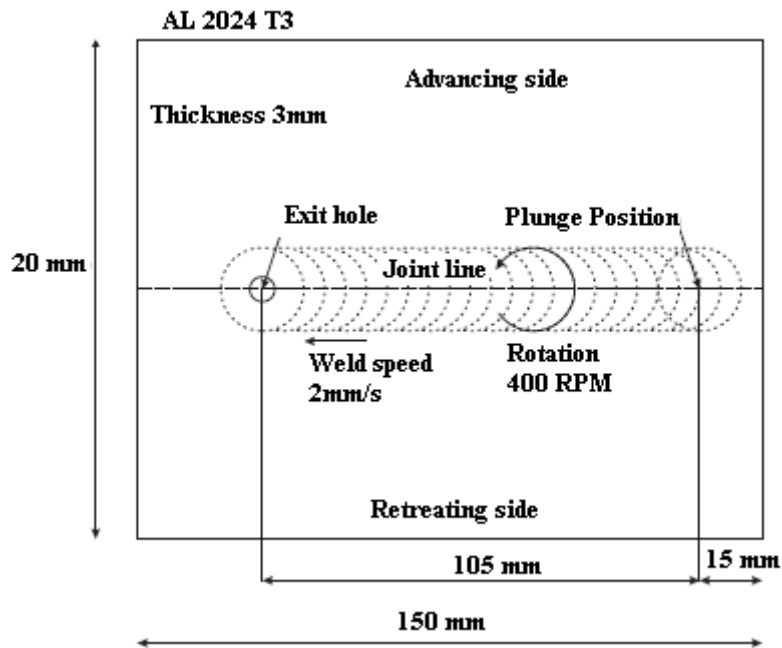
Figure 20: Experimental set up of Schmidt.

The model had three sources of heat. They were the heat generated from the shoulder, heat generated by the plastic deformation of the material due to the stirring action of the pin and heat generated from the bottom surface of the pin. The special thing about this model is that the heat generation equation was developed to satisfy not only flat cylindrical shoulders but also concave or conical shoulders. Some process use conical shoulders for the escape of the material during the submerging phase and enhancing the extrusion process during the operation phase.

The heat generated by the shoulder was given as,

$$q = \int_{0}^{2\pi} \int_{Rprobe}^{Rshoulder} \omega \tau_{contact} r^2 (1 + \tan \alpha) dr d\theta \qquad (20)$$

The heat generated by a cylindrical probe was given as,

$$q = \int_{0}^{2\pi} \int_{0}^{Hprobe} \omega \tau_{contact} R_{probe}^2 dz d\theta \qquad (21)$$

The heat generated by the probe tip flat surface was given as,

$$q = \int_{0}^{2\pi} \int_{0}^{Rprobe} \omega \tau_{contact} r^2 dr d\theta \qquad (22)$$

Equations (20), (21) and (22) were added together for the total heat generated. The result obtained was similar to that of Khandkar[14],[10].

M. Awang and V. H. Mucino [25] have done a finite element modeling of friction stir spot welding (FSSW) process by an explicit finite element code in 2005. The model of FSSW process has been done using Abacus software. They have simulated the material flow and temperature distribution of the process. However they claim that the lack of refinements of several modeling aspects provided them with less realistic results. According to this model, heat is generated by two ways. One is due to the friction between the rotating tool and the work piece. The other is due to the plastic deformation of the material.

Frictional heat input was given by,

$$q = 2\pi \mu R N F_n \qquad (23)$$

Where, μ – Friction coefficient

R - The distance of the calculated point from the tool axis

N - Rotational speed of the tool.

$$F_n$$ - Normal force applied to the work piece.

Heat due to plastic deformation was given by,

$$q = \eta\sigma\xi^{pl} \tag{24}$$

Where, η - Fraction heat dissipated due to plastic straining

σ - Shear stress

ξ^{pl} - The plastic straining rate.
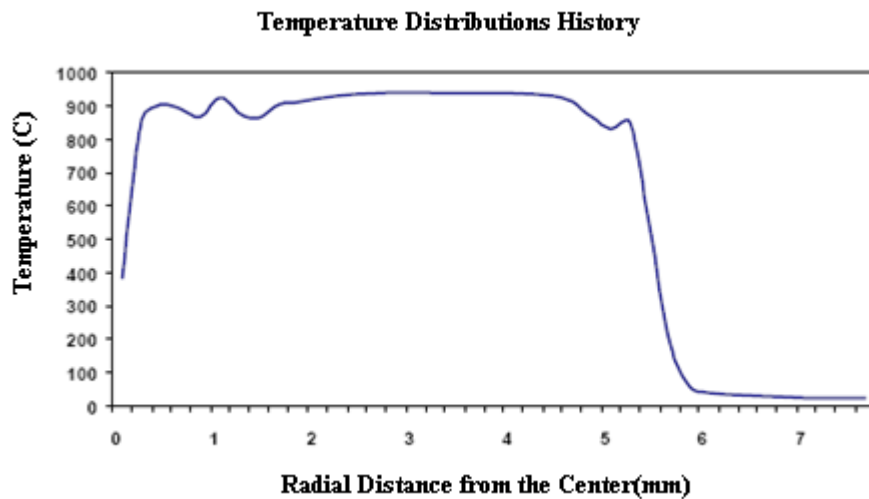
Figure 21: Awang's Predicted result.

Approximated friction coefficients used would be one of the reasons for the unrealistic temperature curves obtained from the model.

There were researchers who also included the heat lost to the atmosphere and the neighboring elements, during the process in their models. Xu [17] , in 2003, developed a model to find the heat generated due to the interaction of the tool with the work piece considering the loss of heat to the tool and the anvil. Xu claims that the result obtained accurately matches with the thermocouple and the infrared camera readings. In this project, Xu had a mica frame inserted between the work piece and the backing plate to reduce the heat dissipated to the backing plate

while thermocouples were used to measure the temperature. The measured temperature was used to combine with the finite element model to find quantitatively the heat lost to anvil, heat lost to the tool, downward pressure, heat lost to the air and the heat generated due to the interaction of the tool and the work piece. The maximum temperature obtained in the model was around 970 F. He concluded, stating that, both the shoulder and the pin contributes significantly for the heat generated in the workpiece and it might vary from 30% to 70% of the total heat generated for both shoulder and the pin. His statement also includes that the heat generated by the shoulder increases with increasing diameter, and the heat generated by the pin increases with the increasing traverse speed there by increasing the peak temperature in the nugget.

Colegrove and Shercliff [26] , used FLUENT to model FSW, in 2003. The experiment was done in aluminum alloy 7071-T7. The heat was assumed to be generated in the tool due to the friction of the tool and the material surface, and viscous dissipation within the deformed material .Some part of heat generated was assumed to be convected from the top surface of the workpiece, and some portion was assumed to be conducted by the backing plate.
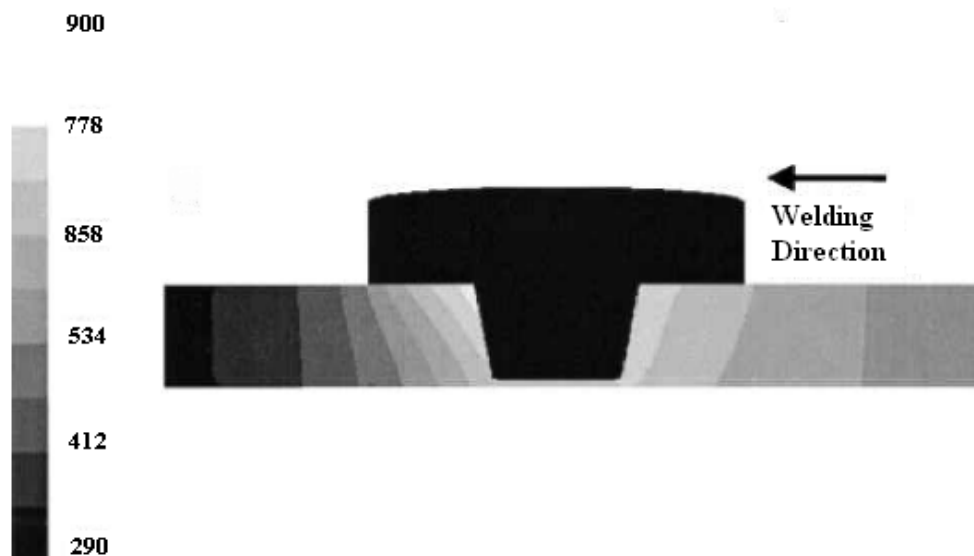
Figure 22: Colegrove's temperature field in Kelvin.

34

Heat generated due to the stirring of material was ignored. This condition was similar to the condition used by Khandkar and Khan [10]. They suggest that the peak temperature of the weld depends on the tool material that is been used, since different tool material would exert different surface shear stress, and they also suggest that the rotation speed of the tool had very little effect on the peak temperature obtained. The peak temperature obtained for aluminum 7075-T7 was very near to the solidus when Tool steel was assumed to be the pin tool.

The documented thermal measurements and temperature models in FSW research and projects were carried out to find the temperature of the tool and the work piece by placing the thermocouples in both of them at different positions with different parameters. No research was done to find the temperature of the advancing shoulder and the retreating shoulder at the same moment. This is true with the pin also. There is no documented research of the simultaneous advancing and retreating side of the pin. Table 1 on the following page summarizes thermal studies conducted in FSW to date.

Researcher	Material	RPM	Radius: Shoulder	Radius: Pin	Traverse speed	Length: Pin	MaxTemp : Shoulder
Chao	AA 2195	240	25.4 mm	10 mm	2.36 mm/sec	-	440 C
Chen	AL 6061	500	24 mm	6 mm	140 mm/min	-	480 C
Song	AL 6061	344, 637, 914	50 mm	12 mm	1.59 ,3.18 mm/sec	-	850 K
McLure	AL 6061	400	0.75 inch	0.215 inch	2 mm/sec	-	430 C
Nunes	AL 6061	400 to 1200	D	D/2	2 mm/sec	-	420 C
Lienert	AA 6082	1250	0.75 inch	-	-	-	360 C
Lambrakos	AL 6061	400	25.4 mm	6.35	2.17 mm/sec	5.72	750 C
Xu	AL-Mg alloy	250	1.65, 1.2 inches	0.35 inch	4 to 7 inches/min	0.996 inch	1000 F
Kovacevic	AL 6061-1018 Steel	914	25 mm	5.5 mm	140 mm/sec	-	490 C - AL 630 C - Steel
Khandkar	AL 6061	390	25 mm	10 mm	142 mm/min	8 mm	460 C
Chang	AL 6061	1600	-	-	87 to 567 mm/min	-	530 C
Lui	AL 6061	350	16.5 mm	6.3 mm	2.5 mm/sec	-	571 C
Schmidt	AA 2024	400	-	6 mm	120 mm/min	3.5 mm	400 C
Colegrove	AA 7075	330	-	-	105 mm/min	-	530 C

Table 1: Maximum temperatures recorded by various researchers with alloys and the

Friction Stir Welding parameters they used in their studies.

Classic Milling Theory applied to Friction Stir Welding

Thermal study and thermal modeling of the process was done in metal cutting also. Tay [27], in 1973, used a two dimensional finite element analysis tool to study the temperature distribution in the workpiece, chip and tool. He obtained the distribution of heat source from quick stop tests and flow field measurements.

Klamecki [28], in 1973, developed a model for the initial stages of the chip formation using a three dimensional finite analysis tool. Stephenson [29], in 1983, attempted to study the temperature distribution in the tool and chip in continuous cutting by developing a finite element program. But he had a difference of 50 C between his predicted temperature and his recorded temperature.

Stephenson and Ali [29], in 1992, modeled the tool tip to study the temperature distribution of the tool temperature in interrupted metal cutting.

Boothroyd [30], in 1963, also tried to measure the radiation from the workpiece, a technique similar to that of Schwerd. He photographed workpieces to find the radiation from the work, tool and the chip after heating the work pieces for about 600 C. To find the point to point radiation intensity a microdensitometer was used.

Shore [31], in USA, Gottwein [32], in Germany and Herbert [33], in Great Britain, simultaneously, found a way to measure the mean temperature, by using thermocouple technique, along the face of a metal cutting tool.

A very valuable insight to the temperature distribution on shear plane, tool and the chip was given by, Schwerd [34] in 1937. But his method of measuring the infrared radiation from the tool, work and the chip to find the temperature distribution on the outside surface of the region did not reveal the temperature inside the workpiece.

Abdel-Hamid [30], in 1996, developed a thermomechanical model to better understand the end milling cutting process using a high speed steel tool. The temperature distribution in both the tool and the chip was predicted during the cutting and as well as in the non-cutting period. He gave the temperature rise at the shear plane by,

$$T_s = (1 - \lambda_s)P_s / \rho c v A_c \qquad (25)$$

Where, P_s - Instantaneous gross rate of energy liberation of shear source.

ρc - Volumetric specific heat

v - Cutting speed

λ_s - Portion of the shear heat source

A_c - Instantaneous chip cross section area, given as

$$A_c = s_t \sin(\varphi_i)d \qquad (26)$$

Where s_t - Feed rate per tooth

φ_i - Instantaneous cutter rotation angle

d - Chip width.

ANSYS was used to simulate the process for the study. He predicted the peak temperature to be around 800 K for a feed rate of 0.1 mm/tooth and a cutting speed of 40 m/min.

Martelloti [35] suggests that in up milling, when the tool enters the work, the relative velocity along the tool path is maximum. He also states that the value of the relative velocity will decrease as the tooth of the tool progress along the tooth path. So, he concludes that the value of velocity has a maximum value when the tool enters the work and has a minimum value when the tool leaves the work. The equation for finding the relative velocity is given by,

$$V = 2\pi n[\{R \pm r\}^2 \pm 2ry]^{\frac{1}{2}} \qquad (27)$$

Where n - RPM

R - Radius of the tool

r - Radius of Pinion

y - Depth of cut.

In equation 1.3, "$+$" will be used for up milling and "$-$" will be used for down milling, thus giving higher value for up milling and a lower value for down milling.

Shaw [33], gave an expression to calculate the total frictional energy generated at the chip- tool interface per unit time per unit area, which is,

$$q = \frac{F_C V_C}{Jab} \tag{28}$$

Where, F_C - Friction force along the tool face.

V_C - Velocity of the chip relative to the tool.

a - Length of contact between chip and tool

b - Width of the chip.

Martelloti's and Shaw's principles were combined by Payton [36] for Friction Stir Welding as a specialized form of slot milling. According to Payton, the pin tool used in the FSW process, works similar to a milling tool. So the numerical equations that apply for a milling tool also apply to the FSW tool. In Machining theory, the leading side or the up milling side of the workpiece would be hotter than the trailing or down milling side. This is due to the velocity of the tool tip would be maximum on the leading side and minimum on the trailing side. In FSW, the leading side is the advancing side and the trailing side is the retreating side. According to this, the advancing side of the piece in FSW is hotter than the retreating side. The heat equation was given as,

$$T = [16,148.58]HP_s\sqrt{\frac{V*t}{k*(pc)}} \qquad (29)$$

Where, HP_s - Specific Horsepower

V - Cutting speed

k - Coefficient of thermal conductivity

pc - Volume specific heat of the work material

t - Uncut chip thickness, given by

$$t = \frac{F_t*d}{R\cos^{-1}(1-\frac{d}{R})+\frac{F_t*n}{\pi*D}\sqrt{D*d-d^2}} \qquad (30)$$

Where, R - Radius of the cutting edge

d – Depth of cut

D – Diameter of the cutter

n – Number of teeth

F_t - Feet per tooth

Payton claims that the above equation could be used to find the temperature of the workpiece during the experiment for a given set of parameters, which would help the welder to design a tool which would avoid the defects. Payton's model forms the basis for this project

Conclusions of the literature review

Although there have been several flow models and heat source models proposed in the refereed literature of Friction Stir Welding, there is a shortage of real world thermal data against which to validate the proposed models. This is largely due to the contained nature of the actual

Friction Stir Welding process. The heat sources of deformation are located within the base metal being welded and underneath the rotating tool shoulder. As such, surface pyrometry measures are ineffective. The limited amount of thermal data in the reported literature is usually coincidental to the primary goal of the experimental design and non-symmetrical.

Thermal studies are also complicated by the complex methods required to embed thermocouples within the work-piece. This is further compounded by the attention to detail which would be required to exactly place the thermocouples in the same place each time within the specimen as it is being prepared.

None of the proposed models have been validated against more than a few data runs. A quick way to collect a statistically valid body of thermal data has eluded researchers attempting to model the FSW process.

IV. MATERIALS, EQUIPMENT AND SOFTWARE

This chapter documents the materials, equipment and software used in the conduct of the experimental research.

Overview

The core of the final experimental setup consists of a steel holder (Alloy 1020) which acts as the Friction Stir Welding anvil, work-holder and thermocouple holder (Figure 23 and Figure 24). The unit allows for a rapid exchange of specimens without the need to place or replace thermocouples needlessly.

Figure 23: Side view of the steel holder with stainless steel wells

Figure 24: End view of the steel holder.   Tool is inserted into the sample

The holder has two slotted provisions, one for the aluminum shoulder specimen and the other for the aluminum pin specimen. The specimens are clamped to the holder using screws on either ends of the holder and through out the length of the stock. The dimensions and the material of the elements in the holder are given below.   Figure 25 provides a schematic representation of the instrument base.
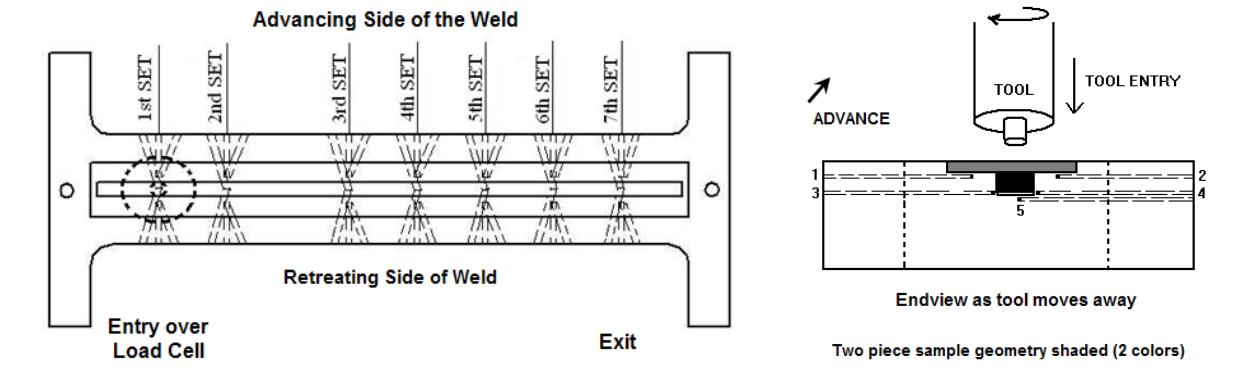
Figure 25: Rough schematic of the instrument above.   The thermocouple wells must be drilled at convergent angles in order to place all 5 thermocouple data points in the same plane as the tool moves through the plane. A load cell is located underneath the entry point on the left.   The advancing side of the weld is located on the side away from the operator as he faces the machine.   The tool enters from the left. Normal rotation is clockwise.

Materials:

The steel base is steel alloy 1020.   The thermocouple wells are made from stainless steel 318.   The specimens (workpiece) used in this experiment was aluminum alloy (AA) 6061 with a T6 temper.   Common commercial dimensions were used to create the top stock and bottom stock quickly using a simple cutoff saw.

> Top (Shoulder) stock dimension:
>
>> Length: 22 inches
>>
>> Breadth: 2 inches
>>
>> Height: 0.125 inches
>
> Bottom (Pin) stock dimension:
>
>> Length: 21 inches
>>
>> Breadth: 0.5 inches
>>
>> Height: 0.5 inches

The actual friction stir welding tools were manufactured from titanium alloy purchased from TIMETAL.   The alloy used was AMS 4928N / HT R6968.   The material machines easily and had outstanding wear characteristics.

OMEGATHERM was used to seal any gaps which may have existed along any boundaries.   High accuracy thermocouples (OMEGA HH-K-20-SLE) with an accuracy of +/- 2 degrees were used in the construction of the base holder.

Closed end stainless steel wells were an OMEGA product (SS-316) with a standard diameter of 0.1875 inches and a uniform wall thickness of 0.025 inches.

Fabricated Devices:

The base holder was fabricated from steel alloy 1020. Basic dimensions are depicted in Figure 26. Overall length was 25 inches. Widest width was 10 inches. Maximum height was 2 inches. Figure 23 above illustrates it photographically.
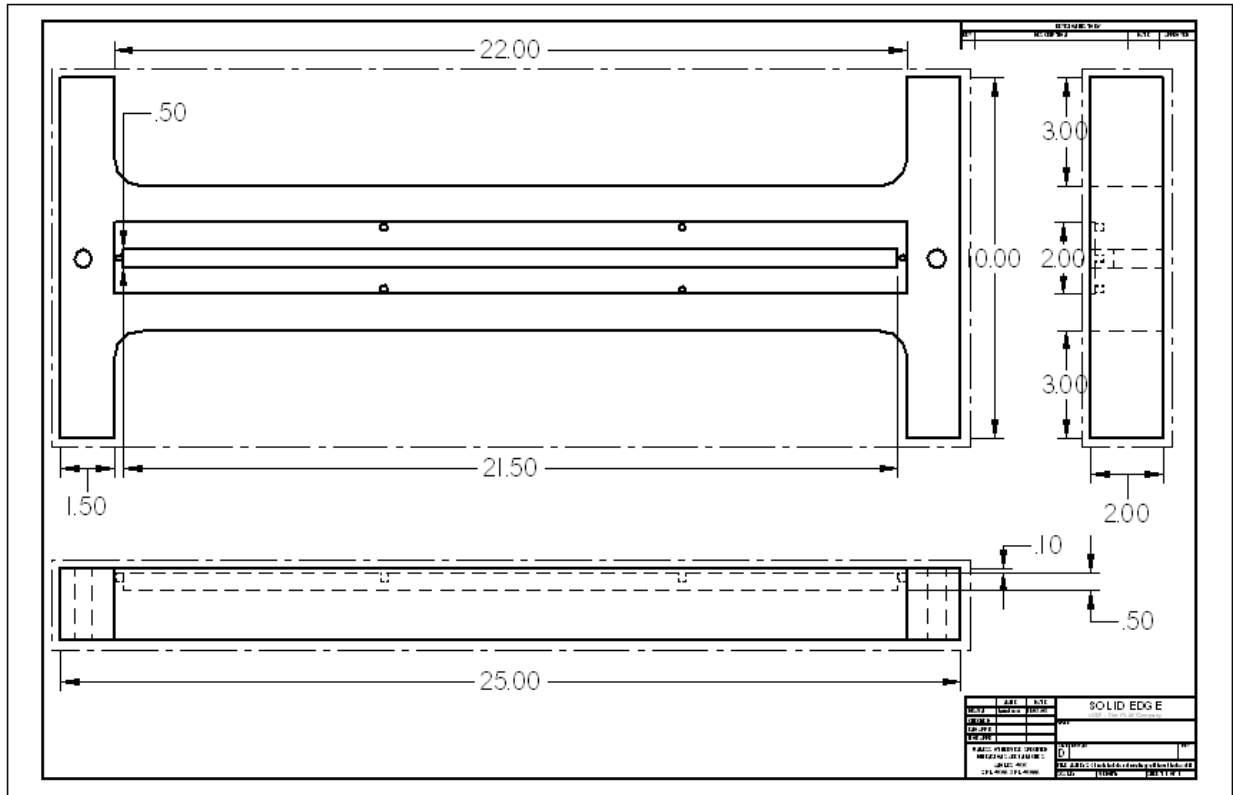
Figure 26: Drawing of the holder with dimensions in inches without the accommodations for steel wells; all dimensions are in inches.

The pin tools used in this experiment were simple pins without threading. Three tools were used for the experiment with three different shoulder diameters as illustrated below. All tools were produced on a computer numerically controlled (CNC) HAAS TL2 tool-room lathe locally.

Shoulder: Titanium alloy (AMS 4928N by TIMETAL)

Pin: Titanium alloy (AMS 4928N by TIMETAL)

45

Shoulder diameter: 0.9 inch, 0.7 inch, 0.5 inch

Pin diameter: 0.25 inch

Length of the pin: 0.3 inch

Radius between the shoulder and the tool: 0.1 inches

The tools were made on the CNC lathe.
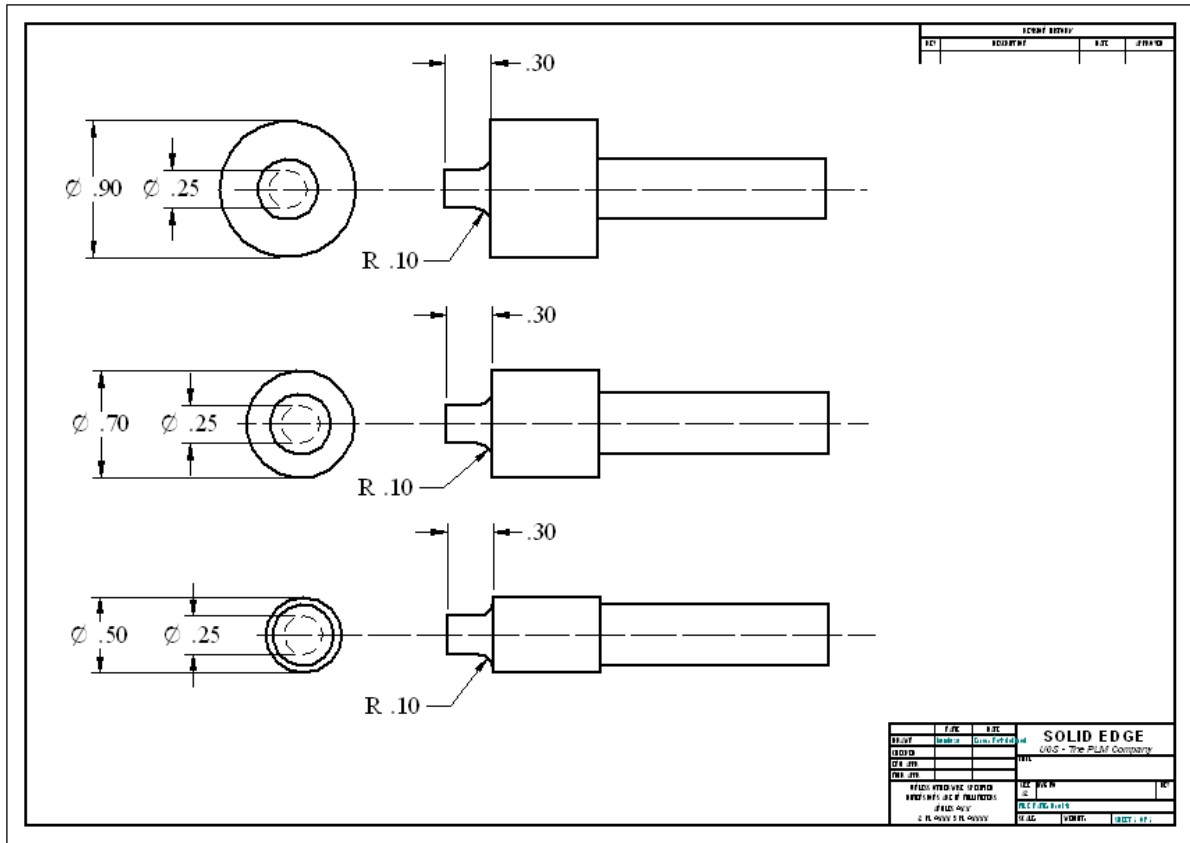
Figure 27: Tool dimensions; All dimensions are in inches.

Instrumentation:

National Instruments' LabVIEW Version 8.3 software was used to collect the data using a NI-CDAQ 9172 backplane chassis combined with NI 9205 instrumentation modules. Figure 28 shows the chassis with modules installed and thermocouples attached. Figure 29 shows the entire final instrument from a distance in Auburn University's Design and Manufacturing Laboratory. Figure 30 and Figure 31 illustrates the software setups used to program the NI 9205 modules for the thermocouples utilized.
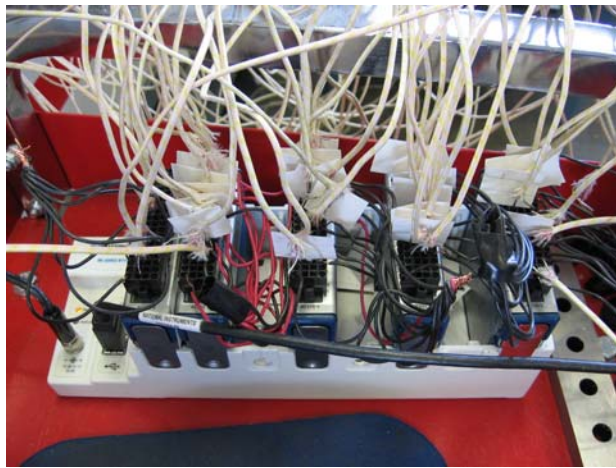
Figure 28: NI 9205 modules installed in NI-CDAQ-9172 chassis.

Figure 29: Entire instrument installed in CINNINATI ARROW CNC Mill
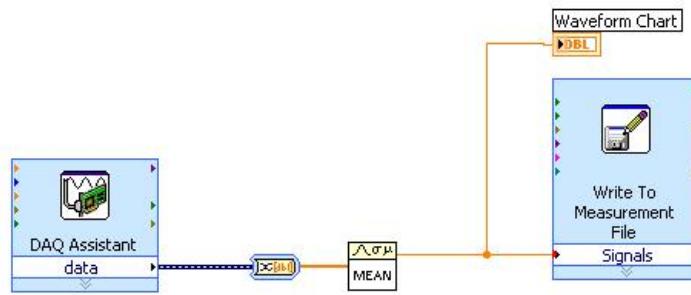
Figure 30: Basic thermocouple setup LABVIEW 8.3 program.
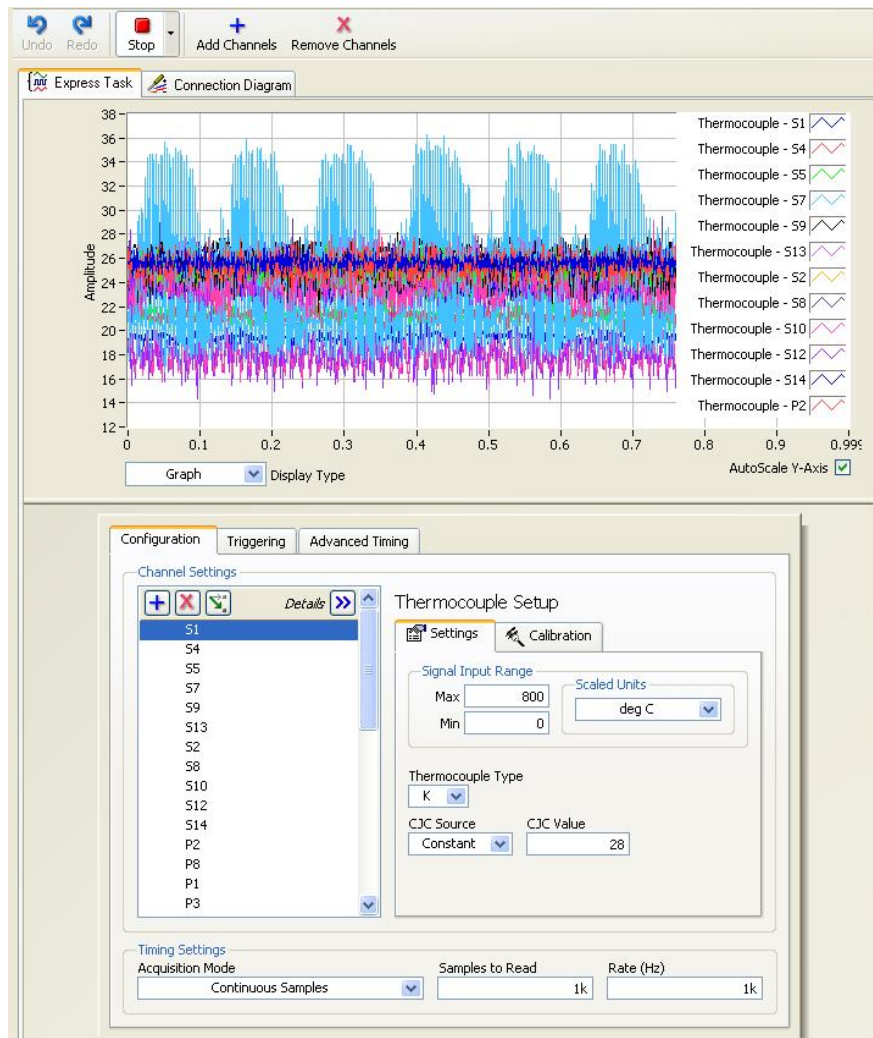
Figure 31: LabVIEW 8.3 setup for multiple thermocouples

Machinery

A Cincinnati ARROW 750 mill was used (see earlier Figure 28) as the friction stir welding platform in this experiment. A HAAS TL-2 CNC lathe was utilized to fabricate the welding tools and a HAAS TM-2 CNC mill was utilized to fabricate the steel 1020 holder of Figures 23, 24 and 26.

Software

National Instruments' LabVIEW version 8.3 was utilized to build the instrumentation circuitry. A commercially available multiphysics finite element modeling software program developed by FEMLAB called COMSOL was utilized to simulate the results. COMSOL was utilized because of its low cost and availability to the major professor and student. Additionally, COMSOL works well with the popular MATLAB software used throughout academia.

V. CONSTRUCTION AND METHODOLOGY OF INSTRUMENT

The experimental objective of the instrument is to simultaneously and symmetrically measure the thermal field around a tool as it passes a given plane. Ideally, this would capture the temperature under the shoulder at its maximum radius, just under the pin as it passes overhead and below the midpoint side of the pin. This "nominal" configuration requires a pairing of 5 thermocouples to completely capture the transverse plane as the tool passes by the observation point. Multiple pairings allow the tool to pass through the thermocouples.

Embedding thermocouples in such a manner for every sample is a very time consuming effort. Controlling the variability of thermocouple fabrication and placement is an extremely daunting prospect for even a skilled technician. Each of the earlier studies was conducted on a limited number of carefully prepared samples. It became apparent that it would be best to construct a standard holder with embedded thermocouples. Instead of changing the thermocouples, the experimentalist changes the sample. This allows the collection of a large body of statistical data rapidly. Figure 25 provides a schematic view. Figure 23 is a photograph of the instrument. The first two sets of thermocouples are separated from the final five sets to allow for the dwell in temperature during tool insertion. The last five sets or pairings all view the approaching tool as a steady state, if transient, heat source.

Advancing Side of the Weld

1st SET   2nd SET   3rd SET   4th SET   5th SET   6th SET   7th SET

Retreating Side of Weld

Entry over Load Cell

Exit

ADVANCE

TOOL   TOOL ENTRY

Endview as tool moves away

Two piece sample geometry shaded (2 colors)
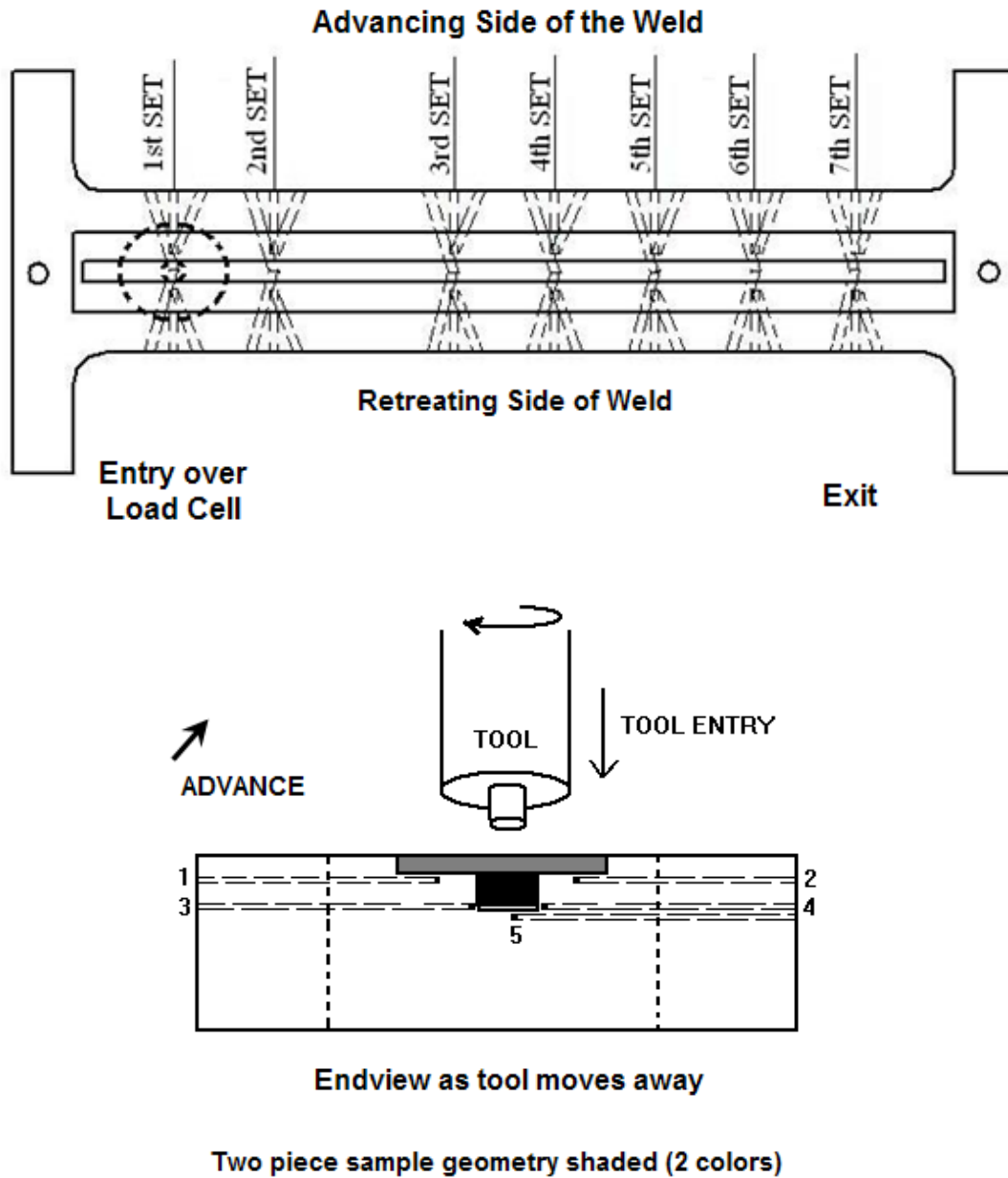
Figure 32: Rough schematic of the instrument above. The thermocouple wells must be drilled at convergent angles in order to place all 5 thermocouple data points in the same plane as the tool moves through the plane. A load cell is located underneath the entry point on the left.   The advancing side of the weld is located on the side away from the operator as he faces the machine.   The tool enters from the left. Normal rotation is clockwise.
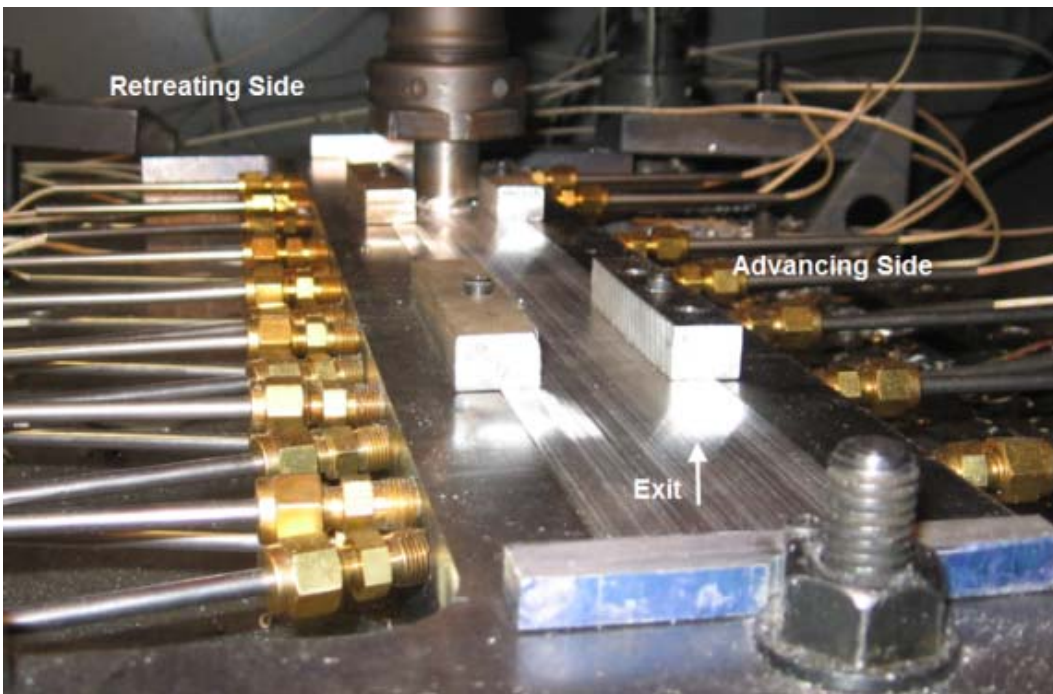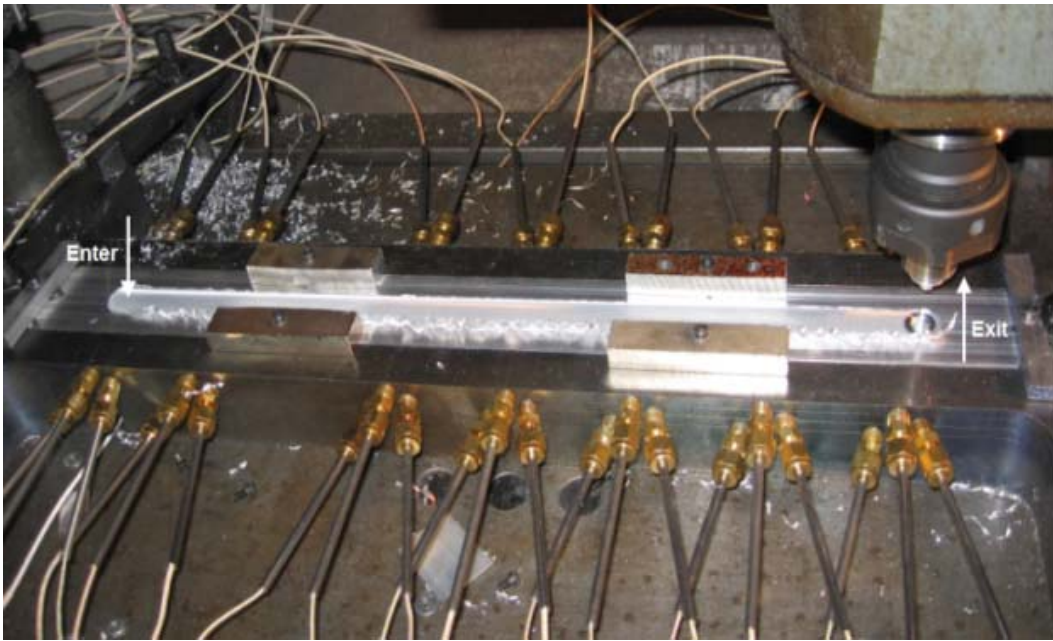
Figure 33:   Side and end view of the thermal profile instrument. In the first photograph,

the tool enters on the left hand side and traverses to the right along a 22 inch long path.

Exit is marked in each view in white. In the first photograph the run is complete (tool up).

A run is in progress in the second photograph (tool down, moving towards the front).

The overall length of the data run is 22 inches measured from the tool entry point until the tool exit point. Seven thermocouple pairs are arranged along the length of the unit in groups of five for a total of 35 thermocouples. Within each planar group, there are two shoulder thermocouples (advancing and retreating side), two pin sides (advancing and retreating sides), and one under the pin thermocouple. The first two of seven pairs are separated by a small offset to the left hand side from the final 5 paired sets. Downward thrust force is also recorded at this time using a small force plate underneath the entry point. This allows for observation of the tool entry and initial traverse independently of the routine weld passage observed through the 5 pairs on the right hand side.

The design objective was to achieve an instrument with a statistical power of 90%. The unit is currently capable of capturing a +/- 2 degree Celsius temperature difference 95% of the time with 7 replicates of each factor level. The long term goal is to achieve 95% confidence with 3 replicates of each factor level. Many samples per hour are possible since only a slight cooling off period is needed between samples.

The holder is designed to accept commercially available stocks in order to fit the cavity in the steel holder. The pin stock (0.5 by 0.5 inches) was dropped in the pin cavity and the shoulder stock (2.0 inches by .125 inches) was dropped in the shoulder cavity. Both the stocks were clamped down to the steel holder with a screw on each corner of the holder and through out the length of the holder. Figure 33 above shows the end view of the holder with thermocouple placements.

Thermal grease (OMEGASEAL) was used to fill the air gap between the aluminum stock and the steel holder. The holder has provision to measure seven sets of data. At each "set" for that plane of the work piece, a total of five holes were drilled at different locations to

53

accommodate five K-type thermocouples.

Force Measurements

Traditionally, Friction Stir Welding machines are run in a method referred to as "load control" where the machine maintains a constant downward force. Auburn University does not have machines capable of performing "load control" welding. In order to ensure a consistent starting downward force, the downward force of the pin tool was measured using a load cell. The load cell was placed under the backside of the steel holder, directly under the point of entry of the tool. A slot was machined in the back side of the holder to accommodate the load cell. Data runs which fell outside the nominal pressure range were rejected for analysis. Figure 34 shows the load cell placement.
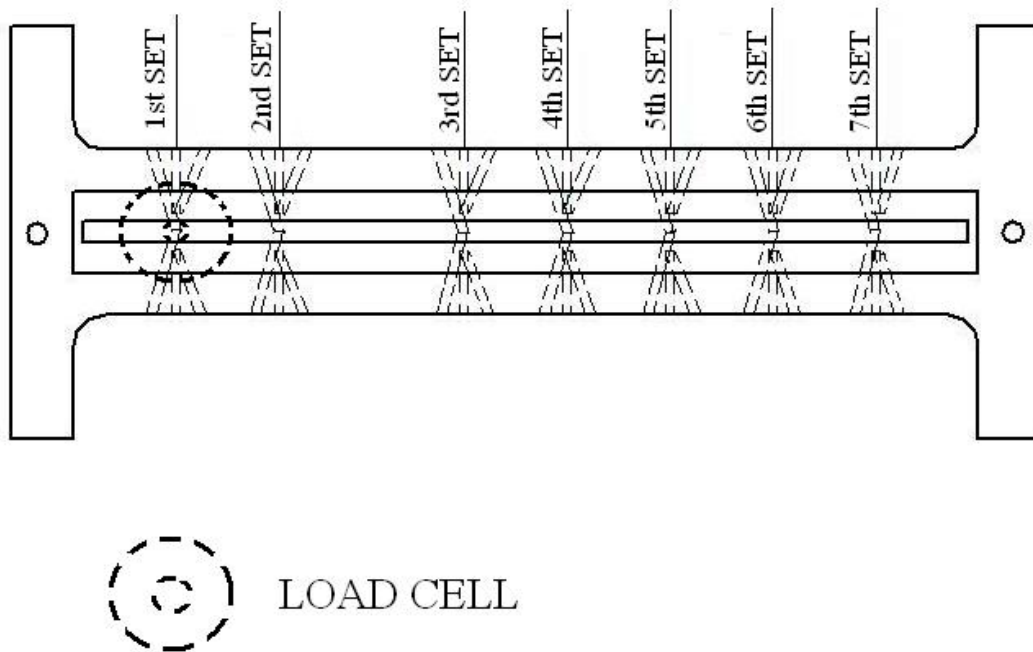
Figure 34: Placement of the load cell for measuring the downward force.

The specification of the load cell:

> Make: Omegadyne Inc
>
> Model: LCGD – 30K
>
> Measuring Range: 0 – 30000 lbs
>
> Sensitivity: 18.1112 mVdc

Data Collection

Lab view software and a data acquisition system were used to record the data from the thermocouples and the load cell.   Details of the software are presented in the section on equipment.   The basic flow diagram representation is depicted in Figure 35 below.
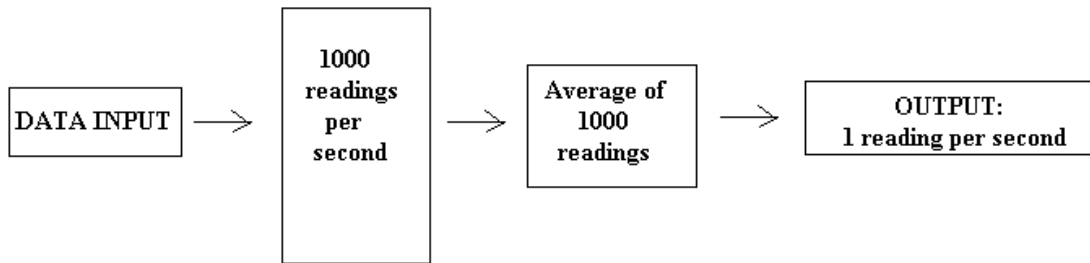
Figure 35: Basic Data Collection Block Diagram

The time versus temperature graph and the time versus force graph obtained has one sample every second. The reading obtained in a second would be the average of one thousand readings obtained in the same second. This was done to reduce the noise disturbances.

Thermocouple Nomenclature and placement

There are seven sets of thermocouples in the apparatus.   Each set includes 5 thermocouples. Figure 36 shows the placement of the terminal thermocouple joints within the apparatus.
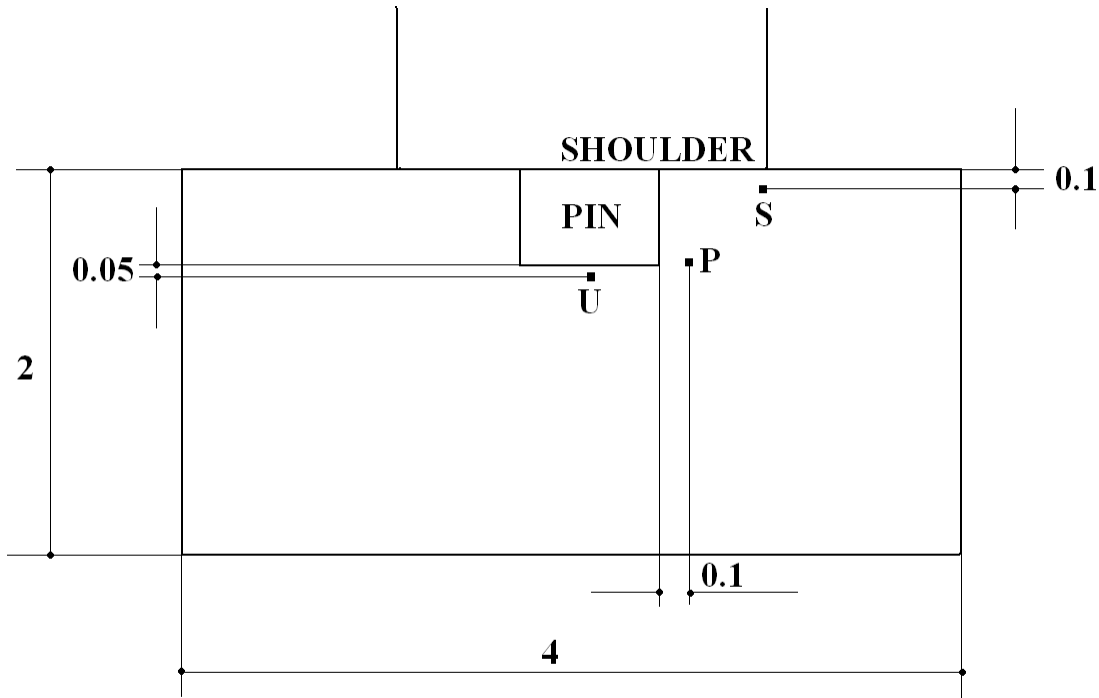
ALL DIMENSIONS ARE IN INCHES

Figure 36: Physical placement of the thermocouples

Thermocouple Designations:

Each Thermocouple was represented by a unique alphabet and number.

S – Shoulder thermocouple. (Retreating side: S_1, S_3... S_{13}; Advancing side: S_2, S_4... S_{14})

P – Pin thermocouple. (Retreating side: P_1, P_3... P_{13}; Retreating side: P_2, P_4... P_{14})

U – Under the pin thermocouple. (U_1, U_2... U_7)

The first two sets of thermocouples are separated from the last five sets of thermocouples. The intention here is that the first two sets are observing the entry of the tool. The last five sets all observe and document the approaching tool as it transits a weld position. This is similar to a long production weld such as on the space shuttle external fuel tank.

<u>Recorded and Calculated Thermodynamic Results</u>

The experimental method used in this project does not directly record the temperature of the specimen. Since the welled thermocouples are placed in the steel holder, the recorded temperatures would be the steel temperature at the thermocouple tip within the well. Steady state, one dimensional heat transfer equations were used to find the approximate temperature in the aluminum specimen. This is necessary in order to compare real world data to the predicted values of the thermodynamic models.

Steady state, one dimensional heat transfer equation is based on Fourier's law of conduction. According to Fourier's law of conduction, the rate of heat flow through a homogenous solid is directly proportional to the area of the section perpendicular to the direction of heat flow, and the temperature difference along the path of heat flow.

$$(dQ/dt) \propto A*(dT/dl), \qquad\qquad (28)$$

where, Q – Heat flux,

A – Area of the section,

T – Temperature.

From equation 28, the one dimensional, steady state equation is derived as,

$$Q = -kA \ (T_2 - T_1)/L \qquad\qquad (29)$$

where, k – Thermal conductivity of the material

Q – Heat flux,

A – Area of the section,

T_2- Lower temperature,

T_1- Higher temperature.

The minus sign for thermal conductivity denotes that the heat is transferred in the direction of the

decreasing temperature.

Equation 29 can be rewritten as,

$$Q = kA \ (T_1 - T_2)/L \hspace{3cm} (30)$$

This project uses equation 30 for finding the temperature of the specimen. For one dimensional steady state condition, heat flux, Q is the same through out the material. In order to find Q, there has to be two known temperatures (T_1, T_2).
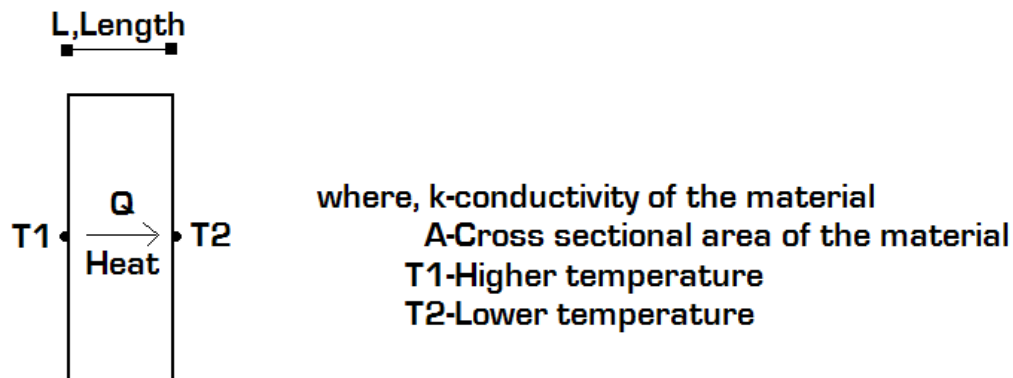
Figure 37: One dimensional heat transfer

Measurement of temperatures (T_1, T_2) in FSW

In this case, temperature is measured only at one single point in the steel holder using the welled thermocouples which provides us with only one temperature, T_1. In order to find T_2, the same set up was used without the wells. Instead of welled thermocouples recording the temperature from the steel holder, plain thermocouples were used to find the temperature of the steel holder thus finding T_2. With two known temperatures (T_1, T_2) the heat flowing through the stainless steel well could be found. The calculated Q could be used to find the temperature of the specimen using equation 30.

Application of One dimensional steady state Conduction to the instrument

Equation 30 was used in the project to find the temperature of the specimen. Cross section view of the holder is shown in figure 38.
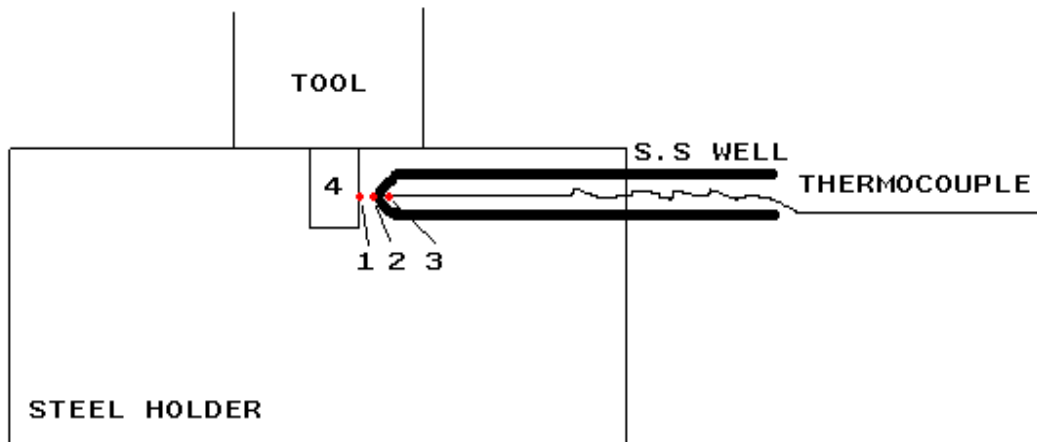
Figure 38: Cross sectional view; Welled thermocouple in the steel Holder

The interfaces represented at each boundary are:

1 – T_s: Temperature of the specimen at the aluminum/steel interface

2 – T_h: Temperature of the steel holder. (Recorded data, T_2)

3 – T_w: Temperature of the stainless steel. (Recorded data, T_1)

4 – T: Temperature at the tool.

In order to calculate the actual temperature at the tool:

CASE 1: To find Q:

$Q = (T_w\text{-}T_h)k_1A/L_1$

CASE 2: To find Ts:

$T_s= (QL_2/k_2A) +T_h$

CASE 3: To find T:

$T= (QL_3/k_3A) +T_s$

Where,

k_1 - Thermal conductivity of steel well

k_2 - Thermal conductivity of steel holder

k_3 - Thermal conductivity of welded metal (Aluminum)

A- Area of cross section.

L_1- Thickness of the well.

L_2- Distance between the aluminum/holder interface and the face of well.

A detailed, worked example is provided in the results appendices. The author shall clearly document all reported results as either "recorded", which is the actual live data without manipulation, or "calculated". Calculated data has been transposed as detailed above. This is necessary so that actual recorded data can be compared against the predicted results of the thermal models in the literature.

VI. VALIDATION OF THE INSTRUMENT

Construction and design of a new instrument requires validation.   One must conduct trials to answer three fundamental questions:

(1) Is the instrument repeatable for constant operating conditions?

(2) Is the instrument sensitive enough to detect small changes?

(3) What is the standard deviation of the instrument?

Once these questions are answered, the confidence level or statistical power of the instrument as an observational tool can be determined.

Two different experimental conditions (factor levels) were chosen to check the repeatability and the sensitivity of the instrument. The different conditions are given in the following table (Table 2).

Factor	Factor Level Combination 1	Factor Level Combination 2
Tool Shoulder Diameter	1 inch	0.7 inch
Tool Pin Diameter	0.25 inch	0.25 inch
RPM	400	400
Traverse speed	4 inches/min	4 inches/min

Table 2: Experimental conditions for repeatability and sensitivity analysis

The basic premise of a repeatability study is that one conducts a number of runs over several days using the same operating parameters.   Then the investigator compares the statistical

61

averages against each other using a T-test. If the instrument is valid, then there should be no difference between the results. Having established repeatability, the investigator then deliberately varies the operating parameters to establish that the instrument is sensitive to changes in parameters.

The instrument has seven sets of thermocouples. The first two capture the entry of the tool and the last five capture the traverse of the tool. Temperatures captured by all the thermocouples were recorded. First two sets which capture the entry of the tool are called "Entry 1" and "Entry 2". The remaining five sets which capture the traverse of the tool are called "Group 1", "Group 2", "Group 3", "Group 4" and "Group 5". The following thermocouple labeling system was used throughout the data capture runs.

Entry 1		Entry 2		Group 1		Group 2		Group 3		Group 4		Group 5	
S1	S2	S3	S4	S5	S6	S7	S8	S9	S10	S11	S12	S13	S14
RE	AD	RE	AD	RE	AD	RE	AD	RE	AD	RE	AD	RE	AD
P1	P2	P3	P4	P5	P6	P7	P8	P9	P10	P11	P12	P13	P14
RE	AD	RE	AD	RE	AD	RE	AD	RE	AD	RE	AD	RE	AD
U1		U2		U3		U4		U5		U6		U7	

Table 3: Thermocouple labeling assignments

Where RE – Retreating side

AD – Advancing side

S – Under the shoulder thermocouple

P – Side of the pin thermocouple

U – Under the pin thermocouple

Repeatability test: Five experiments were done for the 1 inch shoulder tool at different times to validate the instrument's repeatability.   There were five replicates within each experiment.   The standard deviation of the five readings obtained then calculated. If the standard deviation found, lies within the standard deviation of the instrument, the data is said to be repeatable.   If the standard deviation found exceeds the standard deviation of the instrument, the data is considered not repeatable.

The following are the peak temperatures recorded during the experimental runs at different thermocouples.

Experimental condition: 1 Inch Shoulder tool, 400 RPM, 4 IPM

	Entry 1		Entry 2		Group 1		Group 2	
	S1	S2	S3	S4	S5	S6	S7	S8
RUN 1	169.35	171.64	187.07	195.99	170.01	189.3	140.92	154.4
RUN 2	168.74	181.77	181.91	192.58	172.76	184.41	148.84	158.9
RUN 3	162.06	180.14	183.1	190.89	172.41	184.15	142.61	153.5
RUN 4	170.52	179.44	190.17	192.63	174.5	184.23	142.07	154.3
RUN 5	174.41	183.69	178.83	190.75	171.81	182.65	145.97	161.7

	Group 3		Group 4		Group 5	
	S9	S10	S11	S12	S13	S14
RUN 1	158.68	168.73	152.97	178.61	131.49	139.31
RUN 2	168.61	170.69	167.08	182.56	132.34	150.61
RUN 3	158.52	171.27	159.74	180.71	132.97	144.93
RUN 4	163.43	183.76	167.16	189.46	141.67	152.7
RUN 5	162.4	184.26	161.4	190.37	133.93	149.49

Table 4: Recorded Temperature for repeatability analysis for shoulder thermocouples: All values in Celsius

	Entry 1		Entry 2		Group 1		Group 2	
	P1	P2	P3	P4	P5	P6	P7	P8
RUN 1	175.43	196.41	138.98	146.66	142.99	180.93	150.74	161
RUN 2	185.07	195.78	142.99	154.14	147.94	176.77	147.23	163.7
RUN 3	184.89	190.34	136.2	150.83	143.94	164.43	142.62	167.6
RUN 4	186.68	191.26	137.87	147.54	149.46	177.51	152.55	170.2
RUN 5	180.56	195.55	139.43	151.8	153.87	183.84	156.51	177.7

	Group 3		Group 4		Group 5	
	P9	P10	P11	P12	P13	P14
RUN 1	149.66	163.42	128.13	170.88	126.8	139.86
RUN 2	160.51	165.9	139.44	171.73	128.26	148.47
RUN 3	151.28	164.68	135.09	170.13	128.37	138.96
RUN 4	157.94	166.49	140.81	175.81	135.55	146.8
RUN 5	159.35	171.83	142.38	183.25	128.51	147.78

	Entry 1	Entry 2	Group 1	Group 2	Group 3	Group 4	Group 5
	U1	U2	U3	U4	U5	U6	U7
RUN 1	195.8	175.86	179.65	140.48	137.14	164.07	125.92
RUN 2	199.55	177.34	179.61	148.46	143.34	157.32	131.61
RUN 3	210.61	167.6	170.36	142.47	137.5	164.25	124.67
RUN 4	197.8	174.28	174.54	145.03	139.48	170.42	135.17
RUN 5	210.24	168.34	176.76	154.08	148.56	164.16	127.9

Table 5: Recorded Temperature for repeatability analysis for pin and under the pin thermocouples: All values in Celsius

Standard Deviation:

The standard deviation of the instrument was given by,

Standard deviation of the instrument = Standard deviation of the thermocouples +

Standard deviation of the module NI 9205.

The standard deviation of thermocouples is ±2 degree Celsius. The module has a standard deviation of at least ±2% of the recorded temperature. So, the module standard deviation range was ±2% of the average of the five peak temperature readings of the same thermocouple.

The standard deviation of the instrument was compared with the standard deviation of the readings obtained for each thermocouple. The following tables show the comparison of the standard deviations.

	Std deviation of readings (1)	Std dev range of thermoc ouples	Std deviation of modules	Std deviation range of modules	Std deviation range of instrument (2)	Is (1)<(2)	Remarks
S1 RE	4.47	4	3.38	6.76	10.76	Yes	Repeatable
S2 AD	4.61	4	3.59	7.17	11.17	Yes	Repeatable
S3 RE	4.45	4	3.68	7.37	11.37	Yes	Repeatable
S4 AD	2.11	4	3.85	7.70	11.70	Yes	Repeatable
S5 RE	1.62	4	3.45	6.89	10.89	Yes	Repeatable
S6 AD	2.53	4	3.70	7.40	11.40	Yes	Repeatable
S7 RE	3.26	4	2.88	5.76	9.76	Yes	Repeatable
S8 AD	3.57	4	3.13	6.26	10.26	Yes	Repeatable
S9 RE	4.14	4	3.25	6.49	10.49	Yes	Repeatable
S10 AD	7.61	4	3.51	7.03	11.03	Yes	Repeatable
S11 RE	5.89	4	3.23	6.47	10.47	Yes	Repeatable
S12 AD	5.29	4	3.69	7.37	11.37	Yes	Repeatable
S13 RE	4.12	4	2.69	5.38	9.38	Yes	Repeatable
S14 AD	5.35	4	2.95	5.90	9.90	Yes	Repeatable

Table 6: Repeatability of the shoulder sample temperatures

	Std deviation of readings (1)	Std deviatio n of thermoc ouples	Std deviation of modules	Std deviation range of modules	Std deviation of instrument (2)	Is (1)<(2)	Remarks
P1 RE	4.57	4	3.65	7.30	11.30	Yes	Repeatable
P2 AD	2.84	4	3.88	7.75	11.75	Yes	Repeatable
P3 RE	2.51	4	2.78	5.56	9.56	Yes	Repeatable
P4 AD	3.09	4	3.00	6.01	10.01	Yes	Repeatable
P5 RE	4.40	4	2.95	5.91	9.91	Yes	Repeatable
P6 AD	7.42	4	3.53	7.07	11.07	Yes	Repeatable
P7 RE	5.28	4	3.00	6.00	10.00	Yes	Repeatable
P8 AD	6.45	4	3.36	6.72	10.72	Yes	Repeatable
P9 RE	4.94	4	3.11	6.23	10.23	Yes	Repeatable
P10 AD	3.22	4	3.33	6.66	10.66	Yes	Repeatable
P11 RE	5.74	4	2.74	5.49	9.49	Yes	Repeatable
P12 AD	5.43	4	3.49	6.97	10.97	Yes	Repeatable
P13 RE	3.45	4	2.59	5.18	9.18	Yes	Repeatable
P14 AD	4.58	4	2.89	5.78	9.78	Yes	Repeatable

Table 7: Repeatability of the Pin Tool Temperatures

	Std deviation of readings (1)	Std deviation of thermo couples	Std deviation of modules	Std deviation range of modules	Std deviation of instrument (2)	Is (1) < (2)	Remarks
U1	7.09	4	4.06	8.11	12.11	Yes	Repeatable
U2	4.45	4	3.45	6.91	10.91	Yes	Repeatable
U3	3.90	4	3.52	7.05	11.05	Yes	Repeatable
U4	5.37	4	2.92	5.84	9.84	Yes	Repeatable
U5	4.79	4	2.82	5.65	9.65	Yes	Repeatable
U6	4.63	4	3.28	6.56	10.56	Yes	Repeatable
U7	4.31	4	2.58	5.16	9.16	Yes	Repeatable

Table 8: Repeatability analysis for the underside of the pin tool temperatures

The above table indicates that the instrument reliably repeats temperatures. Additionally, T-Tests of between replicate samples indicate that there is no variance in the standard deviation of the instrument between replicate runs.

<u>Sensitivity test</u>

Five additional experiments were done for the second condition and five readings were obtained for all the thermocouples. Since the shoulder diameter was the only change between the two conditions, the data obtained were statistically compared for a change in the shoulder temperature. Since the "Entry 1" and "Entry 2" thermocouples were used to capture the entry point of the tool, these sets were not considered while comparing the two conditions. Groups 1 to 5 were considered for the sensitivity test. Temperature recorded by the shoulder thermocouples from Group 1 to 5 in both the conditions were subjected to statistical T-test to find if there is a difference in the data obtained or not.

Table 8 shows the peak temperatures obtained in the shoulder thermocouples of Group 1 to 4 with the 1 inch shoulder tool. Table 9 shows the peak temperatures for the 0.7 inch shoulder tool.

Condition 1:   1.0 inch shoulder tool, 400 RPM, 4 IPM

	Group 1		Group 2		Group 3		Group 4	
	S5 RE	S6 AD	S7 RE	S8 AD	S9 RE	S10 AD	S11 RE	S12 AD
RUN 1	170.01	189.30	140.92	154.38	158.68	168.73	152.97	178.61
RUN 2	172.76	184.41	148.84	158.88	168.61	170.69	167.08	182.56
RUN 3	172.41	184.15	142.61	153.48	158.52	171.27	159.74	180.71
RUN 4	174.50	184.23	142.07	154.25	163.43	183.76	167.16	189.46
RUN 5	171.81	182.65	145.97	161.67	162.40	184.26	161.40	190.37

Table 9: Peak average temperature readings for 1.0 inch shoulder tool (Condition 1)

Condition 2: 0.7 inch shoulder tool, 400 RPM, 4 IPM

	Group 1		Group 2		Group 3		Group 4	
	S5 RE	S6 AD	S7 RE	S8 AD	S9 RE	S10 AD	S11 RE	S12 AD
RUN 1	130.55	150.87	132.09	146.29	142.54	154.48	140.19	153.06
RUN 2	128.32	151.18	137.28	149.55	146.99	160.35	145.98	151.07
RUN 3	133.80	156.96	133.73	150.98	147.51	163.88	148.95	155.30
RUN 4	141.94	154.45	143.30	148.73	147.38	169.95	141.00	151.21
RUN 5	137.41	155.54	143.03	151.21	155.85	166.05	140.34	156.19

Table 10: Peak average temperature readings for 0.7 inch shoulder tool (Condition 2)

The data obtained by the same thermocouples at different conditions were compared with each other. For example, S5 of condition 1 was compared to S5 of condition 2 and S6 of condition 1 was compared with S6 of condition 2 and so on. A T-test was used to determine if the averages were different.   If they were in fact different, then the instrument is sensitive to the change in variable.

Statistical Analysis: Null Hypothesis: Condition 1 equals Condition 2

Comparison (1) Vs (2)	Diff in Averages of the two sets	Pooled STD DEV	Ratio between diff and pooled STD DEV	P value	Power	Comment	Report
S5(1) Vs S5(2)	37.9	4.01	9.45	0	100%	(1)≠(2)	Sensitive
S6(1) Vs S6(2)	31.15	2.61	11.93	0	100%	(1)≠(2)	Sensitive
S7(1) Vs S7(2)	6.19	4.32	1.43	0.05	51%	(1)=(2)	Not Sensitive
S8(1) Vs S8(2)	7.18	2.89	2.48	0	92%	(1)≠(2)	Sensitive
S9(1) Vs S9(2)	14.27	4.49	3.18	0	99%	(1)≠(2)	Sensitive
S10(1) Vs S10(2)	12.8	6.8	1.88	0.02	74%	(1)=(2)	Not Sensitive
S11(1) Vs S11(2)	18.38	5.02	3.66	0	100%	(1)≠(2)	Sensitive
S12(1) Vs S12(2)	30.97	4.08	7.58	0	100%	(1)≠(2)	Sensitive
S13(1) Vs S13(2)	21.83	5.53	3.94	0	100%	(1)≠(2)	Sensitive

Table 11: Sensitivity analysis. Rejecting the null hypothesis proves sensitivity.

All the thermocouples are sensitive enough to sense the difference in the change in the operating condition, except S7 and S10 due to the low ratio between the difference and the pooled standard deviation. The system should have at least a ratio of 2.4 to sense a difference with a 90% Power, which implies a 90% confidence interval. The system is sensitive enough to capture the difference when the groups are compared as a whole instead of the comparison made individually on the thermocouples.

Power

Statistical power is defined as the probability that a statistical analysis will detect a difference which actually exists between two sets of data. In other words, power is the statistical term used to describe the ability to reject the null hypothesis when it is false, as indicated in the statistical hypothesis diagram (Figure 39).

<table>
<tr><th></th><th>REJECT</th><th>DO NOT REJECT</th></tr>
<tr><td>HYPOTHESIS TRUE</td><td>TYPE I</td><td>CORRECT DECISION</td></tr>
<tr><td>HYPOTHESIS FALSE</td><td>CORRECT DECISION</td><td>TYPE II</td></tr>
</table>

Figure 39: Statistical Hypothesis Diagram

Statistically, power is $1 - \beta$, where β, is the possible chance of committing a Type II error.

The power of an experiment depends on the size of the experiment and the variability of the response. Factors that influence the power are the size of the effect, sample variance, sample size and the criteria for significance. Standard error will also play a vital error in calculating the power. Decreasing the standard error will increase the power. Standard error will be decreased by increasing the sample size or by reducing the sigma of the dependent variable.

Power analysis could be done either before the experiment or after the experiment. Power analysis done before the experiment helps to determine the sample size of the experiment when the repeatability and sensitivity of the instrument have been established. The maximum power a test could have is 1.0 and the minimum is zero (0). Ideally an experiment which has a power close to 1 is considered to be an experiment with high power.   Ninety percent (0.9) is often the goal of the experimentalist.

<u>Number of replicates</u>

Number of replicates for the actual experiments are found considering S1 and S2 in the repeatability test.   A statistical power test is done on the following data to find significant differences between S1 and S2.

	Entry 1	
	S1	S2
RUN 1	169.35	171.64
RUN 2	168.74	181.77
RUN 3	162.06	180.14
RUN 4	170.52	179.44
RUN 5	174.41	183.69

Table 12: Data to find the number of replicates for the experiments

The Power test results for a sample size of 5 is shown below (using MINITAB 15) is:

```
2-Sample t Test

Testing mean 1 = mean 2 (versus not =)
Calculating power for mean 1 = mean 2 + difference
Alpha = 0.05  Assumed standard deviation = 4.53

            Sample
Difference    Size      Power
   -10.32       5   0.882346
```

According to the analysis, S1 and S2 are significantly different stating that both data are not equal with a statistical power of 88%. In statistics, an experiment is considered as a strong experiment if it has a power of 90%. In order to obtain a power of 90%, the sample size of the experiment is increased from 5 to 7. An other power test is done for the same experiment with a sample size of 7.

The Power test result for a sample size of 7 is shown below.

```
2-Sample t Test

Testing mean 1 = mean 2 (versus not =)
Calculating power for mean 1 = mean 2 + difference
Alpha = 0.05  Assumed standard deviation = 4.53


            Sample
Difference    Size      Power
    -10.32       7  0.973899
```
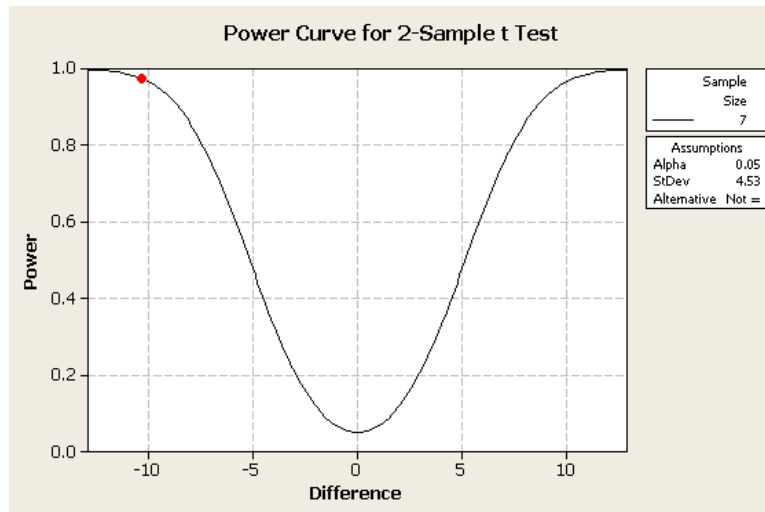

Figure 40: Statistical Power test result for a sample size of 7

For a sample size of 7, statistically S1 and S2 are significantly different with a power of 97%. Since the power of the experiment is above 90%, this is considered to be a statistically strong experiment. In order to maintain a statistical power of 90% for all the experiments, a sample size of 7 is maintained in all the experiments done.

VII. STATISTICAL DESIGN OF THE EXPERIMENT

Upon validating the instrument and determining the number of replicates needed to achieve a confidence level of at least 90 percent, the factor levels of the main experiment could be determined. As in all ANOVA experiments, it is desirable to separate the factor levels by as large a deterministic value as possible while retaining meaningful physical results. For this physical experiment, it was desirable to look at the effects of tool shoulder diameter, revolutions per minute and traverse rate.

Shoulder Diameter	350 RPM	450 RPM
0.500 Inches	Traverse 4 Inches Per Minute	Traverse 7 Inches Per Minute
0.700 Inches	Traverse 4 Inches Per Minute	Traverse 7 Inches Per Minute
0.900 Inches	Traverse 4 Inches Per Minute	Traverse 7 Inches Per Minute

Figure 41: Factor Level Combinations of the Principal Experiment.

73

Two minor additional experiments were also conducted to investigate principal effects suggested by the first experiment. In the first of these experiments, the shoulder pin size was held constant at 0.300 inches while the shoulder diameter was increased incrementally as 0.500 inches, 0.600 inches, 0.700 inches, 0.800 inches, 0.900 inches and finally 1.000 inches. Revolutions were held constant at 400 RPM and the traverse speed was limited to 4 inches per minute (IPM). Two replicates of each combination were conducted (statistical power of 80%). In the final experiment, the top plate of aluminum was replaced by Copper Alloy 10101 to study material effects. Five replicates of this experiment were conducted at 400 RPM, 1.0 inch per minute traverse. The pin tool in this case had a 0.500 inches shoulder and a 0.300 inches pin.

Although experiments can be conducted quite quickly with this setup, financial considerations limited the investigation to the parameters detailed above. The apparatus can collect as much data in a week as was formerly possible in a year of research.

VIII.   RESULTS OF THE EXPERIMENT

The experiments were conducted over a three week period using the factor levels set out in Chapter VII.   Exemplars of each result are discussed in this chapter.   Complete data sets are contained in the appropriate appendix cited below.   General observations are documented in this section.   Comprehensive discussions are conducted in Chapter X.

Principal Experiment:

Three different shoulders, with 2 different RPMs and 2 different traverse rates were used in this experiment. That produced twelve (12) possible factor level combinations in a full factorial experiment. Seven replicates of each factor level combinations were conducted in a random fashion suggested by a random number generator for a total of 84 welds.   This produced an experiment with a confidence factor of at least 95%.

The instruments data was originally organized as entry data (at position E1 and E2), with traverse group points (G1, G2, G3, G4 and G5), corresponding to the 3rd through 7th set of thermocouples.   Post data analysis indicated that the G5 transit point was always lower than G1 through G4 averages.   This is due to the physical fact that the pin was extracted by the computer exactly at position G5, which precluded the passage of the trailing edge of the tool over that portion of the weld.   This prevented the total heat input seen at positions G1 through G4.   Therefore, T5 is more properly referred to as X1, the exit point.

<u>Tabular Data</u>

The complete set of raw recorded data is provided in Appendix A. This data represents the actual "thermocouple data" at the tip of the thermocouple wire. This data was then translated mathematically into the ideal calculated value at the positions specified at the tip shoulder, pin surface and under the base of the pin. The calculated values are listed in Appendix B, along with a worked example of the calculations. The calculated values will allow a direct comparison the simulated model values in the next chapter (IX, Simulation). Table 12 documents the average advancing and retreating temperatures for the advancing (AD) versus retreating (RE) sides of the equipment.

Factor Levels	AD Shoulder	RE: Shoulder	Ad: Pin	Re: Pin	Under Pin
0.9"Sh/4"min/450 RPM	195.53	183.02	189.84	166.08	177.70
0.9"Sh/4"min/350 RPM	182.33	169.32	178.21	158.14	163.98
0.9"Sh/7"min/450 RPM	149.42	140.16	145.00	127.42	137.16
0.9"Sh/7"min/350 RPM	145.74	132.87	140.09	123.04	129.32
0.7"Sh/4"min/450 RPM	162.43	148.43	159.83	139.67	150.54
0.7"Sh/4"min/350 RPM	162.99	149.84	157.18	135.72	148.92
0.7"Sh/7"min/450 RPM	143.36	134.59	138.75	121.75	133.30
0.7"Sh/7"min/350 RPM	141.60	132.97	137.49	121.67	131.76
0.5"Sh/4"min/450 RPM	157.66	143.13	152.05	131.19	141.01
0.5"Sh/4"min/350 RPM	138.10	125.21	135.61	114.73	128.93
0.5"Sh/7"min/450 RPM	139.52	131.65	138.17	121.43	134.25
0.5"Sh/7"min/350 RPM	116.31	103.58	116.77	98.47	106.99

Table 13: Raw experimental data: Average of peak temperatures of Entry 2,

Group 1, 2, 3, and 4; All temperatures are in Celsius.

Table 13 documents the average CALCULATED advancing and retreating temperatures for the advancing (AD) versus retreating (RE) sides of the equipment.

Factor Levels	AD Shoulder	RE Shoulder	AD: Pin	AD: Pin	Under Pin
0.9"Sh/4"min/450 RPM	379.76	367.25	377.83	354.07	370.98
0.9"Sh/4"min/350 RPM	366.56	353.55	366.19	346.13	357.26
0.9"Sh/7"min/450 RPM	333.65	324.39	332.99	315.41	330.44
0.9"Sh/7"min/350 RPM	329.97	317.10	328.07	311.03	322.60
0.7"Sh/4"min/450 RPM	346.66	332.66	347.82	327.66	343.82
0.7"Sh/4"min/350 RPM	347.22	334.07	345.17	323.70	342.20
0.7"Sh/7"min/450 RPM	327.59	318.82	326.74	309.74	326.58
0.7"Sh/7"min/350 RPM	325.83	317.20	325.48	309.66	325.04
0.5"Sh/4"min/450 RPM	341.89	327.36	340.04	319.17	334.29
0.5"Sh/4"min/350 RPM	322.33	309.44	323.60	302.72	322.21
0.5"Sh/7"min/450 RPM	323.75	315.88	326.16	309.42	327.53
0.5"Sh/7"min/350 RPM	300.53	287.81	304.76	286.46	300.27

Table 14: Calculated data: Average of peak temperatures of Entry 2, Group 1, 2, 3, and 4; All temperatures are in Celsius.

Graphical Data

Appendix C provides comparitive graphs of all average values for each directly recorded factor level combination, in the example of Figure 42 on the next page. Appendix D provides comparitive graphs of all average CALCULATED values for each factor level combination, as per the example in Figure 43. This allows quick observation that in general the advancing side will always be hotter than the retreating side.
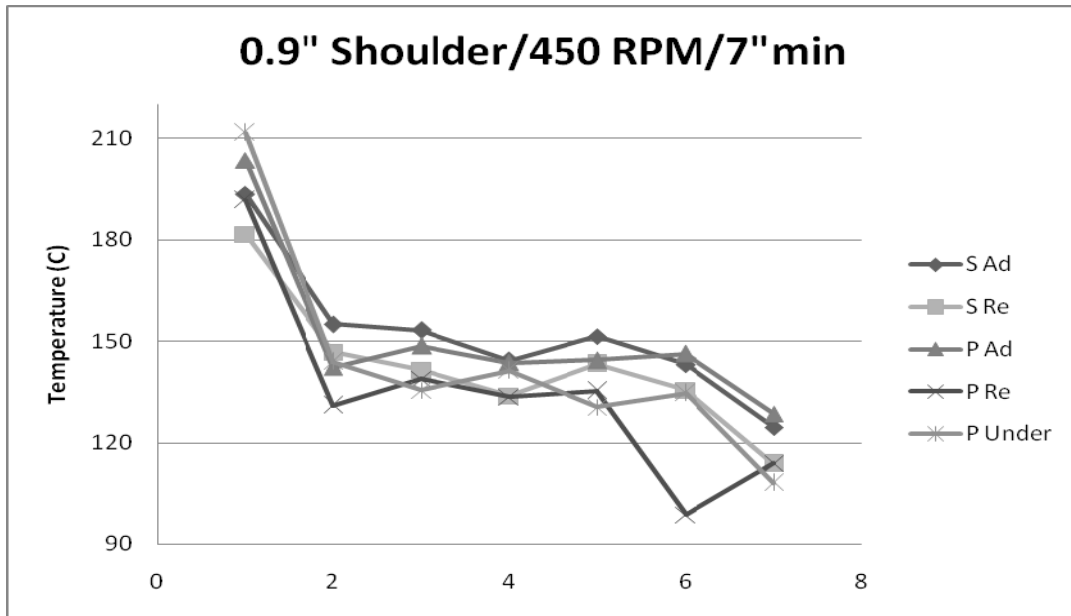
Figure 42: Example of average of seven replicates for a factor level combination (FLC) .

Advancing is higher than corresponding retreating side.
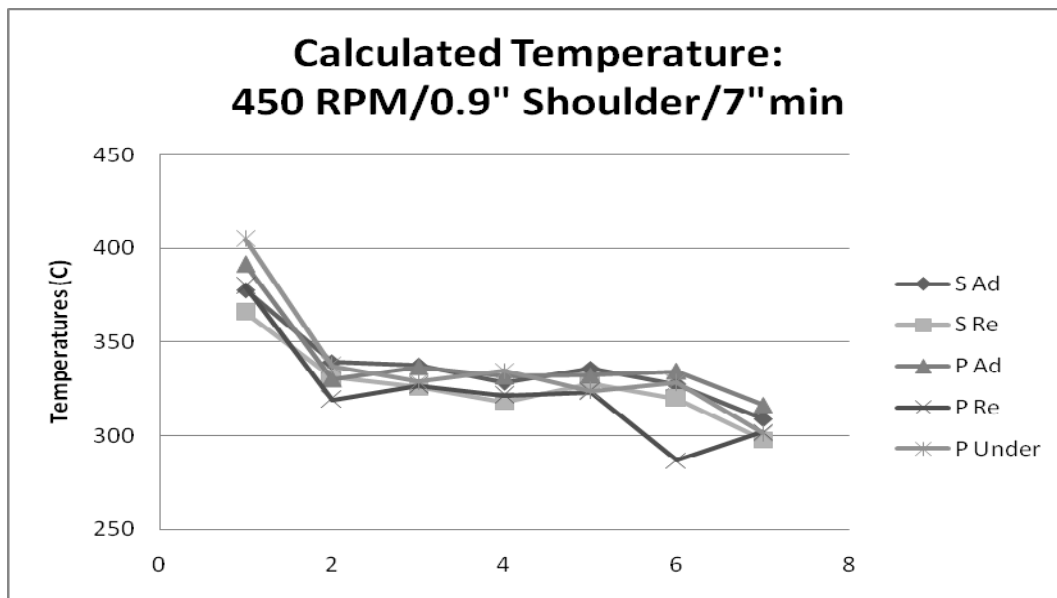
Figure 43: Example of average of seven replicates (calculated temperature) for a factor

level combination (FLC).   Advancing is higher than corresponding retreating side.

Analysis of Variance (ANOVA)

Each response was analyzed individually using ANOVA with the STATEASE software program by DesignEase, Inc. The individual responses are all detailed in Appendix E using the APA approved style format of Figure 44 below. It is thus possible to rank the impact factors of the factor levels using the F-value as a ranking number.

Response   2   S1
ANOVA for selected factorial model
Analysis of variance table [Classical sum of squares - Type II]

Source	Sum of Squares	df	Mean Square	F Value	p-value Prob > F	
Model	30168.58	11	2742.60	123.00	< 0.0001	significant
A-RPM	153.19	1	153.19	6.87	0.0107	
B-Traverse	1814.66	1	1814.66	81.38	< 0.0001	
C-Shoulder	22219.52	2	11109.76	498.25	< 0.0001	
AB	1009.18	1	1009.18	45.26	< 0.0001	
AC	113.18	2	56.59	2.54	0.0861	
BC	1829.35	2	914.67	41.02	< 0.0001	
ABC	3029.50	2	1514.75	67.93	< 0.0001	
Pure Error	1605.43	72	22.30			
Cor Total	31774.01	83				

The Model F-value of 123.00 implies the model is significant. There is only a 0.01% chance that a "Model F-Value" this large could occur due to noise.

Figure 44: ANOVA table comparing the impact factors (F-Value) of the factor levels chosen for S1, the temperature on the advancing side of the shoulder.

Table 15 gives the first, second and third largest impact factors on the individual responses for the shoulders. Table 16 gives the first, second and third largest impact factors for the pin. Table 17 ranks the impact factors for the underside of the pin.

Responses	1st largest Impact Factor	2nd largest Impact Factor	3rd largest Impact Factor
S1	Shoulder	Traverse speed	Shoulder X Speed X RPM
S2	Shoulder	Traverse speed	Shoulder X Speed X RPM
S3	Traverse speed	Shoulder	Shoulder X Speed
S4	Traverse speed	Shoulder	Shoulder X Speed
S5	Traverse speed	Shoulder	Shoulder X Speed X RPM
S6	Traverse speed	Shoulder	Shoulder X Speed X RPM
S7	Traverse speed	Shoulder	RPM X Speed
S8	Traverse speed	Shoulder	RPM X Speed
S9	Traverse speed	Shoulder	RPM X Speed
S10	Traverse speed	Shoulder	RPM X Speed
S11	Traverse speed	Shoulder	RPM X Speed
S12	Traverse speed	Shoulder	RPM X Speed
S13	Traverse speed	Shoulder	RPM X Speed
S14	Traverse speed	Shoulder	RPM X Speed

Table 15: Ranking of Impact Factors for each shoulders thermal response.

Responses	1st largest Impact Factor	2nd largest Impact Factor	3rd largest Impact Factor
P1	Shoulder	Traverse speed	Shoulder X Speed X RPM
P2	Shoulder	Traverse speed	Shoulder X Speed X RPM
P3	Traverse speed	Shoulder	RPM X Speed
P4	Traverse speed	Shoulder	Shoulder X Speed
P5	Traverse speed	Shoulder	Shoulder X Speed
P6	Traverse speed	Shoulder	Shoulder X Speed
P7	Traverse speed	Shoulder	RPM X Speed
P8	Traverse speed	Shoulder	RPM X Speed
P9	Traverse speed	Shoulder	RPM X Speed
P10	Traverse speed	Shoulder	RPM X Speed
P11	Traverse speed	Shoulder	Shoulder X Speed
P12	Traverse speed	Shoulder	Shoulder X Speed
P13	Traverse speed	Shoulder	RPM X Speed
P14	Traverse speed	Shoulder	RPM X Speed

Table 16: Ranking of Impact Factors for each pins thermal response.

Responses	1st largest Impact Factor	2nd largest Impact Factor	3rd largest Impact Factor
U1	Shoulder	Traverse speed	RPM X Speed
U2	Traverse speed	Shoulder	Shoulder X Speed
U3	Traverse speed	Shoulder	RPM X Speed
U4	Traverse speed	Shoulder	RPM X Speed
U5	Traverse speed	Shoulder	RPM X Speed
U6	Traverse speed	Shoulder	Shoulder X Speed
U7	Traverse speed	Shoulder	Shoulder X Speed

Table 17: Impact factors for temperature underneath the pin tool.

T-Tests:

T-Tests were conducted using the 7 replicates of each advancing side versus the seven replicates of the retreating side for each result. The tables below provide the P value of the T-test conducted for different factor level combination. Table 18 documents the shoulder comparisons. Table 19 documents pin comparisons. Tables 20 and 21 document the power/confidence with which we can state the advancing sides are hotter than the retreating sides.

Factor level combination	S1 Vs S2	S3 Vs S4	S5 Vs S6	S7 Vs S8	S9 Vs S10	S11 Vs S12	S13 Vs S14
0.9"Sh/4"min/450 RPM	0.001	0.000	0.001	0.001	0.002	0.000	0.000
0.9"Sh/4"min/350 RPM	0.001	0.002	0.002	0.001	0.002	0.001	0.003
0.9"Sh/7"min/450 RPM	0.000	0.000	0.000	0.000	0.002	0.001	0.000
0.9"Sh/7"min/350 RPM	0.000	0.003	0.001	0.001	0.001	0.002	0.000
0.7"Sh/4"min/450 RPM	0.004	0.000	0.000	0.000	0.000	0.000	0.002
0.7"Sh/4"min/350 RPM	0.001	0.006	0.005	0.005	0.005	0.004	0.004
0.7"Sh/7"min/450 RPM	0.000	0.001	0.000	0.000	0.002	0.000	0.000
0.7"Sh/7"min/350 RPM	0.000	0.001	0.000	0.000	0.003	0.000	0.002
0.5"Sh/4"min/450 RPM	0.001	0.001	0.002	0.002	0.002	0.002	0.000
0.5"Sh/4"min/350 RPM	0.002	0.004	0.001	0.000	0.002	0.000	0.001
0.5"Sh/7"min/450 RPM	0.001	0.002	0.003	0.001	0.000	0.000	0.000
0.5"Sh/7"min/350 RPM	0.000	0.000	0.001	0.001	0.001	0.000	0.001

Table 18: P-Values for the Retreating Versus Advancing Shoulders

Factor level combination	P1 Vs P2	P3 Vs P4	P5 Vs P6	P7 Vs P8	P9 Vs P10	P11 Vs P12	P13 Vs P14
0.9"Sh/4"min/450 RPM	0.000	0.001	0.000	0.001	0.000	0.000	0.000
0.9"Sh/4"min/350 RPM	0.002	0.001	0.000	0.005	0.002	0.000	0.002
0.9"Sh/7"min/450 RPM	0.000	0.000	0.001	0.000	0.000	0.000	0.000
0.9"Sh/7"min/350 RPM	0.000	0.001	0.001	0.001	0.001	0.000	0.001
0.7"Sh/4"min/450 RPM	0.000	0.001	0.000	0.000	0.000	0.000	0.000
0.7"Sh/4"min/350 RPM	0.002	0.000	0.001	0.002	0.001	0.000	0.001
0.7"Sh/7"min/450 RPM	0.000	0.000	0.000	0.000	0.000	0.000	0.002
0.7"Sh/7"min/350 RPM	0.001	0.002	0.000	0.000	0.000	0.000	0.000
0.5"Sh/4"min/450 RPM	0.002	0.004	0.001	0.001	0.001	0.000	0.001
0.5"Sh/4"min/350 RPM	0.002	0.000	0.000	0.000	0.000	0.000	0.006
0.5"Sh/7"min/450 RPM	0.001	0.000	0.000	0.000	0.000	0.000	0.000
0.5"Sh/7"min/350 RPM	0.000	0.001	0.000	0.000	0.000	0.000	0.000

Table 19: P-Values for the Retreating Versus Advancing Pin Temperatures

Factor level combination	S1 Vs S2	S3 Vs S4	S5 Vs S6	S7 Vs S8	S9 Vs S10	S11 Vs S12	S13 Vs S14
0.9"Sh/4"min/450 RPM	98	99	98	98	96	99	99
0.9"Sh/4"min/350 RPM	96	90	95	98	93	95	93
0.9"Sh/7"min/450 RPM	99	99	99	99	95	98	99
0.9"Sh/7"min/350 RPM	99	92	99	99	99	94	99
0.7"Sh/4"min/450 RPM	97	97	96	96	95	95	99
0.7"Sh/4"min/350 RPM	98	90	90	90	90	91	91
0.7"Sh/7"min/450 RPM	99	97	99	99	95	99	99
0.7"Sh/7"min/350 RPM	99	98	97	97	92	99	94
0.5"Sh/4"min/450 RPM	90	99	99	99	99	99	95
0.5"Sh/4"min/350 RPM	95	94	97	99	96	99	97
0.5"Sh/7"min/450 RPM	99	99	97	96	96	99	98
0.5"Sh/7"min/350 RPM	97	97	93	93	97	99	99

Table 20: Power of the Retreating Versus Advancing Shoulders Observation

Factor level combination	P1 Vs P2	P3 Vs P4	P5 Vs P6	P7 Vs P8	P9 Vs P10	P11 Vs P12	P13 Vs P14
0.9"Sh/4"min/450 RPM	99	98	99	98	99	99	99
0.9"Sh/4"min/350 RPM	95	96	90	96	90	94	95
0.9"Sh/7"min/450 RPM	99	99	96	99	99	99	99
0.9"Sh/7"min/350 RPM	99	97	97	97	96	99	97
0.7"Sh/4"min/450 RPM	94	90	98	98	99	99	97
0.7"Sh/4"min/350 RPM	99	99	98	96	98	99	98
0.7"Sh/7"min/450 RPM	99	99	99	99	99	99	95
0.7"Sh/7"min/350 RPM	97	95	99	99	99	99	99
0.5"Sh/4"min/450 RPM	99	98	99	99	99	99	99
0.5"Sh/4"min/350 RPM	99	99	99	99	99	99	90
0.5"Sh/7"min/450 RPM	99	99	99	99	99	99	99
0.5"Sh/7"min/350 RPM	98	99	99	99	99	99	99

Table 21: Power of the Retreating Versus Advancing Pin Temperature observations

Shoulder Experiment

A second, smaller experiment was conducted where the shoulder was varied incrementally from 0.5 to 1.0 inches at a constant speed and RPM to investigate the shoulder radius to pin radius ratio (R/r) as a thermal factor. Due to time and budget constraints, only two replicates were run for each factor level. This results in a confidence level of 30% for the results. Table 22 summarizes the advancing and retreating side temperatures for the shoulder and pin for all different parameters used in this experiment.

	Ad: Shoulder	Re: Shoulder	Ad: Pin	Re: Pin
1.0" Sh/4"min/400RPM	185.25	178.15	186.56	179.88
0.9" Sh/4"min/400RPM	176.10	169.64	176.17	168.42
0.8" Sh/4"min/400RPM	159.47	151.78	160.96	149.71
0.7" Sh/4"min/400RPM	143.63	135.43	145.18	135.30
0.6" Sh/4"min/400RPM	128.32	121.03	133.92	124.54
0.5" Sh/4"min/400RPM	121.85	116.29	126.75	118.66

Table 22: Raw experimental data: Average of peak temperatures of Entry 2,

Group 1, 2, 3, and 4; All temperatures are in Celsius.

Figure 45 shows the plot of the temperature behavior for various size shoulder diameters on the next page
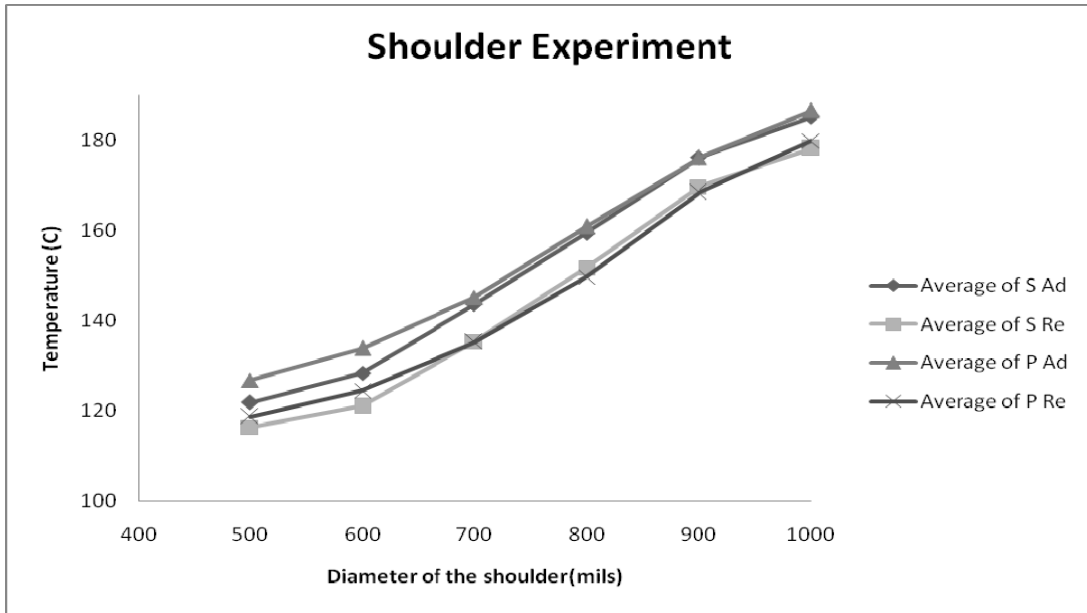
Figure 45: Average of the calculated peak temperatures of the shoulder experiment

Aluminum Copper Experiment

The main objective of this experiment is to study the behavior of the temperature field when two dissimilar metals are welded together, with common tool geometry, common traverse and RPM.

For this experiment, the shoulder stock was selected to be copper 10101 and the pin stock was selected to be aluminum 6061-T6. Tool shoulder diameter was 0.5 inches. Tool pin diameter was 0.3 inches Tool pin height was 0.3 inches. RPM was chosen to be 500 with a traverse rate of 1 inch/min. Five runs were conducted. The complete data set is provided in Appendix F. Average values are depicted in Table 23 below. Figure 46 shows the difference in temperature between copper and aluminum at different points.

Parameter	Sh: Material	Ad: Shoulder	Re: Shoulder	Ad: Pin	Re:Pin
0.5"Sh/1"min/500RPM	Copper	235.67	224.63	231.71	205.35
0.5"Sh/1"min/500RPM	Aluminum	211.11	204.18	209.35	187.24

Table 23: Raw experimental data: Average of peak temperatures of Entry 2, Group 1, 2, 3, and 4; All temperatures are in Celsius.
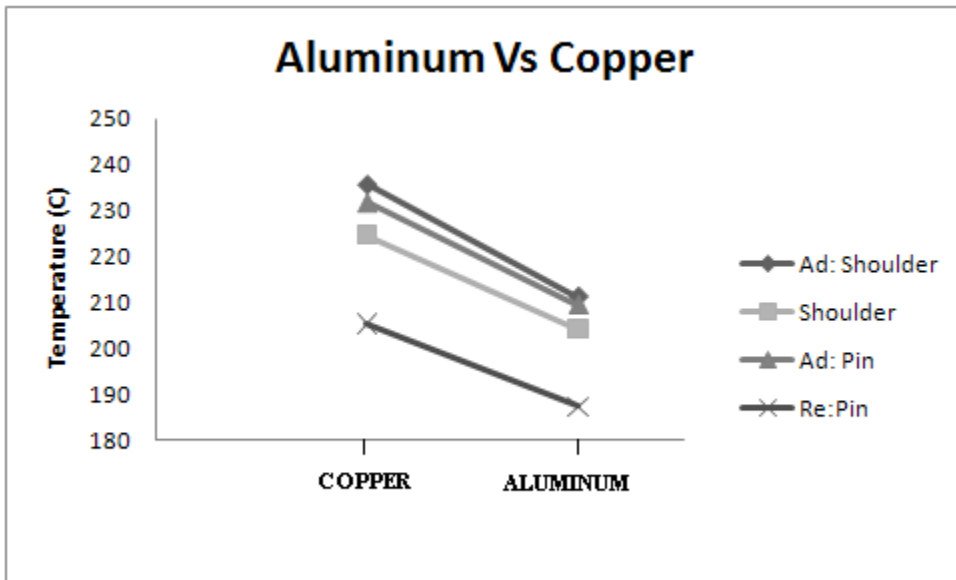
Figure 46: Shoulder and pin temperature of copper and aluminum

IX. SIMULATION OF AN ASYMETRIC THERMAL MODEL

The physical results of Chapter 8 clearly documents that the advancing side will always be the hotter side. Only one model in the literature predicts the asymmetrical thermal field around the tool (Payton [36]). This chapter documents an attempt to simulate the physical results obtained with a readily available, inexpensive finite element modeling software (COMSOL) using the metal cutting model first proposed by Payton [36].

Historically, simulation meant the modeling of one physical phenomenon at a time, such as structural integrity, electromagnetic compatibility or aerodynamic behavior. In reality, though, a component's behavior can depend on a number of physical phenomena combined with each other. Today, thanks to the increasing computer power available for engineers and scientists, simulating multiphysics phenomena is easy, accessible, and affordable using personal computer software such as COMSOL (formerly FEMLAB). COMSOL is based upon the widely available MATLAB family of computational products. It is not as powerful as traditional mainframe simulation software (ANSYS, NASTRAN, LS-DYNA, DEFORM), but it is easily used and inexpensive. Complete screen shots of the software, including equation setups used in this simulation, are provided in Appendix F at the end of this dissertation.

Original Asymmetric Temperature Model of Friction Stir Welding

None of the earlier thermocouple measurements by researchers in the literature review observed a well behaved difference between the advancing and retreating sides. Perhaps as a consequence of this, only one of the researchers has modeled the FSW process as an asymmetric thermal process. Modelers need data in order to formulate realistic models. Simulators need large amounts of data in order to validate their simulations of the various models.

Only one model in the literature review predicted the asymmetric result observed during data collection above. Payton [36] equates the advancing side and retreating sides of FSW with what classical machining theory in general refers to as up milling and down milling. On the leading (up-milling side) side, as the tool enters the work, tool tip velocity (*V*) assumes a maximum value, which decreases as the tool progresses along the tool path. On the trailing side, velocity (*V*) has a minimum value when the tooth leaves the work and a somewhat higher value when the tool enters the work. The tool edge traces out a looped tracheiod path through the material. Incorporating the eccentric geometry and travel features of the tool, and generating the proper coefficients to use the data in ASM Handbook of Metals (9th Edition), Payton generated the following useful expressions for the FSW tool designer in aluminum alloy 6061-T6 which predict a hot advancing side and a colder retreating side using the following equations.

$$T = [16,148.58]HP_s\sqrt{\frac{V*t}{k*(pc)}} \qquad (31)$$

HP_s is the specific horsepower for the alloy or workpiece, k is the coefficient of thermal conductivity for the workpiece, (pc) is the volume specific heat of the work material, V is the cutting speed at the tip of the tool. This is a geometric consideration which varies between left and right side (equation 32).

91

$$V = 2\pi n \sqrt{(R \pm r)^2 \pm 2ry}$$ (32)

One must use a (+) sign in equation (2) for the up-milling side and a (-) sign for the down-milling side of the geometry. The variable t is the uncut chip thickness, generally given by the following equation:

$$t_{avg} = \frac{F_t * d}{R \cos^{-1}\left(1 - \dfrac{d}{R}\right) + \dfrac{F_t * n}{\pi * D} \sqrt{D * d - d^2}}$$ (33)

Where, R is the Radius of the cutting edge (specific to shoulder or pin in this application), d is the depth of the cut (specific to the design of tool), D is the diameter of the cutter, n is the number of teeth, and F_t is the feed per tooth. These equations predict the results of thermocouple measurements in the laboratory to date very exactly, since the velocity term V captures the difference between the advancing and retreating sides. The availability of a large amount of data over different machining values and modern multiphysics based finite element analysis using equations 31 through 33 predict simulate the results accurately. Table 24 summarizes the material and machining parameters associated with equations 31 through 33. English units are used throughout because of the predominance of those units in the applicable literature sources on milling and metal cutting.

Symbol	Nomenclature	Unit
HP_s	Specific horse power	hp/in^3/min
k	thermal conductivity of W/P	BTU/ft.h.F
pc	Volume specific heat of W/P	BTU/lb.F
R	Radius of shoulder	inch
D	Diameter of shoulder	inch
t	Average chip thickness	inch
Ft	Feed per tooth for shoulder	inch
y	depth of cut	inch
n	RPM	RPM
r	Radius of pin	inch
V	Cutting speed	inch/sec

Table 24: Material and machining variables used in equations (1) through (3).

Modification to the Model

In equation (31), the constant 16,148.58, was derived by Payton for specific alloys in use at Marshall Space Flight Center where his research was conducted. It is necessary to adjust this for the current instrument. As Chao points out [9], the maximum temperature increases with decreasing feed rate, the constant used is replaced by a variable that best matches the recorded temperature within the instrument. In order to find the variable, two data runs were conducted to determine the endpoints. Table 25 summarizes the parameters and results.

Parameter	Recorded Temperature, C Advancing side
900 shoulder/4"min/450 RPM	378
900 shoulder/7"min/450 RPM	330

Table 25: Recorded temperatures to find the variable in heat equation

The variable must meet three conditions:

   Condition 1: Temperature decreases with increasing Traverse speed.

   Condition 2: At 4 IPM traverse, 450 RPM, a 0.9 inch shoulder produces 378 C.

   Condition 3: At IPM traverse, 450 RPM, a 0.9 inch shoulder produces 330 C.

In equation (31), let's take the constant as "X".

$$T = [X]HP_S\sqrt{\frac{V*t}{k*(pc)}} \tag{36}$$

From the data obtained, feed rate (F_d) is inversely proportional to the Temperature.

Therefore,

$$X \infty \frac{1}{F_d} \tag{35}$$

$$X = \frac{a}{F_d} + b \tag{36}$$

For parameter 1: 4"min/450 RPM/ 900 shoulder

$$T = [\frac{a}{F_d} + b]HP_S\sqrt{\frac{V*t}{k*(pc)}}$$

$$378 = [\frac{a}{F_d} + b]HP_S\sqrt{\frac{V*t}{k*(pc)}} \tag{37}$$

Where, $F_d = 4$

For parameter 2: 7"min/450 RPM/ 900 shoulder

$$T = [\frac{a}{F_d} + b]HP_S\sqrt{\frac{V*t}{k*(pc)}}$$

$$330 = [\frac{a}{F_d} + b]HP_S\sqrt{\frac{V*t}{k*(pc)}} \tag{38}$$

Where, $F_d = 7$

94

Solving equations (37) and (40),

a = 170000; b = 10000

Substituting a and b in equation in the heat equation,

$$T = [\frac{170000}{F_d} + 10000]HP_S \sqrt{\frac{V*t}{k*(pc)}}$$ (39)

Equation (39) was used in the simulation for both shoulder heat and pin heat. Height of the pin is not considered for the heat generated by the pin.

PHYSICS BASED SIMULATION

Equation 39 provides the heat input at both the pin and shoulder surfaces.
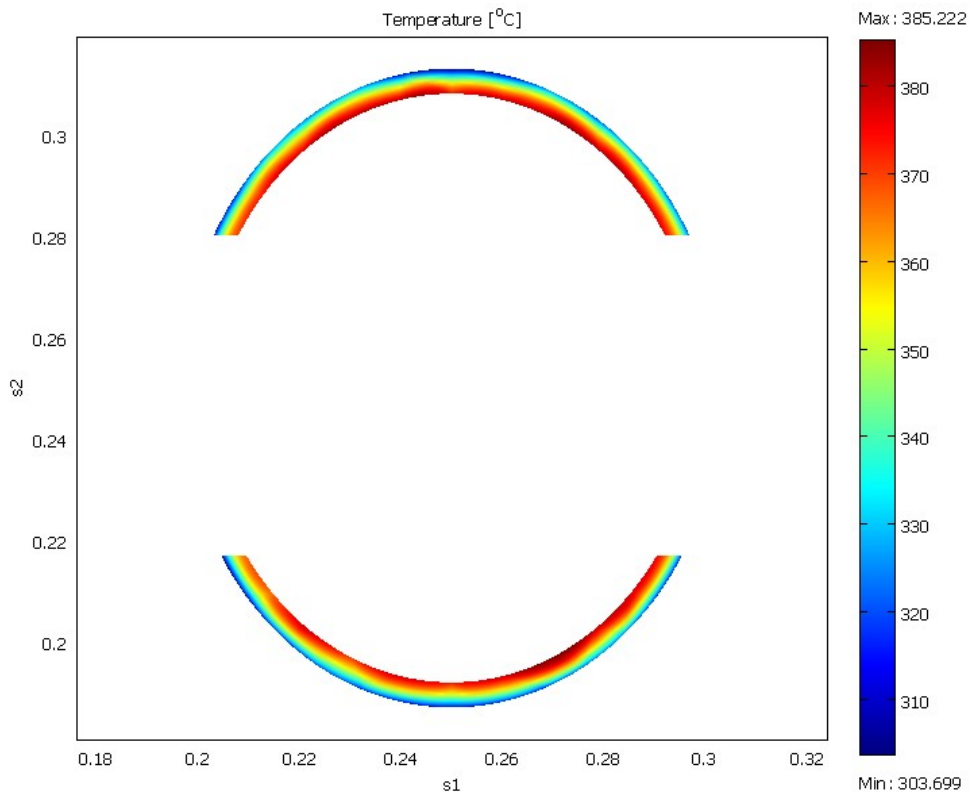
Figure 47: Advancing (top) and retreading (bottom) outer edge of the shoulder. Simulated advancing (385 C) and retreating (381 C) temperatures for 0.9" shoulder at 450 RPM and 4 ipm.

As Song summarizes in his paper [11], most simulation efforts only attempt to model the heat input from the tool shoulder, which is a very great simplification.   Modern physics based software allows the application of physics based expressions such as equations 41 directly to the contact surfaces of the pin and tool.   This model worked well for temperatures under the shoulder at the shoulder thermocouple. For example, at thermocouples S7 and S8, the agreement was almost within the overall error of the instrument (+/- 5.0 degrees).   It did not work well for the pin tool though since COMSOL does not allow the modeler to include combined thermal effects from the shoulder (above) and the pin (below and to the side).   Actual temperatures are a combined result of those two heat sources. Also, increasing the MESH density might improve the results below.

RPM 450, 4 IPM, 0.9 inch	Simulated	Actual
Shoulder Advancing	183.2 Celsius	188.2 Celsius
Shoulder Retreating	169.3 Celsius	174.1 Celsius

Table 26: Comparison of simulated results to actual results AT THE THERMAL WELL.

Meshing Conditions:

The following meshing conditions are for the model with 0.9 inch shoulder, 450 RPM with 4"/min traverse.

Meshing Conditions	# of elements	Peak Temperature (Celsius)
Coarser	11351	390.85
Coarse	17281	387.85
Normal	31525	385.85
Fine	49215	380.85

Table 27: Number of elements generated for default meshing conditions.

The above table shows the number of elements produced for four different meshing conditions.

The table also includes the peak temperature obtained when each condition was used in the FEA tool. It was noted that there was no big difference between the last 3 meshing conditions, "Course", "Normal" and "Fine".
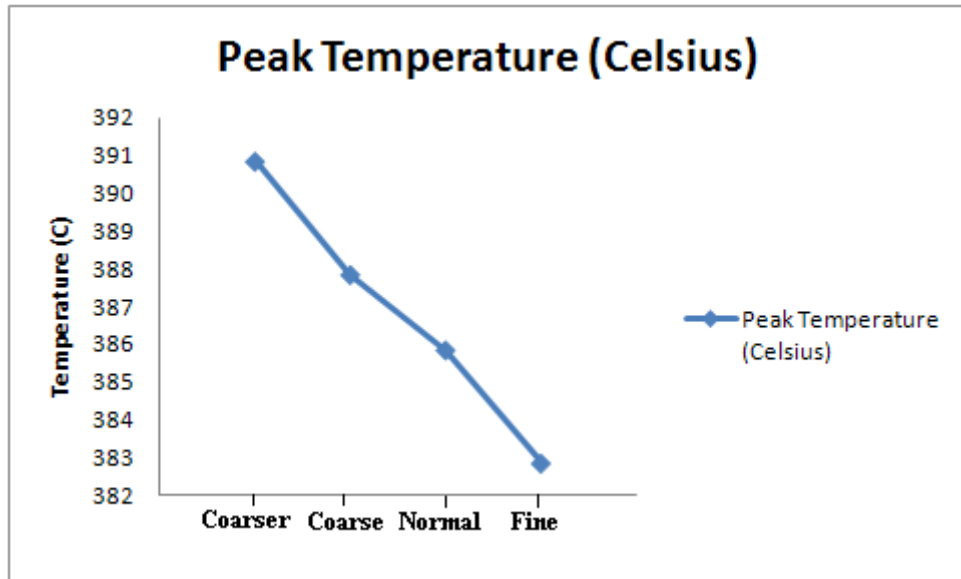
Figure 48: Peak temperature Vs number of elements in meshing.

The graph above shows the peak temperature obtained for different 'number of elements' generated during meshing process. For this model, NORMAL meshing was used and the statistics of the meshing option is given below.

Actual Meshing Values:

A default meshing condition was used for the simulation. NORMAL mesh was used in the model which has 31525 elements. The elements are of tetra, hexahedral and prismatic shapes. Number of degrees of freedom was 45894. There were total of 6240 mesh points and 9477 boundary elements. Increasing the mesh to "FINE" would have improved the computational values of Table 27.

Table 28 gives the simulated temperature at the point where the thermocouples were placed for the experiment and table 29 gives the actual temperature recorded at Group 2 (S7, S8, P7 and P8) thermocouples.

Factor level combination	Simulation at thermocouple			
	Ad: Sh	Re: Sh	Ad: Pin	Re: Pin
0.9"Sh/4"min/450 RPM	183.2	169.3	102.4	101.0
0.9"Sh/4"min/350 RPM	167.5	160.3	96.7	93.4
0.9"Sh/7"min/450 RPM	125.8	118.9	65.3	60.2
0.9"Sh/7"min/350 RPM	118.6	111.1	57.8	52.3
0.7"Sh/4"min/450 RPM	166.3	156.4	95.5	90.2
0.7"Sh/4"min/350 RPM	143.0	131.2	72.3	64.3
0.7"Sh/7"min/450 RPM	128.5	120.9	67.4	62.9
0.7"Sh/7"min/350 RPM	117.8	105.2	55.3	51.1
0.5"Sh/4"min/450 RPM	128.0	115.1	67.7	59.0
0.5"Sh/4"min/350 RPM	105.0	95.1	48.3	46.2
0.5"Sh/7"min/450 RPM	109.7	103.0	49.6	48.2
0.5"Sh/7"min/350 RPM	78.6	69.2	48.3	47.0

Table 28: Simulated thermocouple temperature in Celsius

Direct temperature at thermocouple: Group 2				
Factor level Combination	Ad: Sh	Re: Sh	Ad: Pin	Re: Pin
0.9"/4"min/450 RPM	188.2	174.1	186.4	176.0
0.9"/4"min/350 RPM	178.3	161.8	182.5	168.9
0.9"/7"min/450 RPM	144.3	133.8	143.6	133.4
0.9"/7"min/350 RPM	144.2	130.7	143.1	133.4
0.7"/4"min/450 RPM	160.8	146.0	163.2	147.9
0.7"/4"min/350 RPM	156.6	144.7	157.7	141.8
0.7"/7"min/450 RPM	141.0	132.0	140.5	132.8
0.7"/7"min/350 RPM	138.3	128.6	137.8	127.8
0.5"/4"min/450 RPM	145.6	127.2	153.0	138.7
0.5"/4"min/350 RPM	134.6	121.1	135.3	123.0
0.5"/7"min/450 RPM	136.6	125.9	140.5	129.0
0.5"/7"min/350 RPM	108.8	95.1	110.6	96.5

Table 29: Direct Temperature at Group 2 thermocouples in Celsius

Table 30 gives the temperature calculated manually using the Payton's equation. The values represent the temperature at the tool-workpiece interface. Table 31 gives the simulated tool-workpiece interface temperature.

Factor level combination	Ad: Sh	Re: Sh	Ad: Pin	Re: Pin
0.9"Sh/4"min/450 RPM	382.49	381.17	194.21	191.44
0.9"Sh/4"min/350 RPM	359.59	358.35	169.18	166.74
0.9"Sh/7"min/450 RPM	308.53	306.65	166.19	161.99
0.9"Sh/7"min/350 RPM	287.45	285.7	144.46	140.77
0.7"Sh/4"min/450 RPM	357.93	356.33	194.21	191.44
0.7"Sh/4"min/350 RPM	336.45	334.93	169.18	166.74
0.7"Sh/7"min/450 RPM	307.11	304.68	166.19	161.99
0.7"Sh/7"min/350 RPM	288.53	286.24	144.46	140.77
0.5"Sh/4"min/450 RPM	307.6	305.61	194.21	191.44
0.5"Sh/4"min/350 RPM	286.59	284.73	169.18	166.74
0.5"Sh/7"min/450 RPM	280.68	277.5	166.19	161.99
0.5"Sh/7"min/350 RPM	263.62	260.61	144.46	140.77

Table 30: Temperature calculated using Payton's equation (in Celsius).

Factor level combination	Ad: Sh	Re: Sh	Ad:Pin	Re: Pin
0.9"Sh/4"min/450 RPM	385.16	381.13	320.79	315.76
0.9"Sh/4"min/350 RPM	355.72	352.15	301.97	298.4
0.9"Sh/7"min/450 RPM	305.22	302.57	252.39	249.74
0.9"Sh/7"min/350 RPM	284.35	282.55	231.33	229.53
0.7"Sh/4"min/450 RPM	353.33	349.28	294.52	290.47
0.7"Sh/4"min/350 RPM	333.68	330.53	279.89	276.73
0.7"Sh/7"min/450 RPM	305.08	302.79	250.36	248.08
0.7"Sh/7"min/350 RPM	285.44	282.03	228.02	224.6
0.5"Sh/4"min/450 RPM	304.37	301.31	247.93	244.86
0.5"Sh/4"min/350 RPM	282.85	280.27	229.74	227.16
0.5"Sh/7"min/450 RPM	276.85	272.99	223.56	219.7
0.5"Sh/7"min/350 RPM	260.41	257.32	203.87	200.77

Table 31: Simulated temperature at tool-workpiece interface (in Celsius)

X. DISCUSSION

The apparatus had seven (7) sets of thermocouples.   Paired shoulder and pin thermocouples captured the advancing and retreating temperatures of the shoulder and the pin. A fifth thermocouple in each set captured the temperature at the bottom of the pin. The first set captured the temperature during the entry of the tool and the last set captured the temperature during the exit of the tool. The middle sets captured the temperature during the transient action of the tool. Figure 49 shows the temperature distribution during the process.
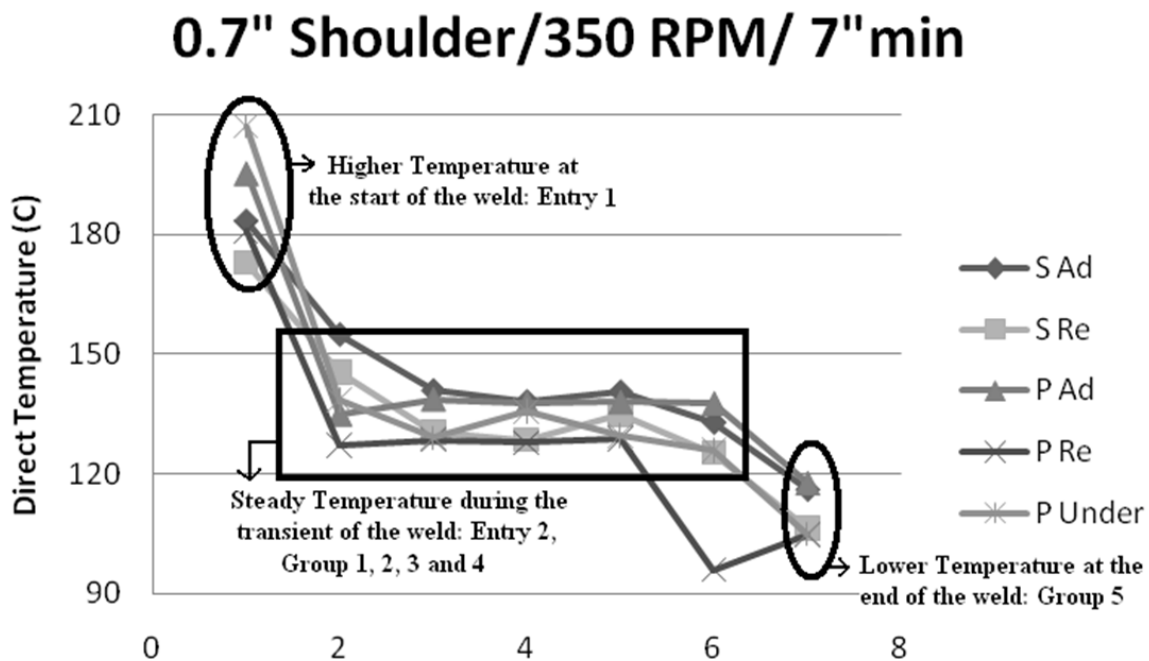
Figure 49: Temperature distribution during the process

It is to be noted that in all the experiments and for all the factor level combinations, the entry set was hotter than any other set and the exit set was cooler than any other set. The highest temperature in the process is obtained when the tool moves in to the work piece. This is the

result of the drilling action of the pin and the shoulder in the work piece at the same position; i.e. the dwell of the tool over the entry point allows the heat to build underneath the rotating tool during entry.

Thermal field mapping was done for the process. The thermocouples used, captured the temperature of the advancing shoulder, retreating shoulder, advancing pin, retreating pin and under the pin. The temperatures recorded were the temperature of the steel holder at fixed points away from the "ideal geometrical points". One dimensional steady state thermodynamic equations were used to find the temperature at the tool tip. These equations do not consider the heat dissipated in the second or the third dimensions. But in real process, heat is lost to the atmosphere, the metal holder and base plate. The calculated temperature does give an approximate value at the tool shoulder tip, the pin radius and the area immediately under the pin.

The temperatures recorded in all the experiments and the statistical test done to compare the difference in the peak temperatures of the advancing and the retreating sides of each pair of thermocouples (S1&S2, S3&S4…..) conclusively demonstrates that the advancing temperature is clearly higher than the retreating temperature. For all the advancing-retreating pairs, the test results document that the advancing side was always hotter than the retreating with a statistical power of at least 90% for all the thermocouple pairs.

From the temperature plots that were obtained for different factor level combinations, it is very clear that the temperature is higher at the entry point because of the temperature dwell. The temperature then stabilizes as the shoulder is fully in contact with the workpiece and stays the same through out the process till the exit set. The last set called the exit set sees a decrease in the temperature. This is because of the tool getting out of the workpiece above that set without the shoulder traversing through it completely. The back half of the tool never transits over the

thermocouple set, therefore the peak temperature never occurs.   Future designs should pass at least two diameters of the maximum shoulder beyond the last thermocouple set.
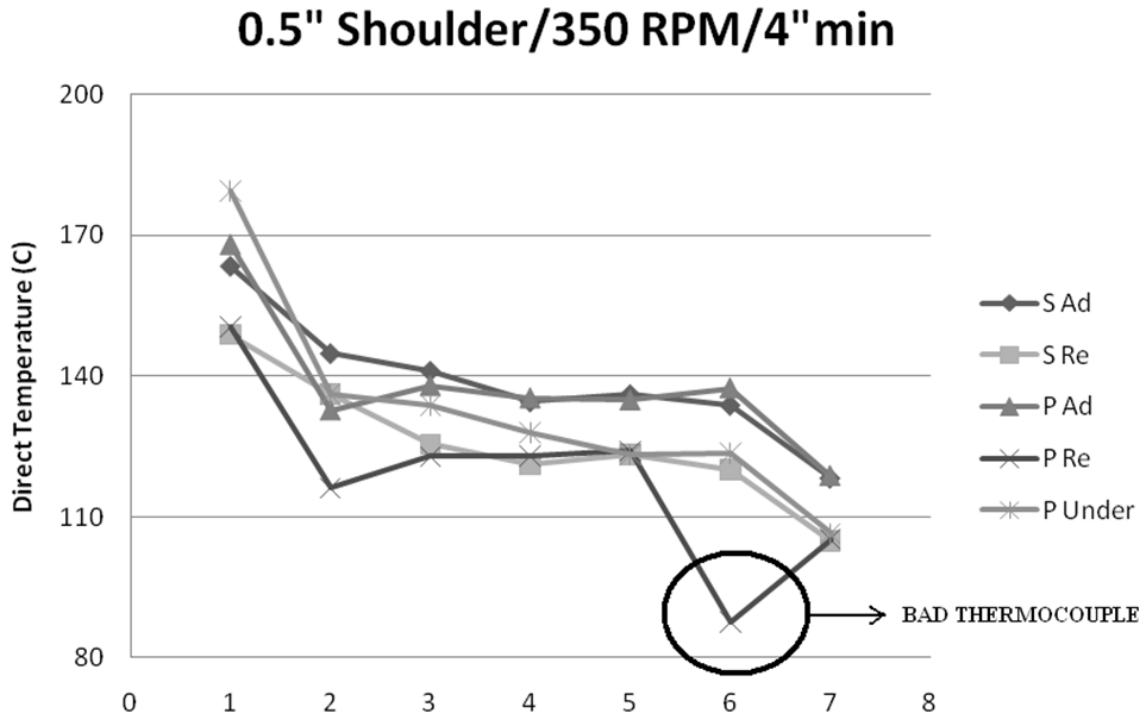
Figure 50: Bad Thermocouple in the experiment.

In most of the factor level combination, the plot having the average of the peak temperatures of the thermocouple clearly shows that the Group 4 retreating pin thermocouple (P11) temperature is always lower than the others (as in Figure 50).   This difference was not immediately apparent to the author until analysis was in progress.   Data collection happens quickly with this instrument, even when doing 84 weld runs.

For the temperatures recorded, analysis of variance was done to check the most influential factor on the responses for different factor level combinations. For any factor level combination, the size of the shoulder had the largest impact on the entry thermocouples (S1, S2, P1, P2 and U1). All other thermocouples sets are most affected by the traverse speed. This indicates that more than the size of the shoulder, the traverse speed of the tool plays a vital role in the

$$T = [X]HP_s\sqrt{\frac{V*t}{k*(pc)}}$$ recrystallization of the metal.   One interesting finding in this analysis is

that the RPM does not have as large a statistical effect comparatively, on any of the

thermocouple.   The results also indicate that the shoulder size and the RPM are directly

proportional to the temperature. As the shoulder size and the RPM goes up, the temperature of

the work piece goes up. But, the traverse speed is inversely proportional to the temperature of

the work piece. As the traverse speed goes up, the temperature goes down.   This is consistent

with Choe's observations [9], [22] and [23].

In the literature, there is no model which reflects two important facts of the process as

documented in these thermal data runs. One is the asymmetry of the temperature field and the

other is the inverse proportionality of the traverse speed. No heat equation is modeled to adapt

these two conditions of the process.   A new model based on Payton's metal cutting model was

presented and simulated here with good results.   These results might be in even better

agreement with more powerful computers or finite element modeling software.

The shoulder experiment conducted had expected results.   The temperature of any

thermocouple increased with the increasing shoulder size of the tool.   The graph plotted was

more or less linear, steadily increasing with increasing tool size. Earlier, from the analysis of the

variance of the experiments, we concluded that traverse speed had more effect on the

thermocouples than the shoulder except at the entry set of thermocouples. Since increasing the

shoulder size of the tool increases the temperature of the workpiece more or less linearly, the

author expects the temperature to increase more steadily and linearly with increasing traverse

speed. Figure 51 demonstrates an interesting observation from the data.   The peak temperature

at a thermocouple is not obtained when the tool is exactly on top of it.
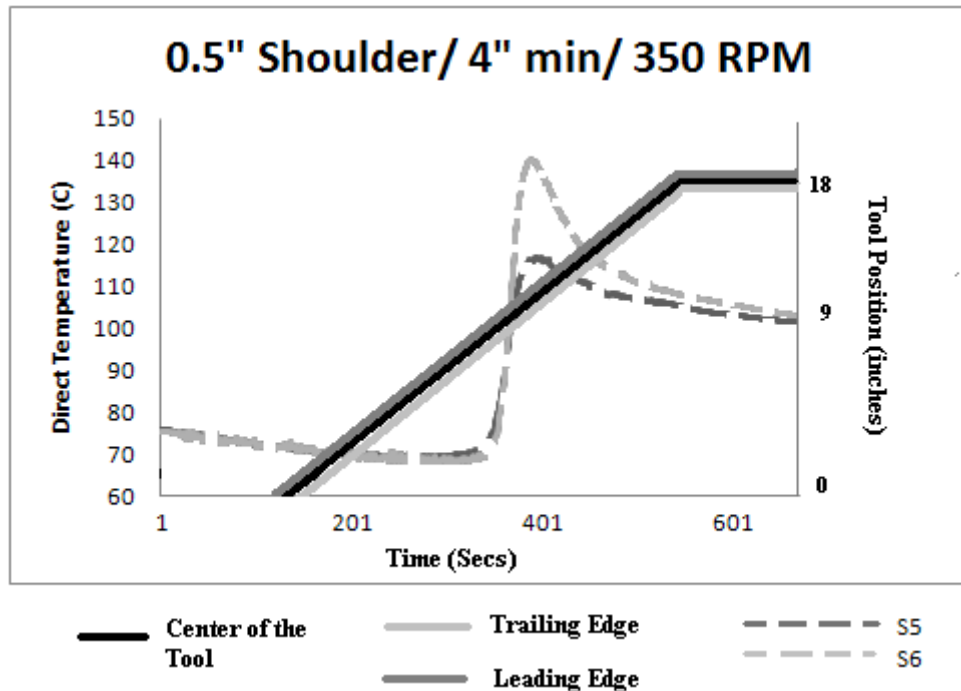
Figure 51: Shoulder temperature with respect to the position of the tool.

Figure 51 shows the temperatures of S5 and S6 thermocouples from the start to the end of the experiment. It is very clear that the peak temperature is obtained only after a certain period after the tool (trailing end of the tool) has gone past the thermocouples. To be specific, the peak temperature is obtained only 18 seconds after the trailing edge of the tool has gone past the thermocouples for the factor level combination involved.

The heat equation used in the model gives the temperature of the advancing shoulder, retreating shoulder, advancing pin and retreating pin. The temperature of the advancing and retreating shoulder, more or less matches with the thermodynamically calculated values. The temperature of the advancing and retreating pin is much less than the thermodynamically calculated temperatures. When simulated using Multiphysics software, the shoulder temperatures were not exactly equal to the calculated temperatures but close to it. The reason for the temperature of the pin when calculated from the heat equation being much less than the

104

simulated or thermodynamically calculated temperature is that the heat equation does not consider the effect of shoulder for pin temperature. It is possible also that instead of a milling equation, an extrusion equation should be utilized in the area of flow around the pin, or perhaps a combination of equations as Choe attempted to do [9], [22] and [23].

<u>Parameterization using tool geometry and material properties</u>

The thermal model described within this paper incorporates the material properties of the alloys being welded and tool designs geometric properties and path. Although the major experiment conducted by Kandaswaamy [37] utilized the very well known results for aluminum alloy 6061-T6 extensively, the researcher validated the sensitivity of the instrument to both material and tool changes using copper alloys and aluminum together along with various tool geometries, RPM's and feed rates across the welds.

The model and simulation capture the "dwell" of the tool's motion as it passes through the material since the shoulder dominates the final passage over the welded junction. It correctly captures the transitions during insertion and initial shoulder contact. Most importantly, the asymmetrical thermal difference on the two sides of the tool, and the variation of the temperature from the shoulder down along the pin are accurately predicted by the simulation of this model presented.

A model such as this lets the operator chose from the classic milling conventions (feed per tooth, RPM, velocity) in order to "target" a sweet spot or temperature range within the alloy of concern. Although the data collected during the initial experiments involved the simple geometry of a "straight" pin with no shoulder ridges or flutes, it is only a straightforward application of conventional milling theory to incorporate the cooling effects of flutes and scrolls in the design of the tool.

XI. CONCLUSIONS

A detailed review was conducted on the previous thermal measurements and thermal models by various researchers. An instrument that measures the temperature of the work piece around the tool was designed and built. A full factorial, detailed observation of the thermal fields was made with the apparatus with the following results:

- The highest temperatures of the friction stir welding process occur during the relatively long insertion into the specimen. Once the transit starts, temperatures fall and reach as lower steady state transient temperature. For aluminum 6061-T6, this occurs within 2 diameters of the tool shoulder (on average).

- The advancing side of the tool is always hotter than the retreating side of the tool, with a statistical power of at least 90% for all the experiments and factor level combinations done.

- The temperature always peaks following passage of the trailing edge of the shoulder. This is an important consideration in applications where a run out tab is not used. The weld properties at the extraction point may be very different because of the lower temperatures at that point.

- The pin, well away from the shoulder, often exceeds the maximum temperature at the shoulder, suggesting that extrusion around the pin has a much greater heating effect than the rotation or radius of the shoulder.

- The rate of traverse dominated temperature responses by a large statistical margin. Shoulder diameter was an important, but not close, second in most cases. RPM, to the surprise of the investigator, was a very distant third.

- Temperature rose linearly as RPM and shoulder diameter increased.

- Temperature decreased inversely as the traverse speed increased.

- Temperature changed with material being welded, all other things constant.

- An extensive body of thermal data is now available upon request. All thermal data is available from the principal advisor to modelers and simulators, along with exact geometry of the holder and material properties.

- An instrument exists which can rapidly collect more data using standard commercially available geometries. An upgrade to the instrument is planned when access to a 5 axis CNC mill is possible.

- Payton's model, being the only model in the literature which describes the asymmetric nature of the temperature field, was used to simulate the process using a multi physics finite element analysis tool. The results obtained were compared to the real world data for the shoulder with excellent results. Software limitations precluded a good simulation of the pin tool area.

- Classic metal cutting theory from the 1950s and 1960s has been successfully applied to a joining process. This suggests that classic extrusion theory and software such as DEFORM 3D might also be very beneficially applied to Friction Stir Welding.

REFERENCES

1. Lee, W.B., Y.M. Yeon, and S.B. Jung, *Evaluation of the microstructure and mechanical properties of friction stir welded 6005 aluminum alloy.* Materials Science and Technology, 2003. **19**(11): p. 1513-1518.

2. Murr, L.E., et al., *Friction-stir welding: Microstructural characterization.* Materials Research Innovations, 1998. **1**(4): p. 211-223.

3. Jata, K.V. and S.L. Semiatin, *Continuous dynamic recrystallization during friction stir welding of high strength aluminum alloys.* Scripta Materialia, 2000. **43**(8): p. 743-749.

4. Murr, L.E., G. Liu, and J.C. McClure, *Dynamic recrystallization in friction-stir welding of aluminium alloy 1100.* Journal of Materials Science Letters, 1997. **16**(22): p. 1801-1803.

5. Murr, L.E., et al., *Intercalation vortices and related microstructural features in the friction-stir welding of dissimilar metals.* Materials Research Innovations, 1998. **2**(3): p. 150-163.

6. James, M.N., et al., *The relationship between process mechanisms and crack paths in friction stir welded 5083-H321 and 5383-H321 aluminium alloys.* Fatigue & Fracture of Engineering Materials & Structures, 2005. **28**(1-2): p. 245-256.

7. Tang, W., et al., *Heat input and temperature distribution in friction stir welding.* Journal of Materials Processing & Manufacturing Science, 1999. **7**(2): p. 163-172.

8.   Chen, C.M. and R. Kovacevic, *Finite element modeling of friction stir welding - thermal and thermomechanical analysis.* International Journal of Machine Tools & Manufacture, 2003. **43**(13): p. 1319-1326.

9.   Chao, Y.J., X. Qi, and W. Tang, *Heat transfer in friction stir welding - Experimental and numerical studies.* Journal of Manufacturing Science and Engineering-Transactions of the Asme, 2003. **125**(1): p. 138-145.

10.   Khandkar, M.Z.H., J.A. Khan, and A.P. Reynolds, *Prediction of temperature distribution and thermal history during friction stir welding: input torque based model.* Science and Technology of Welding and Joining, 2003. **8**(3): p. 165-174.

11.   Song, M. and R. Kovacevic, *Thermal modeling of friction stir welding in a moving coordinate system and its validation.* International Journal of Machine Tools & Manufacture, 2003. **43**(6): p. 605-615.

12.   McClure, J.C., et al. ***A thermal model of friction stir welding*** in *Trends in Welding Research, Proceedings, 5th International Conference* 1998. Pine Mountain, GA; USA

13.   Dong, P., et al., *Coupled thermomechanical analysis of friction stir welding process using simplified models.* Science and Technology of Welding and Joining, 2001. **6**(5): p. 281-287.

14.   Khandkar, M.Z.H. and J.A. Khan, *Thermal modeling of overlap Friction Stir Welding for Al-alloys.* Journal of Materials Processing & Manufacturing Science, 2001. **10**(2): p. 91-105.

15.   Lienert, T.J., W.L. Stellwag, and L.R. Lehman. *Heat Inputs, Peak Temperatures, and Process Efficiencies for FSW.* in *4th International Friction Stir Welding Symposium.* 2003. Park City, Utah: TWI.

16.   Lambrakos, S.G., et al., *Analysis of friction stir welds using thermocouple measurements.* Science and Technology of Welding and Joining, 2003. **8**(5): p. 385-390.

17.   Xu, J., et al. *Experimental and Numerical Study of Thermal Process in Friction Stir Welding.* in *Joining of Advanced and Specialty Materials VI.* 2003. Pittsburg, Pa: ASM International.

18.   Ulysse, P., *Three-dimensional modeling of the friction stir-welding process.* International Journal of Machine Tools & Manufacture, 2002. **42**(14): p. 1549-1557.

19.   Chang, W.S., et al., *Joint properties and thermal behaviors of friction stir welded age hardenable 6061Al alloy*, in *Thermec'2003, Pts 1-5.* 2003, TRANS TECH PUBLICATIONS LTD: Zurich-Uetikon. p. 2953-2958.

20.   Lawrjaniec, D., et al., *Numerical simulation of friction stir welding*, in *Thermec'2003, Pts 1-5.* 2003, TRANS TECH PUBLICATIONS LTD: Zurich-Uetikon. p. 2993-2998.

21.   Liu, S., Y.J. Chao, and C.H. Chien. *Study of thermal and heat transfer phenomenon in friction stir welding of aluminum alloy 6061-T6 thick plates* in *SAE 2004 World Congress and Exhibition.* 2004. Detroit, Michigan, USA Society of Automotive Engineers, Inc., Warrendale, Pennsylvania, USA.

22.   Chao, Y.J. and X.H. Qi, *Thermal and thermo-mechanical modeling of friction stir welding of aluminum alloy 6061-T6.* Journal of Materials Processing & Manufacturing Science, 1999. **7**(2): p. 215-233.

23.   Chao, Y.J. and X. Qi. *Heat Transfer and Thermo-Mechanical Analysis of Friction Stir Joining of AA6061-T6 Plates.* in *1st International Symposium on Friction Stir Welding.* 1999. Thousand Oaks, Ca: TWI.

24.   Schmidt, H., J. Hattel, and J. Wert, *An analytical model for the heat generation in friction stir welding.* Modelling and Simulation in Materials Science and Engineering, 2004. **12**(1): p. 143-157.

25.   Awang, M., et al. *Thermo-Mechanical Modelling of FrictionStir Spot Welding (FSSW) Process: Use of an Explicit Adaptive Meshing Scheme.* in *SAE World Congress.* 2005. Detroit, Michigan, USA: Society of Automotive Engineers, Inc., Warrendale, Pennsylvania, USA.

26.   Colegrove, P.A. and H.R. Shercliff, *Experimental and numerical analysis of aluminium alloy 7075-T7351 friction stir welds.* Science and Technology of Welding and Joining, 2003. **8**(5): p. 360-368.

27.   Tay, A.O, "*A Numerical Study of the Temperature distribution generated during Orthogonal Machining*", Thesis, University of New South Wales.

28.   Klamecki, B.E, "Incipient Chip Formation in Metal Cutting – A 3D Finite Element Analysis", Thesis, University of Illinois.

29.   Stevenson, M.G, Wright P.K and Chow J.C, "Further Developments in Applying the FEM to the calculation of Temperature Distributions in Machining and Camparisons with Experiment", Journal of Engineering for Industry , Trans. ASME, pp. 149-154.

30.   Abdel-Hamid, "*A three dimensional finite element thermo-mechanical analysis of intermittent cutting process*", Dept of Mechanical Design and Production, Cairo University.

31.   Shore, H, *Tool and chip temperatures in Machine shop Practice*, M.S Dissertation, M.I.T

32.   Shaw, M.C, *Metal cutting Principles,* Oxford University Press, 594(1984).

33.   Herbert, E.G. (1926), *Proc. Instn mech. Engrs 1*, 289.

34.   Schwerd, F. (1937). *Z.des Ver. Deutsche Ing.* 77, 211.

35.   Martelloti, M.E, *An analysis of the Milling process, Part II-Down Milling*, Trans ASME, 233(1945).

36.   Payton, L.N, *Metal Cutting theory and Friction stir welding*, Industrial and systems Engineering, Auburn University.

37.   Payton, L.N, Thermal field mapping of Friction stir welding process, Mechanical Engineering, Auburn University.

APPENDICES

APPENDIX A

Direct Data: With 2 RPMs, 2 traverse speed and 3 shoulder diameters, there is a combination of 12 different parameters. For each parameter, 7 experiments were done to achieve at least a 90% statistical power that advancing was hotter than retreating side. The peak temperatures for all the 12 different parameters are given below.

Nomenclature: Each Thermocouple was represented by a unique alphabet and number:

S – Shoulder thermocouple. (Retreating side: S_1, $S_{3...}$ $S_{13;}$

Advancing side: S_2, $S_{4...}$ S_{14})

P – Pin thermocouple. (Retreating side: P_1, $P_{3...}$ $P_{13;}$ Retreating side: P_2, P_4... P_{14})

U – Under the pin thermocouple. (U_1, $U_{2...}$ U_7)

Factor level combination 1: 450 RPM / 7 inch per min traverse / 0.9 inch shoulder

Entry data:

| | Entry 1 | | Entry 2 | | Entry 1 | | Entry 2 | | Entry 1 | Entry 2 |
	S1	S2	S3	S4	P1	P2	P3	P4	U1	U2
RUN 1	177.5	189.01	146.8	150.1	191.3	197	123.2	124.5	203	139.2
RUN 2	176.5	180.38	156.3	165.6	188.5	189.4	130.2	136.6	208.8	147.9
RUN 3	191.6	198.02	146.2	153.9	207.7	216.3	136.7	140	221.2	140.8
RUN 4	181.4	193.49	146.2	155.2	195.7	208.8	135.6	140.9	207.6	147.1
RUN 5	183.2	186.77	144	157.5	191.7	195	131.3	145.6	210.9	153.6
RUN 6	182.1	184.16	147.8	155	199.2	203.3	127.7	133.1	212.3	142.3
RUN 7	189.4	193.29	150.5	157.8	198.4	205.1	132.2	134.7	217.8	136.7

(450 RPM / 7 inch per min traverse / 0.9 inch shoulder)

Traverse data:

	Group 1		Group 2		Group 3		Group 4	
	S5	S6	S7	S8	S9	S10	S11	S12
RUN 1	127	147	130.5	133.4	141	145	139	141
RUN 2	137.5	151.3	135.9	147.8	147	148	143	147
RUN 3	145.8	148.7	135	140.7	141	152	132	142
RUN 4	145	147.4	133.6	147.4	144	158	135	146
RUN 5	145.1	145.2	135	144.2	142	156	130	144
RUN 6	143.5	145	132.3	136.8	143	144	139	142
RUN 7	146.4	148.1	134.1	139.8	144	147	140	140

	Group 1		Group 2		Group 3		Group 4	
	P5	P6	P7	P8	P9	P10	P11	P12
RUN 1	131.2	143.7	127	139.9	136	136	98.6	142
RUN 2	143.2	148.4	141.4	146.3	140	144	102	150
RUN 3	142.2	153.5	128.8	141.8	137	148	79.1	143
RUN 4	141.2	144.5	133.1	144.8	138	141	82	141
RUN 5	148.4	152.3	144.6	150.1	136	150	88.1	154
RUN 6	140	141.6	132.9	140.6	139	140	100	146
RUN 7	145.1	146	136.2	141.7	141	142	101	147

	Group 1	Group 2	Group 3	Group 4
	U3	U4	U5	U6
RUN 1	136.1	132.4	126.9	132.1
RUN 2	140.6	142.7	130.3	134.8
RUN 3	133.1	145.1	132	132.9
RUN 4	131.7	141.6	135.4	134.8
RUN 5	139.8	149.7	124.5	141
RUN 6	131.7	137.4	128	133
RUN 7	134.9	140.1	136.3	134.3

(450 RPM / 7 inch per min traverse / 0.9 inch shoulder)

Exit data:

	Exit		Exit		Exit
	S13	S14	P13	P14	U7
RUN 1	110.6	121.6	118.5	121.1	104
RUN 2	117.1	128.9	126	133.6	108
RUN 3	100	117.7	97.81	131.3	104
RUN 4	117.4	119.1	86.5	132.6	105
RUN 5	118.8	112.1	105.4	128.8	119
RUN 6	109.1	115.2	112.9	117	106
RUN 7	112.7	127.4	119.9	125.4	110

(450 RPM / 7 inch per min traverse / 0.9 inch shoulder)

Factor level combination 2: 450 RPM / 4 inch per min traverse / 0.9 inch shoulder

Entry data

	Entry 1		Entry 2		Entry 1		Entry 2		Entry 1	Entry 2
	S1	S2	S3	S4	P1	P2	P3	P4	U1	U2
RUN 1	184.7	198.9	193.7	199.2	198	224	162	165	228.8	177.7
RUN 2	209.6	222.5	203.9	205.1	226	239	171	173	235.5	183
RUN 3	202.4	212.4	205.1	211.1	218	229	173	176	232.8	186.9
RUN 4	199	199.1	199.6	202.7	214	223	171	181	221.3	171.1
RUN 5	202.3	209.3	197.1	204.3	214	219	168	171	233.2	187.3
RUN 6	193.8	211.5	193.3	203.8	214	215	167	172	228.7	178.4
RUN 7	197.5	207	195.8	205.7	213	214	168	173	226.7	172.1

Traverse data:

	Group 1		Group 2		Group 3		Group 4	
	S5	S6	S7	S8	S9	S10	S11	S12
RUN 1	183.5	191.7	163.3	182	184	188	179	185
RUN 2	188.9	203.1	177.8	192.5	199	200	187	193
RUN 3	202.9	208.7	180.6	197.8	201	202	189	198
RUN 4	190.7	203.7	178.1	179.3	186	190	188	193
RUN 5	190	196.1	171.8	179.7	188	189	184	188
RUN 6	182.1	190.8	171.8	172.9	191	193	179	191
RUN 7	199.1	201.2	175.4	183.6	188	190	188	199

	Group 1		Group 2		Group 3		Group 4	
	P5	P6	P7	P8	P9	P10	P11	P12
RUN 1	180	188	175.4	181.2	177	180	125	193
RUN 2	188.4	199.3	187.4	197.1	193	193	132	204
RUN 3	192.3	204.7	189.9	200.3	193	195	132	206
RUN 4	180.3	199.4	178.1	186	181	193	124	197
RUN 5	187.3	192.2	175.4	183.7	181	183	129	190
RUN 6	180.5	188.1	170.1	186.5	185	186	127	196
RUN 7	180.4	192.9	175.5	189.8	180	193	123	196

(450 RPM / 4 inch per min traverse / 0.9 inch shoulder)

	Group 1	Group 2	Group 3	Group 4
	U3	U4	U5	U6
RUN 1	175.3	171.8	167.9	172.3
RUN 2	183.8	176.4	170.2	178.4
RUN 3	191.6	186.2	175.1	183.1
RUN 4	181.1	175.6	179.9	174.5
RUN 5	180.2	180.1	167.1	178.1
RUN 6	179.3	185.9	161.4	165.4
RUN 7	183	190	171.6	178

(450 RPM / 4 inch per min traverse / 0.9 inch shoulder)

Exit data:

	Exit		Exit		Exit
	S13	S14	P13	P14	U7
RUN 1	156	171.4	163.7	165.2	151
RUN 2	160.8	167.5	161.1	170.3	152
RUN 3	165.8	174.6	167.9	177	153
RUN 4	155.4	171.2	166.9	174.4	154
RUN 5	153.1	162.8	156.6	163.7	150
RUN 6	139.4	157.3	140.3	164.5	134
RUN 7	156.9	150	166.5	170.2	153

(450 RPM / 4 inch per min traverse / 0.9 inch shoulder)

Factor level combination 3: 350 RPM / 7 inch per min traverse / 0.9 inch shoulder

Entry data:

	Entry 1		Entry 2		Entry 1		Entry 2		Entry 1
	S1	S2	S3	S4	P1	P2	P3	P4	U1
RUN 1	189.6	191.6	130.5	140.5	177.5	201.7	128.1	140.5	215.1
RUN 2	185.7	192	142.6	154.8	174.8	202.7	118.2	126.5	215.7
RUN 3	197.3	199.5	141.5	152.5	48.05	207.5	125.9	130.3	222.3
RUN 4	196.3	200.4	148.3	161.2	189	214.9	128.1	136.6	217.5
RUN 5	186.1	193.8	138	144	40.49	198.6	117.9	120.3	216.8
RUN 6	196.5	198.6	152	162.6	203.9	211.9	135.2	141.1	224
RUN 7	188.5	196.7	154.6	163.2	203.8	207.3	136.4	141.2	220.8

Traverse data:

	Group 1		Group 2		Group 3		Group 4	
	S5	S6	S7	S8	S9	S10	S11	S12
RUN 1	145.6	146.3	135.5	144.2	136.2	141.8	136.9	141.8
RUN 2	128.5	140.8	130.1	139.1	137.8	139.7	135.8	136
RUN 3	139.4	147.1	130.1	137	136.6	145.2	131.6	135
RUN 4	141.9	148	130	137.3	140.6	144.8	131.5	134.5
RUN 5	128.5	130.5	117.2	123.9	127	130.7	121.6	123.3
RUN 6	146.6	147.4	137.3	142.9	144.9	149.3	137.9	144.8
RUN 7	147.7	147.9	135.1	145.3	143.4	149.5	137.7	138.3

	Group 1		Group 2		Group 3		Group 4	
	P5	P6	P7	P8	P9	P10	P11	P12
RUN 1	134	145.5	133.8	148	130.9	135.9	97.73	112.9
RUN 2	131.6	137.8	132.1	137.1	129.9	132.4	96.01	137.7
RUN 3	137.1	138.7	134.4	136.2	131.4	139.5	98.37	135.5
RUN 4	137.8	139.6	133.7	135.9	132.2	139.3	97.53	136
RUN 5	124	126.8	119.4	124.2	121.4	124.1	88.41	127.5
RUN 6	143.5	145	139	145.1	142.7	143.9	101.4	150
RUN 7	145.4	147.6	141.5	145.1	140.4	145.1	100.7	144.2

(350 RPM / 7 inch per min traverse / 0.9 inch shoulder)

	Group 1	Group 2	Group 3	Group 4
	U3	U4	U5	U6
RUN 1	133.2	142.7	121.4	124.9
RUN 2	135.5	134.8	124.3	128.2
RUN 3	126.5	142.1	132.5	125.7
RUN 4	124.4	138.2	126	115.4
RUN 5	111.3	126.8	118	109.6
RUN 6	135.9	143.5	139.7	138
RUN 7	137.6	142.9	138.3	134.3

(350 RPM / 7 inch per min traverse / 0.9 inch shoulder)

Exit data:

	Exit		Exit		Exit
	S13	S14	P13	P14	U7
RUN 1	94.95	103.2	96.75	98.94	86
RUN 2	110.1	123	118.3	119.5	101.5
RUN 3	98.48	109.4	106.8	106.8	101
RUN 4	107.9	120	110.1	116.5	97.92
RUN 5	95.33	103.6	98.32	104.6	87.64
RUN 6	112.1	117.9	113.8	124.8	109
RUN 7	108.2	110	104.8	121.2	108.3

(350 RPM / 7 inch per min traverse / 0.9 inch shoulder)

Factor level combination 4: 350 RPM / 4 inch per min traverse / 0.9 inch shoulder

Entry Data:

	Entry 1		Entry 2		Entry 1		Entry 2		Entry 1	Entry 2
	S1	S2	S3	S4	P1	P2	P3	P4	U1	U2
RUN 1	197.4	206.5	182.5	199.8	208.8	218.5	156.4	171.6	223	164.2
RUN 2	195.2	204.1	183.3	191.8	210.9	219.3	152.1	156.2	217.3	165.6
RUN 3	197.6	205.7	198.8	206.8	210.2	220.6	168.8	172	222.1	180.6
RUN 4	195.3	203	184	193.6	209.8	218.8	171.9	181.9	210.9	178.2
RUN 5	188.3	195.8	178.8	184.6	197.3	203.4	144.3	168.4	214.5	162.1
RUN 6	193.9	204	173.1	184.8	208	211.2	151.5	157.2	223.7	169
RUN 7	197.2	200.1	183.6	195.7	203.7	214.3	159.4	164.2	226.1	177

Traverse Data:

	Group 1		Group 2		Group 3		Group 4	
	S5	S6	S7	S8	S9	S10	S11	S12
RUN 1	185.8	192.1	163	173.4	163.2	178.1	156.9	159.9
RUN 2	178.3	186.4	160.6	171.2	180.9	182.2	157.8	175.4
RUN 3	199.6	199.9	172.6	191.7	173.2	193.7	162.9	171.2
RUN 4	181.5	194.3	179.2	187.6	178	181.3	162.3	174
RUN 5	180.3	194.4	166.1	171.7	167.1	175.6	141.3	170.5
RUN 6	174.1	178.3	152.5	177.2	168	172.4	169.7	170.9
RUN 7	181.8	182.5	158.6	175.7	169.7	170.9	167	172.3

	Group 1		Group 2		Group 3		Group 4	
	P5	P6	P7	P8	P9	P10	P11	P12
RUN 1	179.2	187.9	176.2	182.3	176.3	178.2	127.7	163.8
RUN 2	174.7	181	174.1	180.8	173.7	174.5	122.7	177.5
RUN 3	187.3	195	184.9	191.7	186.8	188.5	130.1	169
RUN 4	171.6	186.5	191.1	197	180.6	194.3	134.9	172.7
RUN 5	160.7	171	177	180.1	174.1	178.9	122.7	155.7
RUN 6	171	171.1	165.2	172.4	163.2	168.1	119.7	177.5
RUN 7	174.5	179.3	163.7	173.3	165.7	176.9	121.3	170.8

(350 RPM / 4 inch per min traverse / 0.9 inch shoulder)

	Group 1	Group 2	Group 3	Group 4
	U3	U4	U5	U6
RUN 1	154.5	151.6	139.7	154.3
RUN 2	166.5	161.8	152.4	166.1
RUN 3	182.1	167.7	157.1	181.1
RUN 4	180.8	169.8	151	168.8
RUN 5	169.3	163	143.4	168.3
RUN 6	160.9	157.2	159	163.9
RUN 7	168.5	164.2	155.3	164.6

Exit Data:

	Exit		Exit		Exit
	S13	S14	P13	P14	U7
RUN 1	131.5	139.4	130.9	137.1	125.7
RUN 2	134	148.2	142.6	142.6	145.9
RUN 3	141	147.4	140.1	151.6	137.6
RUN 4	144	155.2	146.6	157.3	141.1
RUN 5	125.5	130.8	122.6	138.3	123.8
RUN 6	131	135.6	129.2	143	130
RUN 7	126.2	149.9	142.1	143.2	135.1

(350 RPM / 4 inch per min traverse / 0.9 inch shoulder)

Factor level combination 5: 450 RPM / 7 inch per min traverse / 0.7 inch shoulder

Entry Data:

	Entry 1		Entry 2		Entry 1		Entry 2		Entry 1	Entry 2
	S1	S2	S3	S4	P1	P2	P3	P4	U1	U2
RUN 1	168.3	176.7	138.7	159.3	185.1	201.9	126.5	130.9	198.3	134.5
RUN 2	169	189.1	138.7	148.9	183.8	195.9	126.6	130.3	210.9	139.8
RUN 3	172.5	184.1	147	148.5	182.9	194.6	126.3	130.3	202.2	136.5
RUN 4	174.2	187.9	142.1	149.4	183.9	192.8	123.6	128.3	215.6	134.9
RUN 5	176.6	182.1	147.4	154.6	189.9	196	120.9	134.5	209.8	143.4
RUN 6	175.6	186.4	143.1	156.4	192.3	195.3	122.9	136.6	210.6	142.8
RUN 7	174.9	177.8	148.5	154.9	190.3	202.8	120.6	132.8	204.1	139.5

Traverse Data:

	Group 1		Group 2		Group 3		Group 4	
	S5	S6	S7	S8	S9	S10	S11	S12
RUN 1	134.2	146.7	133.2	147.1	128.2	145.5	126.2	139.7
RUN 2	135.3	147.9	133.4	139.5	138.6	141.8	127.4	136.4
RUN 3	138.2	141.2	130.4	137.6	134.2	139.4	129.4	133.7
RUN 4	131.1	144.2	132.4	141.9	136	138.6	128.9	137.5
RUN 5	135.6	146.9	135	138.6	133.9	145.1	125.7	136.5
RUN 6	131.6	139.7	128.3	141.3	134.9	140.3	132.4	137.7
RUN 7	129.6	144.4	131.2	141.3	137	138.6	132.9	136.6

	Group 1		Group 2		Group 3		Group 4	
	P5	P6	P7	P8	P9	P10	P11	P12
RUN 1	128.1	148.9	130.9	142.8	127.3	141.6	94.4	144.2
RUN 2	122.8	143.3	137.5	140	125.1	135.8	99.59	143
RUN 3	135.1	139	135.3	137.7	129.8	141.2	97.6	134.2
RUN 4	129.8	140.7	132.1	139.5	131.6	133.5	94.63	137.9
RUN 5	124	145.3	136.7	143.2	120.4	142.3	100.1	141.1
RUN 6	131.1	138.5	127.2	139.8	123.5	136.1	96.79	142
RUN 7	129.7	142.9	130.2	140.7	123	136.7	99.63	140.8

(450 RPM / 7 inch per min traverse / 0.7 inch shoulder)

	Group 1	Group 2	Group 3	Group 4
	U3	U4	U5	U6
RUN 1	136.1	137.6	131.4	124.2
RUN 2	134.5	140.6	134	128.3
RUN 3	135.3	138	128.6	121.8
RUN 4	124.6	137.1	125.5	124.1
RUN 5	135.2	142.9	133.7	130.9
RUN 6	129.1	140.5	131	128.3
RUN 7	132.5	135.4	126	127.2

Exit Data:

	Exit		Exit		Exit
	S13	S14	P13	P14	U7
RUN 1	102.4	127.3	110.3	125.4	108.5
RUN 2	109.5	120.2	119	121.1	109.2
RUN 3	107.9	118.3	117.5	119.1	104.8
RUN 4	115.3	121.6	120.1	124.4	113.3
RUN 5	106.6	117.8	115.2	125.8	109.3
RUN 6	102.7	115.2	111.1	119.4	104.6
RUN 7	107.7	118.7	115.9	121.4	104.3

(450 RPM / 7 inch per min traverse / 0.7 inch shoulder)

Factor level combination 6: 450 RPM / 4 inch per min traverse / 0.7 inch shoulder

Entry Data:

| | Entry 1 | | Entry 2 | | Entry 1 | | Entry 2 | | Entry 1 | Entry 2 |
	S1	S2	S3	S4	P1	P2	P3	P4	U1	U2
RUN 1	161.8	166.2	154.3	164.6	169.55	181	148.3	150.9	192.4	153.3
RUN 2	163.6	166.8	149.8	165	175.66	176.1	143.3	150.2	191.2	158.5
RUN 3	166.4	175.1	152.8	172.8	165.22	184.5	144.3	160.9	201.5	135.6
RUN 4	165.1	166.8	151.2	163	169.37	181.5	136.2	163.7	201.6	159.3
RUN 5	164.2	169.1	149.6	165.7	169.15	180.3	142.8	164	197.8	160.3
RUN 6	162.2	170.5	152.7	164.7	167.21	179	141.9	162.9	198.2	158.3
RUN 7	164.4	178	153.1	164.9	173.55	184.5	145.1	148.4	200.1	155.9

Traverse Data:

| | Group 1 | | Group 2 | | Group 3 | | Group 4 | |
	S5	S6	S7	S8	S9	S10	S11	S12
RUN 1	150.5	163	143.1	163.3	147.22	165.7	150.5	158.6
RUN 2	145.6	161	145.9	161.9	143.68	163.5	150.4	153.9
RUN 3	141.8	170.8	151.4	163.9	145.63	172.4	140.5	163.3
RUN 4	143.2	157.2	140	163.6	150.03	161.2	146.3	168.8
RUN 5	148.7	160.1	146.1	152.1	155.27	156.3	144.5	156.6
RUN 6	146.4	163.2	147.2	168	146.99	160	149.2	154.5
RUN 7	153.6	164.3	148.3	153.1	157.53	161.8	152	162.4

| | Group 1 | | Group 2 | | Group 3 | | Group 4 | |
	P5	P6	P7	P8	P9	P10	P11	P12
RUN 1	152.8	161	145.3	165.2	153.13	162.7	107.2	148.4
RUN 2	143.9	155.6	145.6	162.5	152.05	157.2	106.1	147.5
RUN 3	144.4	170.5	152.8	171.5	150.07	167.8	99.3	137.8
RUN 4	145.4	156.4	142.1	156.9	146.43	169.8	106.4	156.8
RUN 5	152.2	160.6	150.9	161.4	153.44	166.9	106.7	162.4
RUN 6	149.8	161.8	146.6	161.4	153.24	156.2	108.3	159.3
RUN 7	155.5	163.9	151.9	163.3	154.6	168.7	110.5	160

(450 RPM / 4 inch per min traverse / 0.7 inch shoulder)

124

	Group 1	Group 2	Group 3	Group 4
	U3	U4	U5	U6
RUN 1	157	156.9	141	150.7
RUN 2	154.5	154.5	141.4	148.2
RUN 3	144.3	140.4	134.2	138
RUN 4	145.9	144.8	140.1	149.1
RUN 5	156.2	163.2	148.5	146.7
RUN 6	155.4	157.6	151	152.8
RUN 7	155	159.7	148.5	152.4

Exit Data:

	Exit		Exit		Exit
	S13	S14	P13	P14	U7
RUN 1	126.4	134.8	133.9	144.4	128.09
RUN 2	126.3	136.4	129.2	145.7	121.69
RUN 3	124.4	145.9	121.5	153.6	134.48
RUN 4	129.4	134.9	133.3	140.6	128.07
RUN 5	133.3	136	133.3	148	127.97
RUN 6	128.7	129.8	125.5	139.5	129.87
RUN 7	126.4	136.3	133.6	145.3	126.06

(450 RPM / 4 inch per min traverse / 0.7 inch shoulder)

Factor level combination 7: 350 RPM / 7 inch per min traverse / 0.7 inch shoulder

Entry Data:

	Entry 1		Entry 2		Entry 1		Entry 2		Entry 1	Entry 2
	S1	S2	S3	S4	P1	P2	P3	P4	U1	U2
RUN 1	179.3	183.6	139.1	148.1	182.47	192.6	121.2	134.4	202.2	134.9
RUN 2	173.9	187.7	149	161.6	179.71	204.4	130.9	140.7	212.1	142.7
RUN 3	172.1	190	146.3	158.6	178.01	206.7	129.5	136.5	209.3	140
RUN 4	170.9	181.2	146.8	153	179.22	197.5	129.3	131.5	207.5	138
RUN 5	172.9	178.5	143.9	153.1	176.41	181.6	127.2	139.5	203.1	135.4
RUN 6	168.3	180.2	145.6	156.5	185.54	195.1	128.5	131.5	209.4	136.4
RUN 7	173.6	181.9	147.9	154	184.25	189.9	123.4	131	206.8	142.4

Traverse Data:

	Group 1		Group 2		Group 3		Group 4	
	S5	S6	S7	S8	S9	S10	S11	S12
RUN 1	130	134.2	124.4	139.9	132.03	135.1	120.1	130.1
RUN 2	135.3	146.2	134.2	144.6	134.12	145	127	137.1
RUN 3	131.1	142.1	127	137.5	133.36	141.5	129.2	129.3
RUN 4	131	141.3	128.8	135.2	137.54	140.9	124.9	135.7
RUN 5	129.2	140.1	128	136.1	135.84	139.5	127.6	132.5
RUN 6	127.1	141	128.2	136.1	139.44	140.8	126.2	133.9
RUN 7	130.3	142.1	129.6	138.4	131.71	142	122.2	132.7

	Group 1		Group 2		Group 3		Group 4	
	P5	P6	P7	P8	P9	P10	P11	P12
RUN 1	127.2	132.8	127	142.3	128.06	138.4	94.98	136.1
RUN 2	122.9	144.4	122.3	142.5	128.28	142.4	100.8	139.2
RUN 3	128	138.3	125	135.5	128.91	137	96.4	136.5
RUN 4	128.9	139.1	132.1	136.4	125.07	135.9	93.28	139.6
RUN 5	135.6	138	132.1	135.8	132.02	136.7	96.08	134.9
RUN 6	127.9	138.6	131.8	134.3	133.83	137.3	93.49	139.2
RUN 7	129.3	140.5	124.6	138.1	125.93	138.8	96.74	138.6

(350 RPM / 7 inch per min traverse / 0.7 inch shoulder)

	Group 1	Group 2	Group 3	Group 4
	U3	U4	U5	U6
RUN 1	128.5	128.8	121.8	116.2
RUN 2	135	143.2	137.6	132.3
RUN 3	132	136.6	132.5	126.5
RUN 4	125.3	133.9	128.4	125.9
RUN 5	124.6	136.9	129.8	125.1
RUN 6	126.9	133.8	127.9	126.7
RUN 7	131.5	136.4	129.5	128.5

Exit Data:

	Group 5		Group 5		Group 5
	S13	S14	P13	P14	U7
RUN 1	107.7	119.7	107.7	113.3	100.44
RUN 2	112.3	121.8	107.9	121.3	109.95
RUN 3	100.4	117.8	105.3	115.8	106.96
RUN 4	106.1	110.4	108.4	117.5	104.03
RUN 5	105.4	118.1	94.65	118.7	106.99
RUN 6	104.7	106.6	103.8	114.9	98.12
RUN 7	108.7	119.7	106.8	122.6	108.26

(350 RPM / 7 inch per min traverse / 0.7 inch shoulder)

Factor level combination 8: 350 RPM / 4 inch per min traverse / 0.7 inch shoulder

Entry Data:

	Entry 1		Entry 2		Entry 1		Entry 2		Entry 1	Entry 2
	S1	S2	S3	S4	P1	P2	P3	P4	U1	U2
RUN 1	171.3	181.5	151	161.8	182.54	194.5	125.2	147.4	201.8	146.5
RUN 2	176.5	188.1	154	174.4	179.61	191.9	129.7	142.3	204.5	147.5
RUN 3	177.4	189.3	161.4	170.7	190.25	193.8	129.4	150.1	209.1	155.7
RUN 4	183	192.9	166	186	181.79	211.5	140.5	155.7	215.4	157.5
RUN 5	178.1	179.9	162	165.7	179.17	193.6	135.2	145.9	209.8	160.6
RUN 6	174.9	183.2	161.1	183.1	180.68	194.9	140.9	147.2	212.5	152.5
RUN 7	169.4	193.3	168.5	176.1	185.74	188.7	136.8	149	209.9	157

Traverse Data:

	Group 1		Group 2		Group 3		Group 4	
	S5	S6	S7	S8	S9	S10	S11	S12
RUN 1	145.8	156.1	140.3	158.8	150.2	160.7	131.9	143.4
RUN 2	144	163.9	134.7	154.1	149.22	164.7	149.8	152.2
RUN 3	157.7	164	144.8	153.6	159.18	160.7	152.8	157.4
RUN 4	141	173.1	154.7	167.7	141.04	172.6	142.7	167.2
RUN 5	154.9	157.2	142.6	146.2	147.48	152.6	135.5	152.2
RUN 6	164.1	164.7	145.4	158	160.62	160.7	136	166.6
RUN 7	148.1	171.1	150.5	157.8	146.79	167	149	163

	Group 1		Group 2		Group 3		Group 4	
	P5	P6	P7	P8	P9	P10	P11	P12
RUN 1	149.1	163.3	134.6	148.6	151.89	162.4	100.6	145.9
RUN 2	144.3	151.2	149.9	156.8	142.09	153.1	107.4	154.4
RUN 3	153.1	160.8	130.5	157.7	152.35	154.5	111.5	158.5
RUN 4	146.1	171.6	144.9	171	147.27	167.4	115.5	165.9
RUN 5	148.2	151.7	143.8	148.2	146.05	157.7	106.6	162.5
RUN 6	147.6	161.5	146	159.5	134.88	157.4	111.2	162.1
RUN 7	150.6	168.5	143	162.5	140.62	162.3	112.8	166.6

(350 RPM / 4 inch per min traverse / 0.7 inch shoulder)

	Group 1	Group 2	Group 3	Group 4
	U3	U4	U5	U6
RUN 1	141	149.1	128.7	145.3
RUN 2	148.5	143.7	134.1	149.3
RUN 3	153.1	146.2	137.7	144.3
RUN 4	164.1	163.9	155.8	149.5
RUN 5	162.4	142.3	140.1	131.6
RUN 6	146.2	154.1	143.4	149.9
RUN 7	155.9	150.6	147.9	156.7

Exit Data:

	Exit		Exit		Exit
	S13	S14	P13	P14	U7
RUN 1	119.4	131.8	127.9	128	116.91
RUN 2	113.9	135.1	120.4	131.3	121.89
RUN 3	125.3	142.7	129.3	140.2	123.31
RUN 4	137.7	146.2	131.7	148.4	137.42
RUN 5	126.1	140	118.9	142.9	114.54
RUN 6	120.5	142.5	126	138.5	126.13
RUN 7	136.3	137	123.4	145.1	131.65

(350 RPM / 4 inch per min traverse / 0.7 inch shoulder)

Factor level combination 9: 450 RPM / 7 inch per min traverse / 0.5 inch shoulder

Entry Data

| | Entry 1 | | Entry 2 | | Entry 1 | | Entry 2 | | Entry 1 | Entry 2 |
	S1	S2	S3	S4	P1	P2	P3	P4	U1	U2
RUN 1	128.3	138.4	100.2	120.7	135.16	155.2	107.1	111.9	150.9	101.3
RUN 2	134.1	145.5	110.6	115.9	141.33	144.2	90.54	117.3	165.9	105.5
RUN 3	141.8	147.2	104.6	119.7	129.19	149.5	93.88	121.9	161.3	109.8
RUN 4	125	149.4	112.8	119	130.6	152	105	111.6	164.4	120.4
RUN 5	126.4	147	104.8	123.2	129.36	149.9	106.6	115.2	161.4	113.4
RUN 6	126.6	140	114.4	114.7	143.46	148.1	100.2	111.9	160.2	110
RUN 7	120.6	148	103.9	125.6	143.22	158.5	107.3	119.1	163.1	119.9

Traverse Data

| | Group 1 | | Group 2 | | Group 3 | | Group 4 | |
	S5	S6	S7	S8	S9	S10	S11	S12
RUN 1	94.73	108.1	92.87	108	109.68	116.8	105.1	116.4
RUN 2	99.21	114.6	87	95.32	100.91	121.9	104.4	119.5
RUN 3	98.66	110.1	93.71	109.7	97.51	128.1	106.7	114.3
RUN 4	110.5	120.8	96.79	111.9	112.83	122.5	116	120.3
RUN 5	102.1	117.3	100.4	115.7	117.16	125.5	112.6	119.8
RUN 6	101.1	107.2	93.28	108.3	105.24	116.8	101.7	115.8
RUN 7	106	121.1	102	112.5	104.59	112.1	101.3	121.7

| | Group 1 | | Group 2 | | Group 3 | | Group 4 | |
	P5	P6	P7	P8	P9	P10	P11	P12
RUN 1	104.2	116	91.62	112.7	105.09	121.5	81.4	110.1
RUN 2	99.62	122.6	95.9	110.3	107.59	116.6	89.08	112.9
RUN 3	105.9	118.4	92.75	105.4	94.67	112.3	70.82	117.6
RUN 4	110.5	118.5	100.5	116.8	109.46	116.8	86.17	118.3
RUN 5	112.9	125.9	100.2	113.4	105.23	121.8	84.7	126.2
RUN 6	109	116.2	93.02	104.5	102.94	124.5	75.78	113
RUN 7	114.7	121	101.6	111.5	102.65	126.9	87.89	126.7

(450 RPM / 7 inch per min traverse / 0.5 inch shoulder)

	Group 1	Group 2	Group 3	Group 4
	U3	U4	U5	U6
RUN 1	98.54	103.9	104.5	95.08
RUN 2	96.36	106.6	109.3	98.17
RUN 3	102.8	102.6	106.4	94.67
RUN 4	113.3	117.2	108.6	101.2
RUN 5	107.7	117.7	110.6	93.49
RUN 6	93.53	116.3	100.8	100.7
RUN 7	112.2	120	121.3	110.7

Exit Data

	Exit		Exit		Exit
	S13	S14	P13	P14	U7
RUN 1	90.85	94.25	73.03	99.64	86.03
RUN 2	80.81	92.11	79.86	92.2	97.27
RUN 3	78.9	92.07	77.31	88.56	81.47
RUN 4	91.01	97.53	86.47	94.77	98.62
RUN 5	91.04	98.64	80.05	90.44	95.11
RUN 6	83.76	95.44	74.37	97.18	85.49
RUN 7	81.91	99.63	87.97	93.86	99.41

(450 RPM / 7 inch per min traverse / 0.5 inch shoulder)

Factor level combination 10: 450 RPM / 4 inch per min traverse / 0.5 inch shoulder

Entry Data:

| | Entry 1 | | Entry 2 | | Entry 1 | | Entry 2 | | Entry 1 | Entry 2 |
	S1	S2	S3	S4	P1	P2	P3	P4	U1	U2
RUN 1	177.9	191.9	153.9	165.3	178.75	191.7	135.4	137.6	211.6	151.9
RUN 2	166.8	185.9	141.8	164.2	170.43	181.6	123.1	143.5	197.8	128.7
RUN 3	169.5	175.2	158.5	157.2	174.4	190.1	124.8	142.6	198.2	143.2
RUN 4	171	189.5	152.8	178.1	168.45	187	133.6	147.2	222.1	156.4
RUN 5	173.6	186.4	157	165.7	179.2	192	131.5	142.8	205.3	154.4
RUN 6	166.4	177.3	151.1	162.7	174.9	186.2	127.9	131	201.9	142.4
RUN 7	174.1	185.3	145.5	163.3	174.22	172.8	124.3	130.7	203	154.2

Traverse Data:

| | Group 1 | | Group 2 | | Group 3 | | Group 4 | |
	S5	S6	S7	S8	S9	S10	S11	S12
RUN 1	146.2	161.1	139.7	149.4	151.87	155.6	155.1	155.7
RUN 2	124.8	160.2	111.4	139.7	131.52	163.5	144.6	163.2
RUN 3	144.2	157.7	124.9	139.8	139.52	157.8	145.3	156.8
RUN 4	155.2	166.2	123.4	161.4	134.9	165.4	142.2	162.4
RUN 5	146.1	168.9	134.6	144.6	154.46	158.3	155.2	158.9
RUN 6	148.4	160.7	130.3	142.5	146.75	158	145.4	157.8
RUN 7	147.9	150.5	126.1	141.4	147.04	151.3	151.9	152.7

| | Group 1 | | Group 2 | | Group 3 | | Group 4 | |
	P5	P6	P7	P8	P9	P10	P11	P12
RUN 1	145.5	158.2	134.7	154.5	146.08	149.2	109.6	161
RUN 2	140.6	156.6	138.3	154.2	122.58	156.9	92.99	134.1
RUN 3	140.3	154.2	135.2	148.7	135.13	153.3	103.5	152.7
RUN 4	158.5	164.6	147.8	161.8	139.24	161.1	114.4	171.5
RUN 5	146	166.5	135.4	160.1	138.32	153.3	112.7	164.6
RUN 6	143.6	156.7	140.7	143.6	142.66	155.2	103.3	155.7
RUN 7	141.4	153.9	139	148.1	142.52	145.7	101.1	150.5

(450 RPM / 4 inch per min traverse / 0.5 inch shoulder)

	Group 1	Group 2	Group 3	Group 4
	U3	U4	U5	U6
RUN 1	154.8	154.6	141.4	136.5
RUN 2	116.7	119.3	113.8	115.9
RUN 3	144.4	135	131.4	147.7
RUN 4	159.3	155.6	150.8	143.7
RUN 5	155.2	143.5	140.9	149.9
RUN 6	145.1	139.6	131.5	138.9
RUN 7	141.9	140.3	130.4	126.2

Exit Data:

	Exit		Exit		Exit
	S13	S14	P13	P14	U7
RUN 1	120	135.2	131.8	138.6	118.28
RUN 2	118.3	121.3	119.6	146.8	103.83
RUN 3	124.2	130.2	124.7	134.1	126.31
RUN 4	113.9	126.8	126.7	148.6	104.99
RUN 5	123.2	133.4	130.4	142.5	124.71
RUN 6	116.4	135.9	132.1	132.3	116.39
RUN 7	118.3	134.2	123.8	141	110.41

(450 RPM / 4 inch per min traverse / 0.5 inch shoulder)

Factor level combination 11: 350 RPM / 7 inch per min traverse / 0.5 inch shoulder

Entry Data:

| | Entry 1 | | Entry 2 | | Entry 1 | | Entry 2 | | Entry 1 | Entry 2 |
	S1	S2	S3	S4	P1	P2	P3	P4	U1	U2
RUN 1	158.2	169.7	137.8	149.9	154.34	175	128.4	130.1	189.6	142
RUN 2	142.6	163.7	132.9	143.6	155.64	168.2	123	127.2	195.1	139.3
RUN 3	155.1	175.6	139.9	158.4	162.85	183.9	122.7	136.2	203.1	143.3
RUN 4	146	155.8	134.1	141.6	166.92	175.2	124.3	133.8	184.6	137
RUN 5	159.5	171.3	144.8	148	165.82	177	128.1	138.3	194.9	141.2
RUN 6	152.6	170.7	135.7	146.6	169.23	179.9	125.7	138.1	189.2	141
RUN 7	152.9	164.4	133.7	144.8	161.35	171.6	125.5	138.2	197.1	139.7

Traverse Data:

| | Group 1 | | Group 2 | | Group 3 | | Group 4 | |
	S5	S6	S7	S8	S9	S10	S11	S12
RUN 1	135.8	143.5	120.1	140.3	132.42	140.1	124.6	131.8
RUN 2	131.9	141.6	127.6	139.3	135.28	139	125.3	133.1
RUN 3	142.2	146.9	131.8	137.5	129.47	139.6	121.9	132.9
RUN 4	136.6	139.2	121.3	137.6	130.56	137.9	126.3	127.4
RUN 5	132.9	142.1	128.1	130.3	134.28	138.5	127	128.3
RUN 6	139.9	142.4	124.6	140.8	137.69	142.2	127	132.4
RUN 7	135.5	141.6	127.8	130.4	134.45	138.8	126.6	134.9

| | Group 1 | | Group 2 | | Group 3 | | Group 4 | |
	P5	P6	P7	P8	P9	P10	P11	P12
RUN 1	130.7	141.1	128.5	139.4	131.42	136.1	92.6	137.6
RUN 2	128.5	141.3	126.7	141.3	123.26	136.3	92.92	138.7
RUN 3	137.3	146.3	135.4	145.1	127.02	138	96.49	141.2
RUN 4	127.9	138.2	120.2	137.3	127.79	133.4	92.42	134.5
RUN 5	132.5	141.7	129.8	139.5	132.79	135.3	93.35	135.8
RUN 6	135.9	141.7	133	140.6	125.16	137.6	92.73	135
RUN 7	132.3	142.3	129.4	140.6	122.98	137.9	93.52	140.7

(350 RPM / 7 inch per min traverse / 0.5 inch shoulder)

	Group 1	Group 2	Group 3	Group 4
	U3	U4	U5	U6
RUN 1	130.6	136.9	127.3	129.7
RUN 2	133.7	140.5	127.8	132
RUN 3	137.7	137.4	129.9	130.9
RUN 4	129.9	135.9	125.8	128.9
RUN 5	132.9	139.8	128.7	130.4
RUN 6	135.1	140	124.1	126.4
RUN 7	136	142.5	130	134.1

Exit Data:

	Exit		Exit		Exit
	S13	S14	P13	P14	U7
RUN 1	106.7	112.8	109.9	122.2	103.06
RUN 2	111.8	112	111.9	124.5	111.71
RUN 3	106	122.7	118.3	125.6	105.81
RUN 4	104.9	115.7	113.1	122.2	106.72
RUN 5	102.8	116.3	111.8	119.1	106.62
RUN 6	101.6	112.2	110.3	125	101.14
RUN 7	107.6	114.8	113.7	123.3	111.08

(350 RPM / 7 inch per min traverse / 0.5 inch shoulder)

Factor level combination 12: 350 RPM / 4 inch per min traverse / 0.5 inch shoulder

Entry Data

	Entry 1		Entry 2		Entry 1		Entry 2		Entry 1	Entry 2
	S1	S2	S3	S4	P1	P2	P3	P4	U1	U2
RUN 1	148.6	165.5	131.7	145.5	150.16	161.8	111	132.2	173.3	131.1
RUN 2	149.6	161.1	133.9	144.4	137.75	161.6	113.6	134	186.7	139.2
RUN 3	165.7	168.3	148.2	150	147.92	171.7	129.7	131.3	182.3	146
RUN 4	143.2	168.9	133.6	146.6	152.78	170.7	115.4	132.5	176.6	129.4
RUN 5	147.9	160.4	136	146.4	161.97	164.5	115.6	135.8	186.3	135.5
RUN 6	149.5	160.6	134.2	143.2	148.37	160.2	113.8	136.8	171.5	139
RUN 7	137.3	159.3	135.2	138.1	153.89	185.4	113.8	126.1	179.6	132.2

Traverse Data

	Group 1		Group 2		Group 3		Group 4	
	S5	S6	S7	S8	S9	S10	S11	S12
RUN 1	117	140.3	119.9	133.1	126.43	135.8	125.3	133.1
RUN 2	124.5	141.4	118.8	134.7	124.67	135.3	123.6	132.3
RUN 3	142.3	146.2	129	134.5	126.34	142.1	122.2	142.9
RUN 4	121.8	139.3	120.3	136.3	128.45	138.6	118.2	135.3
RUN 5	125.7	141.8	121.7	135.9	124.23	134.4	119.2	136.2
RUN 6	126.2	146.7	122	137.7	106.82	128.4	108.4	129.7
RUN 7	121	132	116.3	129.7	125.44	138.4	124	127.5

	Group 1		Group 2		Group 3		Group 4	
	P5	P6	P7	P8	P9	P10	P11	P12
RUN 1	117.8	137.3	120	133.5	123.19	139.3	90.67	135.8
RUN 2	121	138.8	118.6	136.3	120.73	130.2	89.88	134.2
RUN 3	136.2	147	133.4	140.7	132.88	139.9	92.03	151
RUN 4	121.6	137	120.4	135.4	123.6	131.9	87.78	135.1
RUN 5	123.7	140.1	122	137.8	120.97	131.1	88.67	138.6
RUN 6	119.7	134.7	127.9	134	124.22	135.6	76.14	135.4
RUN 7	120	130.2	118.9	129.2	122.8	135.8	87.94	131.6

(350 RPM / 4 inch per min traverse / 0.5 inch shoulder)

	Group 1	Group 2	Group 3	Group 4
	U3	U4	U5	U6
RUN 1	131.7	120.5	115.7	121.1
RUN 2	131.9	127	120.9	128.8
RUN 3	144.6	140.6	133.7	125.1
RUN 4	133.2	126.9	122.3	127.6
RUN 5	135.5	130	124.1	125.3
RUN 6	136.4	122.9	127.2	109.3
RUN 7	122.9	128.2	119.2	127.5

Exit Data

	Group 5		Group 5		Group 5
	S13	S14	P13	P14	U7
RUN 1	103.7	119.3	102.2	118	107.76
RUN 2	106.7	115.1	104.8	117.4	110.57
RUN 3	118.8	123.2	121.5	135.3	110.71
RUN 4	100.5	117.2	99.84	114.5	107.24
RUN 5	102.9	122.4	103	119.7	107.32
RUN 6	95.06	112.3	99.89	113.4	95.8
RUN 7	105.9	119.1	105.6	112.6	105.96

(350 RPM / 4 inch per min traverse / 0.5 inch shoulder)

APPENDIX B

Calculated Data: With 2 RPMs, 2 traverse speed and 3 shoulder diameters, there is a combination of 12 different parameters. For each parameter, 7 experiments were done to achieve at least a 90% statistical power that advancing was hotter than retreating side. The peak temperatures calculated for all the 12 different parameters are given below.

Nomenclature: Each Thermocouple was represented by a unique alphabet and number:

S – Shoulder thermocouple. (Retreating side: S_1, $S_{3...}$ $S_{13;}$

Advancing side: S_2, $S_{4..}$ S_{14})

P – Pin thermocouple. (Retreating side: P_1, $P_{3...}$ $P_{13;}$ Retreating side: P_2, P_4... P_{14})

U – Under the pin thermocouple. (U_1, $U_{2...}$ U_7)

Factor level combination 1: 450 RPM / 7 inch per min traverse / 0.9 inch shoulder

Entry Data:

	Entry 1		Entry 2		Entry 1		Entry 2		Entry 1	Entry 2
	S1	S2	S3	S4	P1	P2	P3	P4	U1	U2
RUN 1	361.7	383.2	331.1	334.3	379.28	395	311.2	332.5	396.3	332.5
RUN 2	360.7	374.6	330.6	339.8	376.51	387.4	318.2	324.6	402.1	341.2
RUN 3	365.9	382.3	330.4	338.1	375.64	394.3	324.7	328	414.5	334.1
RUN 4	365.6	377.7	330.5	339.4	383.72	396.8	323.6	328.8	400.9	340.4
RUN 5	367.4	371	328.2	341.7	379.72	383	319.3	333.6	404.2	346.8
RUN 6	366.3	378.4	332	339.2	377.2	391.2	315.7	331.1	405.6	335.6
RUN 7	373.6	377.5	334.8	342	386.36	393.1	320.2	332.7	411.1	330

(450 RPM / 7 inch per min traverse / 0.9 inch shoulder)

Traverse Data:

	Group 1		Group 2		Group 3		Group 4	
	S5	S6	S7	S8	S9	S10	S11	S12
RUN 1	321.2	341.2	314.7	327.6	324.73	329.3	323.3	324.9
RUN 2	321.7	335.5	320.1	332	330.97	331.9	317.5	331.2
RUN 3	330	333	319.3	324.9	325.5	336.2	316.3	326.7
RUN 4	329.2	331.6	317.9	331.6	328.64	342	319.6	329.9
RUN 5	329.3	339.5	319.3	328.4	326.03	340.6	314.6	327.9
RUN 6	327.7	339.2	316.5	331	327.66	338.7	322.8	326.5
RUN 7	320.7	342.3	318.4	324	328.59	331.4	323.9	324.4

	Group 1		Group 2		Group 3		Group 4	
	P5	P6	P7	P8	P9	P10	P11	P12
RUN 1	319.2	331.7	325	327.9	323.81	334.1	286.6	330.4
RUN 2	331.2	336.4	319.4	334.3	318.16	331.9	289.6	338.4
RUN 3	330.2	341.5	316.8	329.8	324.83	335.8	287.1	331.4
RUN 4	329.2	332.5	321.1	332.8	326.25	328.7	280	329
RUN 5	326.4	340.3	322.6	338.1	323.85	337.7	286.1	342.1
RUN 6	328	339.6	320.9	328.6	327.15	328	288	333.7
RUN 7	323.1	334	324.2	329.7	319.03	330.1	289	335

	Group 1	Group 2	Group 3	Group 4
	U3	U4	U5	U6
RUN 1	329.4	325.7	320.2	325.4
RUN 2	333.9	335.9	323.6	328.1
RUN 3	326.4	338.4	325.3	326.2
RUN 4	325	334.9	328.7	328.1
RUN 5	333.1	343	317.7	334.3
RUN 6	325	330.7	321.2	326.2
RUN 7	328.2	333.3	329.6	327.6

(450 RPM / 7 inch per min traverse / 0.9 inch shoulder)

Exit Data:

	Group 5		Group 5		Group 5
	S13	S14	P13	P14	U7
RUN 1	294.8	305.8	306.5	309.1	297.39
RUN 2	301.4	313.1	294	321.6	301.4
RUN 3	294.3	311.9	305.8	319.3	297.27
RUN 4	301.7	303.4	304.5	320.6	298.21
RUN 5	303	306.3	293.4	316.8	312.31
RUN 6	293.3	309.4	300.9	314.9	299.55
RUN 7	296.9	311.6	307.9	313.4	303.25

(450 RPM / 7 inch per min traverse / 0.9 inch shoulder)

Factor level combination 2: 450 RPM / 4 inch per min traverse / 0.9 inch shoulder

Entry Data:

	Entry 1		Entry 2		Entry 1		Entry 2		Entry 1	Entry 2
	S1	S2	S3	S4	P1	P2	P3	P4	U1	U2
RUN 1	379	383.1	377.9	383.4	395.61	412	350.3	372.7	422.1	371
RUN 2	383.8	386.7	378.1	389.3	394.18	407.4	359.2	361	428.8	376.3
RUN 3	386.7	396.6	369.3	395.4	395.55	417.4	361.2	363.9	426	380.2
RUN 4	383.2	393.4	383.8	386.9	402.26	411.1	358.6	368.7	414.6	364.4
RUN 5	376.5	393.5	381.3	388.5	391.95	407.1	355.5	369.5	426.5	380.5
RUN 6	378	395.8	377.5	388	391.83	402.7	355.4	370.2	421.9	371.7
RUN 7	381.8	391.2	380	389.9	391.12	401.7	355.7	360.6	419.9	365.4

Traverse Data:

	Group 1		Group 2		Group 3		Group 4	
	S5	S6	S7	S8	S9	S10	S11	S12
RUN 1	367.8	376	347.5	366.2	368.65	371.8	362.9	369.1
RUN 2	373.1	387.4	362	376.8	362.77	384.6	371.7	377.2
RUN 3	367.2	392.9	364.8	382	365	386.4	363	382.7
RUN 4	354.9	387.9	362.4	373.5	370.66	374	362.3	376.7
RUN 5	374.2	380.4	356	373.9	362.7	373.1	367.7	371.9
RUN 6	366.3	375	356.1	367.1	365.15	377.5	363.5	375.5
RUN 7	373.3	385.5	359.6	367.8	372.2	374.3	362.5	382.9

	Group 1		Group 2		Group 3		Group 4	
	P5	P6	P7	P8	P9	P10	P11	P12
RUN 1	368	376	363.4	369.2	365.37	378.2	312.9	380.8
RUN 2	366.4	387.2	365.4	385.1	360.83	381	319.8	391.7
RUN 3	360.3	392.7	367.9	368.3	360.93	382.8	320.1	394.2
RUN 4	368.3	387.4	366.1	374	369.44	381	312.4	385.3
RUN 5	375.3	380.2	363.3	371.6	368.9	371	316.5	378
RUN 6	368.5	386.1	358	374.5	373.29	373.7	314.8	383.6
RUN 7	368.4	380.9	363.5	377.8	367.77	381.4	310.6	383.6

(450 RPM / 4 inch per min traverse / 0.9 inch shoulder)

	Group 1	Group 2	Group 3	Group 4
	U3	U4	U5	U6
RUN 1	368.6	365.1	361.2	365.6
RUN 2	377.1	369.7	363.5	371.7
RUN 3	384.9	379.5	368.4	376.4
RUN 4	374.4	368.9	373.1	367.8
RUN 5	373.5	373.4	360.3	371.4
RUN 6	372.5	379.2	354.6	358.7
RUN 7	376.2	383.3	364.9	371.3

Exit Data:

	Exit		Exit		Exit
	S13	S14	P13	P14	U7
RUN 1	340.2	355.7	341.7	353.2	344.38
RUN 2	345.1	351.8	339.1	358.3	345.19
RUN 3	350	358.9	345.9	365	346.11
RUN 4	339.7	355.4	344.9	362.3	346.81
RUN 5	337.3	347	344.5	351.7	342.84
RUN 6	333.6	351.5	328.3	352.5	327.1
RUN 7	341.1	354.3	344.5	358.2	346.35

(450 RPM / 4 inch per min traverse / 0.9 inch shoulder)

Factor level combination 3: 350 RPM / 7 inch per min traverse / 0.9 inch shoulder

Entry Data:

	Entry 1		Entry 2		Entry 1		Entry 2		Entry 1	Entry 2
	S1	S2	S3	S4	P1	P2	P3	P4	U1	U2
RUN 1	373.9	375.8	314.7	324.7	365.52	389.7	316.1	328.5	408.4	328.5
RUN 2	369.9	376.3	326.8	339	362.78	390.7	306.2	334.5	409	329
RUN 3	371.5	383.7	325.8	336.7	366.04	395.5	313.9	328.3	415.6	329.9
RUN 4	370.5	384.6	322.6	345.5	376.97	402.9	316	324.6	410.8	330.4
RUN 5	370.3	378.1	322.2	328.2	368.48	386.6	305.9	328.2	410.1	225
RUN 6	370.7	382.9	326.2	346.8	381.88	399.9	323.2	329.1	417.2	343
RUN 7	372.8	381	328.8	347.5	371.8	395.3	324.4	329.1	414.1	342.1

Traverse Data:

	Group 1		Group 2		Group 3		Group 4	
	S5	S6	S7	S8	S9	S10	S11	S12
RUN 1	319.8	330.5	319.7	328.5	320.46	326	321.1	326.1
RUN 2	312.7	325	314.3	333.3	312.06	323.9	320	320.3
RUN 3	313.7	331.3	314.4	331.2	320.86	329.4	315.8	329.2
RUN 4	316.1	332.2	314.2	321.5	314.84	329	315.7	328.7
RUN 5	312.8	314.8	301.5	328.1	311.27	315	305.8	327.6
RUN 6	320.8	331.6	321.5	327.1	309.17	333.5	322.1	329.1
RUN 7	312	332.2	319.3	329.5	307.64	333.7	321.9	332.5

	Group 1		Group 2		Group 3		Group 4	
	P5	P6	P7	P8	P9	P10	P11	P12
RUN 1	322	333.5	321.8	336	318.9	323.9	285.7	300.9
RUN 2	319.6	325.8	320.1	335.1	317.92	330.4	284	325.7
RUN 3	315.1	326.7	322.4	324.2	319.43	327.5	286.4	323.5
RUN 4	315.8	327.6	321.7	323.9	320.17	327.3	285.5	323.9
RUN 5	312	314.8	317.4	332.2	309.38	332.1	276.4	315.5
RUN 6	311.5	333	327	333.1	310.69	331.9	289.4	337.9
RUN 7	313.4	335.6	319.5	333.1	328.4	333.1	288.6	332.2

(350 RPM / 7 inch per min traverse / 0.9 inch shoulder)

	Group 1	Group 2	Group 3	Group 4
	U3	U4	U5	U6
RUN 1	326.5	336	314.6	318.2
RUN 2	328.8	328	317.5	321.5
RUN 3	319.7	335.4	325.8	318.9
RUN 4	317.6	331.5	319.3	308.7
RUN 5	304.6	320	311.3	302.9
RUN 6	329.1	336.8	332.9	331.3
RUN 7	330.9	336.2	331.6	327.6

Exit Data

	Group 5		Group 5		Group 5
	S13	S14	P13	P14	U7
RUN 1	279.2	297.4	284.7	296.9	279.28
RUN 2	284.3	307.2	286.3	307.4	294.82
RUN 3	282.7	293.7	294.8	304.8	294.32
RUN 4	292.1	304.2	298.1	304.5	291.2
RUN 5	279.6	297.9	286.3	302.6	280.92
RUN 6	286.3	302.2	301.8	312.8	302.23
RUN 7	292.4	294.3	292.8	309.2	301.53

(350 RPM / 7 inch per min traverse / 0.9 inch shoulder)

Factor level combination 4: 350 RPM / 4 inch per min traverse / 0.9 inch shoulder

Entry Data:

	Entry 1		Entry 2		Entry 1		Entry 2		Entry 1	Entry 2
	S1	S2	S3	S4	P1	P2	P3	P4	U1	U2
RUN 1	381.7	390.7	366.8	384.1	386.8	406.4	344.3	359.6	416.3	357.5
RUN 2	379.4	388.3	367.5	376.1	398.92	407.3	340.1	364.1	410.6	358.9
RUN 3	381.9	389.9	363	391	398.13	408.6	356.8	370	415.4	373.9
RUN 4	379.6	387.3	368.2	377.8	387.83	406.8	359.9	369.9	404.2	371.4
RUN 5	372.6	380	363	368.8	385.29	391.4	342.2	356.3	407.8	355.4
RUN 6	378.2	388.2	357.3	369	386	399.2	349.5	365.2	417	362.3
RUN 7	381.4	384.3	367.8	379.9	391.66	402.3	347.4	362.2	419.4	370.2

Traverse Data:

	Group 1		Group 2		Group 3		Group 4	
	S5	S6	S7	S8	S9	S10	S11	S12
RUN 1	360.1	376.3	347.3	357.6	347.41	362.3	341.2	344.1
RUN 2	362.5	370.6	344.8	355.5	345.16	366.5	342.1	359.6
RUN 3	363.8	384.1	356.8	375.9	357.46	378	347.2	355.4
RUN 4	365.8	378.5	343.4	371.8	342.22	365.5	346.6	358.2
RUN 5	364.6	378.7	340.3	355.9	351.33	359.8	345.6	354.7
RUN 6	358.4	362.5	346.7	361.4	352.23	356.6	343.9	355.1
RUN 7	356.1	366.7	342.8	359.9	353.96	355.1	351.2	356.6

	Group 1		Group 2		Group 3		Group 4	
	P5	P6	P7	P8	P9	P10	P11	P12
RUN 1	357.2	375.9	354.2	370.3	354.3	366.2	315.7	351.8
RUN 2	362.7	369	362.1	368.8	361.72	362.5	310.7	365.5
RUN 3	355.3	373	352.9	379.7	354.74	376.5	318.1	357
RUN 4	359.6	374.5	359.1	385	348.57	382.3	322.9	360.7
RUN 5	348.7	369	365	368.1	352.08	366.9	310.7	343.6
RUN 6	359	369	353.2	360.4	351.21	356.1	307.7	365.5
RUN 7	362.5	367.3	351.7	361.2	353.66	364.9	309.3	358.8

(350 RPM / 4 inch per min traverse / 0.9 inch shoulder)

	Group 1	Group 2	Group 3	Group 4
	U3	U4	U5	U6
RUN 1	347.7	344.9	333	347.6
RUN 2	359.8	355	345.7	359.4
RUN 3	375.4	361	350.4	374.3
RUN 4	374.1	363.1	344.2	362.1
RUN 5	362.5	356.2	336.7	361.6
RUN 6	354.1	350.5	352.2	357.2
RUN 7	361.8	357.5	348.6	357.9

Exit Data

	Exit		Exit		Exit
	S13	S14	P13	P14	U7
RUN 1	315.7	323.6	318.9	325.1	319.01
RUN 2	318.3	332.4	330.6	330.6	339.13
RUN 3	315.2	331.7	308.1	339.6	330.91
RUN 4	318.2	339.4	314.6	345.3	334.36
RUN 5	309.7	315	310.6	326.3	317.05
RUN 6	315.2	319.8	317.2	331	323.3
RUN 7	310.4	334.1	320.1	331.2	328.35

(350 RPM / 4 inch per min traverse / 0.9 inch shoulder)

Factor level combination 5: 450 RPM / 7 inch per min traverse / 0.7 inch shoulder

Entry Data

	Entry 1		Entry 2		Entry 1		Entry 2		Entry 1	Entry 2
	S1	S2	S3	S4	P1	P2	P3	P4	U1	U2
RUN 1	352.5	360.9	322.9	343.5	373.09	389.9	314.5	318.9	391.6	327.7
RUN 2	353.3	373.4	323	333.2	371.75	383.8	314.5	318.3	404.2	333.1
RUN 3	356.7	368.3	331.3	332.8	370.88	382.6	314.3	318.3	395.5	329.7
RUN 4	358.4	372.2	326.3	333.6	371.86	380.8	311.6	316.3	408.9	328.2
RUN 5	360.9	366.3	331.6	338.8	377.88	383.9	308.9	322.5	403.1	336.6
RUN 6	359.8	370.6	327.3	340.6	380.29	383.3	310.9	324.6	403.9	336
RUN 7	359.1	362.1	332.8	339.1	378.25	390.8	308.6	320.8	397.4	332.8

Traverse Data

	Group 1		Group 2		Group 3		Group 4	
	S5	S6	S7	S8	S9	S10	S11	S12
RUN 1	318.4	330.9	317.5	331.3	312.47	329.7	310.4	323.9
RUN 2	319.6	332.2	317.6	323.7	322.79	326.1	311.6	320.7
RUN 3	322.4	325.4	314.6	321.9	318.43	323.6	313.7	318
RUN 4	315.4	328.4	316.7	326.1	320.18	322.9	313.1	321.8
RUN 5	319.9	331.2	319.2	322.8	318.14	329.4	309.9	320.7
RUN 6	315.8	324	312.5	325.5	319.12	324.5	316.6	321.9
RUN 7	313.8	328.6	315.4	325.5	321.19	322.9	317.1	320.8

	Group 1		Group 2		Group 3		Group 4	
	P5	P6	P7	P8	P9	P10	P11	P12
RUN 1	316.1	336.9	318.9	330.8	315.32	329.6	282.4	332.1
RUN 2	310.8	331.3	325.5	328	313.09	323.8	287.6	331
RUN 3	323.1	327	323.3	325.7	317.83	329.2	285.6	322.2
RUN 4	317.8	328.7	320.1	327.5	319.62	321.4	282.6	325.9
RUN 5	312	333.3	324.7	331.2	308.36	330.3	288	329.1
RUN 6	319.1	326.5	315.1	327.7	311.51	324.1	284.8	330
RUN 7	317.6	330.9	318.2	328.6	311.01	324.7	287.6	328.8

(450 RPM / 7 inch per min traverse / 0.7 inch shoulder)

	Group 1	Group 2	Group 3	Group 4
	U3	U4	U5	U6
RUN 1	329.4	330.9	324.6	317.5
RUN 2	327.8	333.9	327.3	321.5
RUN 3	328.6	331.3	321.8	315.1
RUN 4	317.9	330.3	318.8	317.3
RUN 5	328.5	336.2	327	324.2
RUN 6	322.4	333.8	324.2	321.6
RUN 7	325.8	328.7	319.2	320.4

Exit Data

	Group 5		Group 5		Group 5
	S13	S14	P13	P14	U7
RUN 1	286.6	311.5	298.3	313.4	301.73
RUN 2	293.7	304.4	307	309.1	302.46
RUN 3	292.2	302.5	305.5	307.1	298.06
RUN 4	299.6	305.9	308.1	312.4	306.55
RUN 5	290.9	302.1	303.2	313.7	302.58
RUN 6	287	299.4	299.1	307.4	297.89
RUN 7	291.9	302.9	303.9	309.4	297.6

(450 RPM / 7 inch per min traverse / 0.7 inch shoulder)

Factor level combination 6: 450 RPM / 4 inch per min traverse / 0.7 inch shoulder

Entry Data:

	Entry 1		Entry 2		Entry 1		Entry 2		Entry 1	Entry 2
	S1	S2	S3	S4	P1	P2	P3	P4	U1	U2
RUN 1	346.1	350.4	338.5	348.8	357.53	369	336.3	338.9	385.7	346.5
RUN 2	347.8	351	334	349.2	363.65	364.1	331.3	338.2	384.4	351.8
RUN 3	350.7	359.3	337.1	357	353.21	372.5	332.2	348.9	394.8	328.9
RUN 4	349.3	351	335.5	347.3	357.36	369.5	324.2	351.6	394.9	352.6
RUN 5	348.4	353.4	333.9	349.9	357.13	368.3	330.8	352	391.1	353.6
RUN 6	346.4	354.7	337	348.9	355.19	367	329.9	350.9	391.5	351.6
RUN 7	348.6	362.2	337.4	349.2	361.54	372.4	333.1	336.4	393.4	349.2

Traverse Data:

	Group 1		Group 2		Group 3		Group 4	
	S5	S6	S7	S8	S9	S10	S11	S12
RUN 1	334.7	347.2	327.3	347.6	331.45	349.9	334.7	342.8
RUN 2	329.8	345.2	330.1	346.2	327.91	347.8	334.6	338.1
RUN 3	326.1	355	335.6	348.1	329.86	356.7	324.7	347.6
RUN 4	327.4	341.4	324.2	347.8	334.26	345.4	330.5	353.1
RUN 5	332.9	344.4	330.3	336.3	339.5	340.6	328.8	340.9
RUN 6	330.6	347.4	331.5	352.2	331.22	344.2	333.5	338.7
RUN 7	337.9	348.5	332.5	337.3	341.76	346	336.2	346.7

	Group 1		Group 2		Group 3		Group 4	
	P5	P6	P7	P8	P9	P10	P11	P12
RUN 1	340.8	349	333.3	353.2	341.12	350.7	295.2	336.3
RUN 2	331.9	343.5	333.6	350.5	340.04	345.2	294.1	335.5
RUN 3	332.4	358.5	340.8	359.5	338.06	355.8	287.3	325.8
RUN 4	333.4	344.3	330.1	344.9	334.42	357.8	294.4	344.8
RUN 5	340.2	348.6	338.9	349.4	341.43	354.9	294.6	350.4
RUN 6	337.8	349.8	334.6	349.4	341.23	344.2	296.3	347.3
RUN 7	343.4	351.9	339.9	351.2	342.59	356.7	298.5	348

(450 RPM / 4 inch per min traverse / 0.7 inch shoulder)

	Group 1	Group 2	Group 3	Group 4
	U3	U4	U5	U6
RUN 1	350.3	350.2	334.3	344
RUN 2	347.8	347.8	334.6	341.4
RUN 3	337.6	333.7	327.5	331.3
RUN 4	339.2	338	333.4	342.4
RUN 5	349.5	356.5	341.8	340
RUN 6	348.7	350.9	344.3	346
RUN 7	348.3	353	341.8	345.7

Exit Data:

	Exit		Exit		Exit
	S13	S14	P13	P14	U7
RUN 1	310.6	319.1	321.9	332.4	321.37
RUN 2	310.5	320.6	317.2	333.7	314.97
RUN 3	308.6	330.1	309.4	341.6	327.76
RUN 4	313.6	319.1	321.3	328.6	321.35
RUN 5	317.5	320.3	321.3	336	321.25
RUN 6	312.9	314	313.5	327.5	323.15
RUN 7	310.6	320.5	321.6	333.3	319.34

(450 RPM / 4 inch per min traverse / 0.7 inch shoulder)

Factor level combination 7: 350 RPM / 7 inch per min traverse / 0.7 inch shoulder

Entry Data

	Entry 1		Entry 2		Entry 1		Entry 2		Entry 1	Entry 2
	S1	S2	S3	S4	P1	P2	P3	P4	U1	U2
RUN 1	363.5	367.8	323.3	332.3	370.46	380.5	309.2	322.4	395.5	328.2
RUN 2	358.1	372	333.3	345.9	367.7	392.4	318.9	328.7	405.4	336
RUN 3	356.3	374.3	330.6	342.8	366	394.7	317.5	324.5	402.5	333.3
RUN 4	355.2	365.5	331	337.2	367.2	385.5	317.3	319.5	400.8	331.3
RUN 5	357.1	362.7	328.1	337.3	364.39	369.6	315.2	327.5	396.4	328.7
RUN 6	352.5	364.4	329.8	340.7	373.53	383.1	316.5	319.4	402.7	329.7
RUN 7	357.8	366.1	332.1	338.2	372.23	377.9	311.4	319	400.1	335.7

Traverse Data

	Group 1		Group 2		Group 3		Group 4	
	S5	S6	S7	S8	S9	S10	S11	S12
RUN 1	314.3	318.4	308.6	324.1	316.26	319.4	304.3	314.3
RUN 2	319.5	330.5	318.4	328.9	318.35	329.2	311.2	321.3
RUN 3	315.3	326.4	311.2	321.8	317.59	325.7	313.4	313.6
RUN 4	315.2	325.6	313.1	319.4	321.77	325.1	309.2	319.9
RUN 5	313.4	324.3	312.3	320.4	320.07	323.8	311.8	316.8
RUN 6	311.3	325.3	312.4	320.3	323.67	325.1	310.4	318.1
RUN 7	314.5	326.4	313.8	322.6	315.94	326.2	306.4	317

	Group 1		Group 2		Group 3		Group 4	
	P5	P6	P7	P8	P9	P10	P11	P12
RUN 1	315.2	320.7	315	330.3	316.05	326.4	283	324
RUN 2	310.9	332.4	310.3	330.5	316.27	330.4	288.8	327.2
RUN 3	316	326.3	313	323.5	316.9	325	284.4	324.5
RUN 4	316.9	327.1	320	324.4	313.06	323.9	281.3	327.6
RUN 5	323.6	325.9	320.1	323.8	320.01	324.7	284.1	322.9
RUN 6	315.9	326.5	319.8	322.3	321.82	325.3	281.5	327.2
RUN 7	317.3	328.5	312.6	326.1	313.92	326.8	284.7	326.6

(350 RPM / 7 inch per min traverse / 0.7 inch shoulder)

	Group 1	Group 2	Group 3	Group 4
	U3	U4	U5	U6
RUN 1	321.8	322.1	315.1	309.5
RUN 2	328.2	336.5	330.9	325.5
RUN 3	325.3	329.9	325.8	319.8
RUN 4	318.6	327.2	321.7	319.2
RUN 5	317.9	330.2	323.1	318.4
RUN 6	320.2	327.1	321.2	320
RUN 7	324.8	329.7	322.8	321.8

Exit Data

	Exit		Exit		Exit
	S13	S14	P13	P14	U7
RUN 1	291.9	304	295.6	301.3	293.72
RUN 2	296.5	306	295.8	309.2	303.23
RUN 3	284.6	302	293.3	303.8	300.24
RUN 4	290.3	294.7	296.4	305.5	297.31
RUN 5	289.6	302.3	282.6	306.7	300.27
RUN 6	288.9	290.8	291.8	302.9	291.4
RUN 7	292.9	304	294.8	310.6	301.54

(350 RPM / 7 inch per min traverse / 0.7 inch shoulder)

Factor level combination 8: 350 RPM / 4 inch per min traverse / 0.7 inch shoulder

Entry Data:

	Entry 1		Entry 2		Entry 1		Entry 2		Entry 1	Entry 2
	S1	S2	S3	S4	P1	P2	P3	P4	U1	U2
RUN 1	355.5	365.8	335.2	346	370.53	382.5	313.2	335.4	395.1	339.8
RUN 2	360.7	372.3	338.2	358.6	367.6	379.9	317.7	330.3	397.8	340.8
RUN 3	361.6	373.6	345.6	354.9	378.24	381.7	317.4	338.1	402.4	348.9
RUN 4	367.2	377.2	350.2	370.2	369.78	399.5	328.5	343.7	408.6	350.8
RUN 5	362.4	364.2	346.2	349.9	367.16	381.6	323.2	333.9	403.1	353.8
RUN 6	359.1	367.4	345.3	367.3	368.67	382.9	328.9	335.1	405.8	345.7
RUN 7	353.6	377.5	352.7	360.3	373.73	376.7	324.8	337	403.2	350.3

Traverse Data:

	Group 1		Group 2		Group 3		Group 4	
	S5	S6	S7	S8	S9	S10	S11	S12
RUN 1	330.1	340.3	324.5	343	334.43	345	316.1	327.6
RUN 2	328.2	348.2	319	338.3	333.45	348.9	334.1	336.4
RUN 3	341.9	348.2	329	337.9	343.41	345	337	341.6
RUN 4	325.3	357.3	338.9	351.9	325.27	356.9	326.9	351.5
RUN 5	339.1	341.5	326.8	330.4	331.71	336.9	319.8	336.4
RUN 6	348.4	348.9	329.6	342.2	344.85	344.9	320.2	350.8
RUN 7	332.3	355.4	334.7	342.1	331.02	351.2	333.2	347.2

	Group 1		Group 2		Group 3		Group 4	
	P5	P6	P7	P8	P9	P10	P11	P12
RUN 1	337.1	351.3	322.6	336.6	339.88	350.4	288.6	333.9
RUN 2	332.3	339.2	337.9	344.8	330.08	341.1	295.4	342.4
RUN 3	341.1	348.8	318.5	345.7	340.34	342.5	299.5	346.5
RUN 4	334	359.6	332.9	359	335.26	355.4	303.5	353.9
RUN 5	336.2	339.7	331.8	336.2	334.04	345.7	294.6	350.4
RUN 6	335.6	349.5	334	347.5	322.87	345.3	299.2	350.1
RUN 7	338.6	356.5	331	350.5	328.61	350.3	300.8	354.6

(350 RPM / 4 inch per min traverse / 0.7 inch shoulder)

	Group 1	Group 2	Group 3	Group 4
	U3	U4	U5	U6
RUN 1	334.3	342.3	322	338.6
RUN 2	341.8	337	327.4	342.6
RUN 3	346.4	339.5	331	337.5
RUN 4	357.4	357.2	349	342.8
RUN 5	355.7	335.6	333.4	324.9
RUN 6	339.4	347.4	336.7	343.2
RUN 7	349.2	343.9	341.2	349.9

Exit Data:

	Group 5		Group 5		Group 5
	S13	S14	P13	P14	U7
RUN 1	303.7	316.1	315.9	316	310.19
RUN 2	298.2	319.3	308.4	319.3	315.17
RUN 3	309.5	326.9	317.3	328.2	316.59
RUN 4	322	330.4	319.7	336.4	330.7
RUN 5	310.3	324.3	306.9	330.9	307.82
RUN 6	304.8	326.7	314	326.5	319.41
RUN 7	320.6	321.2	311.4	333.1	324.93

(350 RPM / 4 inch per min traverse / 0.7 inch shoulder)

Factor level combination 9: 450 RPM / 7 inch per min traverse / 0.5 inch shoulder

Entry Data

| | Entry 1 | | Entry 2 | | Entry 1 | | Entry 2 | | Entry 1 | Entry 2 |
	S1	S2	S3	S4	P1	P2	P3	P4	U1	U2
RUN 1	342.5	353.9	322	334.2	342.33	363	316.4	318.1	382.9	335.3
RUN 2	326.8	347.9	317.2	327.8	343.63	356.2	310.9	315.2	388.4	332.6
RUN 3	339.4	359.9	324.1	342.6	350.83	371.9	310.7	324.2	396.4	336.6
RUN 4	330.3	340	318.4	325.8	354.9	363.2	312.3	321.8	377.9	330.3
RUN 5	343.8	355.5	329.1	332.2	353.81	365	316.1	326.2	388.2	334.5
RUN 6	336.9	354.9	319.9	330.9	357.22	367.9	313.7	326.1	382.5	334.3
RUN 7	337.2	348.6	318	329	349.34	359.6	313.5	326.2	390.4	333

Traverse Data

| | Group 1 | | Group 2 | | Group 3 | | Group 4 | |
	S5	S6	S7	S8	S9	S10	S11	S12
RUN 1	320	327.8	304.3	324.5	316.65	324.4	308.8	316.1
RUN 2	316.2	325.8	311.8	323.6	319.51	323.3	309.5	317.3
RUN 3	326.5	331.2	316.1	321.7	313.7	323.9	306.1	317.1
RUN 4	320.9	323.4	305.6	321.9	314.79	322.1	310.5	311.6
RUN 5	317.1	326.3	312.3	314.6	318.51	322.7	311.2	312.5
RUN 6	324.1	326.6	308.8	325	321.92	326.4	311.2	316.6
RUN 7	319.7	325.8	312	314.6	318.68	323	310.9	319.2

| | Group 1 | | Group 2 | | Group 3 | | Group 4 | |
	P5	P6	P7	P8	P9	P10	P11	P12
RUN 1	318.7	329.1	316.5	327.4	319.41	324.1	280.6	325.5
RUN 2	316.5	329.3	314.7	329.3	311.25	324.3	280.9	326.7
RUN 3	325.3	334.3	323.3	333.1	315	326	284.5	329.2
RUN 4	315.9	326.2	308.2	325.3	315.77	321.3	280.4	322.4
RUN 5	320.5	329.7	317.8	327.5	320.78	323.3	281.3	323.8
RUN 6	323.9	329.7	321	328.6	313.14	325.6	280.7	323
RUN 7	320.3	330.3	317.4	328.6	310.97	325.9	281.5	328.7

(450 RPM / 7 inch per min traverse / 0.5 inch shoulder)

	Group 1	Group 2	Group 3	Group 4
	U3	U4	U5	U6
RUN 1	323.9	330.2	320.5	323
RUN 2	327	333.7	321.1	325.3
RUN 3	330.9	330.7	323.2	324.2
RUN 4	323.1	329.2	319.1	322.2
RUN 5	326.2	333.1	322	323.7
RUN 6	328.4	333.3	317.4	319.7
RUN 7	329.2	335.8	323.3	327.4

Exit Data:

	Group 5		Group 5		Group 5
	S13	S14	P13	P14	U7
RUN 1	290.9	297	297.9	310.1	296.34
RUN 2	296.1	296.3	299.9	312.5	304.99
RUN 3	290.2	306.9	306.3	313.6	299.09
RUN 4	289.1	300	301.1	310.2	300
RUN 5	287.1	300.5	299.8	307.1	299.9
RUN 6	285.8	296.5	298.3	313	294.42
RUN 7	291.8	299	301.7	311.3	304.36

(450 RPM / 7 inch per min traverse / 0.5 inch shoulder)

Factor level combination 10: 450 RPM / 4 inch per min traverse / 0.5 inch shoulder

Entry Data

| | Entry 1 | | Entry 2 | | Entry 1 | | Entry 2 | | Entry 1 | Entry 2 |
	S1	S2	S3	S4	P1	P2	P3	P4	U1	U2
RUN 1	362.1	376.2	338.2	349.5	366.73	379.7	323.4	325.6	404.9	345.2
RUN 2	351.1	370.2	326.1	348.4	358.42	369.6	311.1	331.5	391.1	321.9
RUN 3	353.7	359.4	342.8	341.5	362.39	378.1	312.8	330.6	391.5	336.5
RUN 4	355.2	373.8	337	362.3	356.44	375	321.6	335.2	415.4	349.7
RUN 5	357.9	370.7	341.3	349.9	367.19	380	319.5	330.8	398.6	347.7
RUN 6	350.6	361.5	335.3	347	362.89	374.2	315.8	318.9	395.2	335.7
RUN 7	358.3	369.6	329.7	347.5	362.21	360.8	312.3	318.7	396.2	347.5

Traverse Data

| | Group 1 | | Group 2 | | Group 3 | | Group 4 | |
	S5	S6	S7	S8	S9	S10	S11	S12
RUN 1	330.4	345.3	324	333.7	336.1	339.8	339.3	339.9
RUN 2	309	344.5	295.6	323.9	315.75	347.8	328.9	347.4
RUN 3	328.5	341.9	309.1	324	323.75	342	329.6	341
RUN 4	339.4	350.4	307.6	345.7	319.13	349.6	326.5	346.7
RUN 5	330.3	353.1	318.8	328.9	338.69	342.5	339.5	343.2
RUN 6	332.6	345	314.5	326.7	330.98	342.3	329.7	342.1
RUN 7	332.2	334.7	310.3	325.6	331.27	335.6	336.1	336.9

| | Group 1 | | Group 2 | | Group 3 | | Group 4 | |
	P5	P6	P7	P8	P9	P10	P11	P12
RUN 1	333.5	346.2	322.6	342.4	334.07	337.2	297.5	349
RUN 2	328.6	344.6	326.3	342.2	310.57	344.9	281	322
RUN 3	328.3	342.2	323.1	336.7	323.12	341.3	291.5	340.7
RUN 4	346.5	352.6	335.8	349.8	327.23	349.1	302.4	359.5
RUN 5	334	354.5	323.3	348.1	326.31	341.3	300.7	352.5
RUN 6	331.6	344.7	328.7	331.6	330.65	343.2	291.3	343.7
RUN 7	329.4	341.9	327	336.1	330.51	333.7	289.1	338.5

(450 RPM / 4 inch per min traverse / 0.5 inch shoulder)

	Group 1	Group 2	Group 3	Group 4
	U3	U4	U5	U6
RUN 1	348.1	347.8	334.7	329.8
RUN 2	310	312.6	307.1	309.1
RUN 3	337.6	328.3	324.7	340.9
RUN 4	352.6	348.9	344	337
RUN 5	348.5	336.8	334.1	343.1
RUN 6	338.3	332.9	324.8	332.2
RUN 7	335.2	333.6	323.7	319.5

Exit Data

	Exit		Exit		Exit
	S13	S14	P13	P14	U7
RUN 1	304.2	319.5	319.8	326.6	311.56
RUN 2	302.5	305.5	307.6	334.8	297.11
RUN 3	308.4	314.4	312.6	322.1	319.59
RUN 4	298.1	311.1	314.7	336.6	298.27
RUN 5	307.5	317.7	318.4	330.5	317.99
RUN 6	300.6	320.1	320.1	320.3	309.67
RUN 7	302.5	318.4	311.8	329	303.69

(450 RPM / 4 inch per min traverse / 0.5 inch shoulder)

Factor level combination 11: 350 RPM / 7 inch per min traverse / 0.5 inch shoulder

Entry Data

	Entry 1		Entry 2		Entry 1		Entry 2		Entry 1	Entry 2
	S1	S2	S3	S4	P1	P2	P3	P4	U1	U2
RUN 1	312.5	322.6	284.4	304.9	323.14	343.1	295.1	299.9	344.2	294.6
RUN 2	318.3	329.7	294.8	300.2	329.32	332.2	278.5	305.3	359.2	298.8
RUN 3	326	331.4	288.8	303.9	317.18	337.5	281.9	309.9	354.6	303.1
RUN 4	309.3	333.6	297	303.2	318.58	340	293	299.6	357.7	313.7
RUN 5	310.7	331.3	289.1	307.5	317.35	337.9	294.6	303.2	354.7	306.7
RUN 6	310.8	324.2	298.7	298.9	331.45	336.1	288.2	299.9	353.4	303.3
RUN 7	304.8	332.2	288.2	309.8	331.21	346.4	295.3	307.1	356.4	313.2

Traverse Data

	Group 1		Group 2		Group 3		Group 4	
	S5	S6	S7	S8	S9	S10	S11	S12
RUN 1	279	292.3	277.1	292.2	293.91	301	289.3	300.7
RUN 2	283.4	298.9	271.2	279.6	285.14	306.1	288.7	303.7
RUN 3	282.9	294.3	277.9	293.9	281.74	312.4	290.9	298.5
RUN 4	294.7	305	281	296.1	297.06	306.7	300.2	304.6
RUN 5	286.3	301.5	284.6	300	301.39	309.7	296.9	304.1
RUN 6	285.3	291.4	277.5	292.5	289.47	301	286	300.1
RUN 7	290.3	305.3	286.2	296.7	288.82	296.3	285.5	305.9

	Group 1		Group 2		Group 3		Group 4	
	P5	P6	P7	P8	P9	P10	P11	P12
RUN 1	292.2	304	279.6	300.7	293.08	309.5	269.4	298.1
RUN 2	287.6	310.6	283.9	298.3	295.57	304.6	277.1	300.9
RUN 3	293.9	306.4	280.7	293.3	282.66	300.3	258.8	305.5
RUN 4	298.5	306.5	288.5	304.8	297.45	304.8	274.2	306.3
RUN 5	300.9	313.9	288.2	301.4	293.21	309.7	272.7	314.2
RUN 6	297	304.2	281	292.5	290.93	312.5	263.8	301
RUN 7	302.7	309	289.6	299.5	290.64	314.9	275.9	314.7

(350 RPM / 7 inch per min traverse / 0.5 inch shoulder)

	Group 1	Group 2	Group 3	Group 4
	U3	U4	U5	U6
RUN 1	291.8	297.2	297.8	288.4
RUN 2	289.6	299.9	302.6	291.5
RUN 3	296.1	295.8	299.7	288
RUN 4	306.6	310.4	301.9	294.5
RUN 5	301	311	303.9	286.8
RUN 6	286.8	309.6	294	294
RUN 7	305.5	313.3	314.6	304

Exit Data

	Group 5		Group 5		Group 5
	S13	S14	P13	P14	U7
RUN 1	275.1	278.5	261	287.6	279.31
RUN 2	265	276.3	267.9	280.2	290.55
RUN 3	263.1	276.3	265.3	276.6	274.75
RUN 4	275.2	281.8	274.5	282.8	291.9
RUN 5	275.3	282.9	268	278.4	288.39
RUN 6	268	279.7	262.4	285.2	278.77
RUN 7	266.1	283.9	276	281.9	292.69

(350 RPM / 7 inch per min traverse / 0.5 inch shoulder)

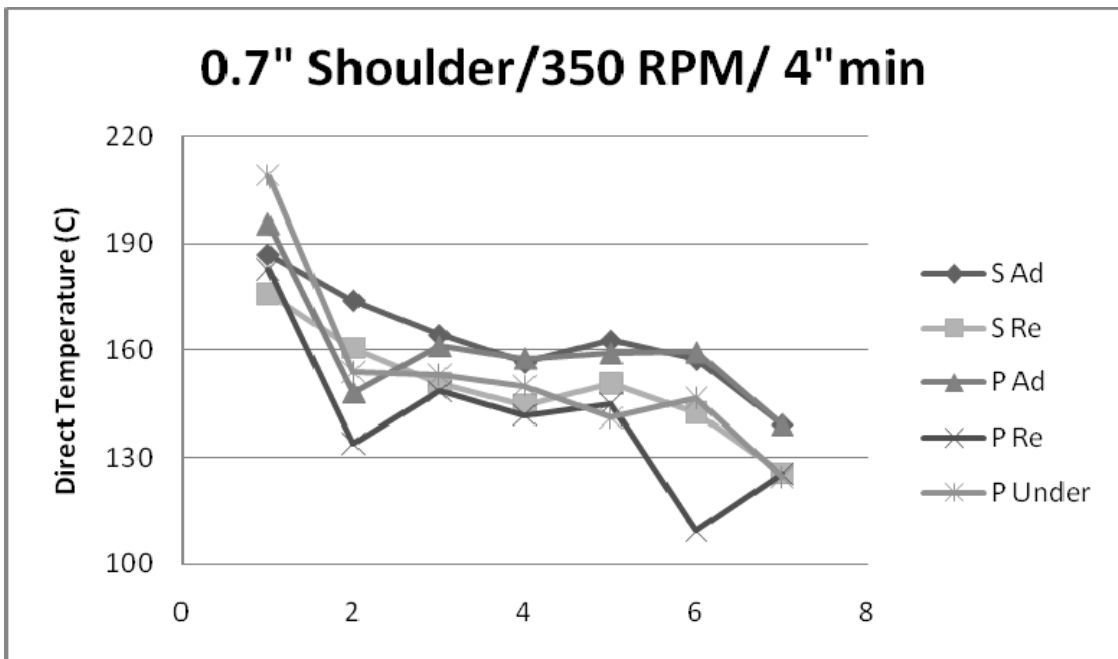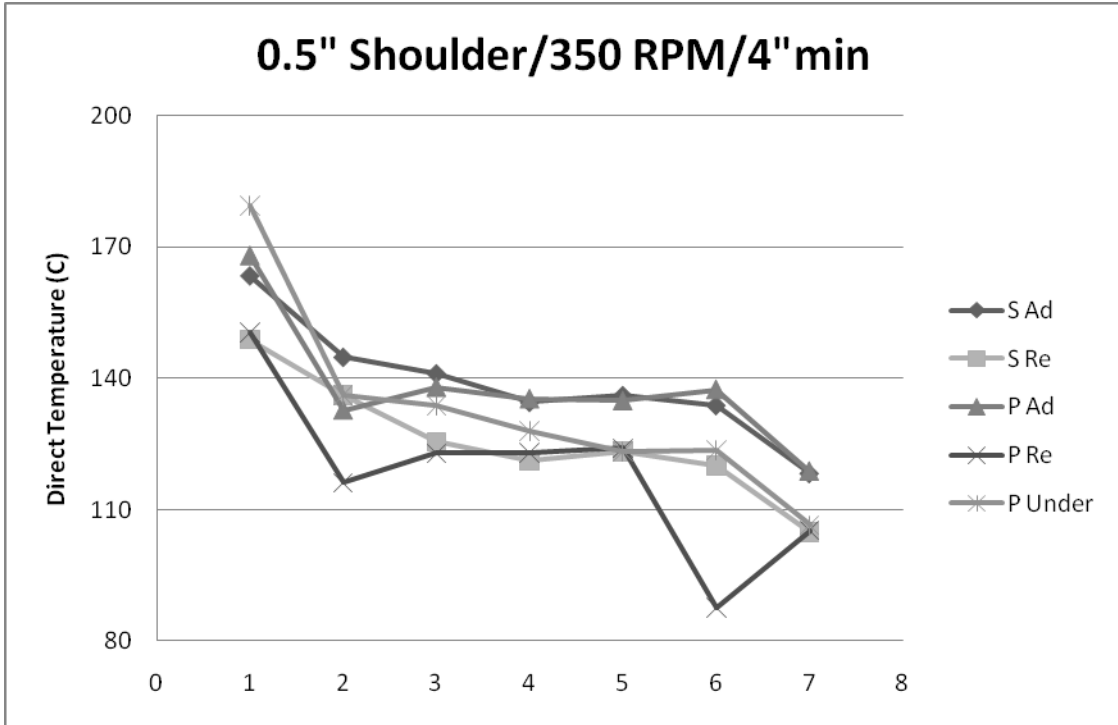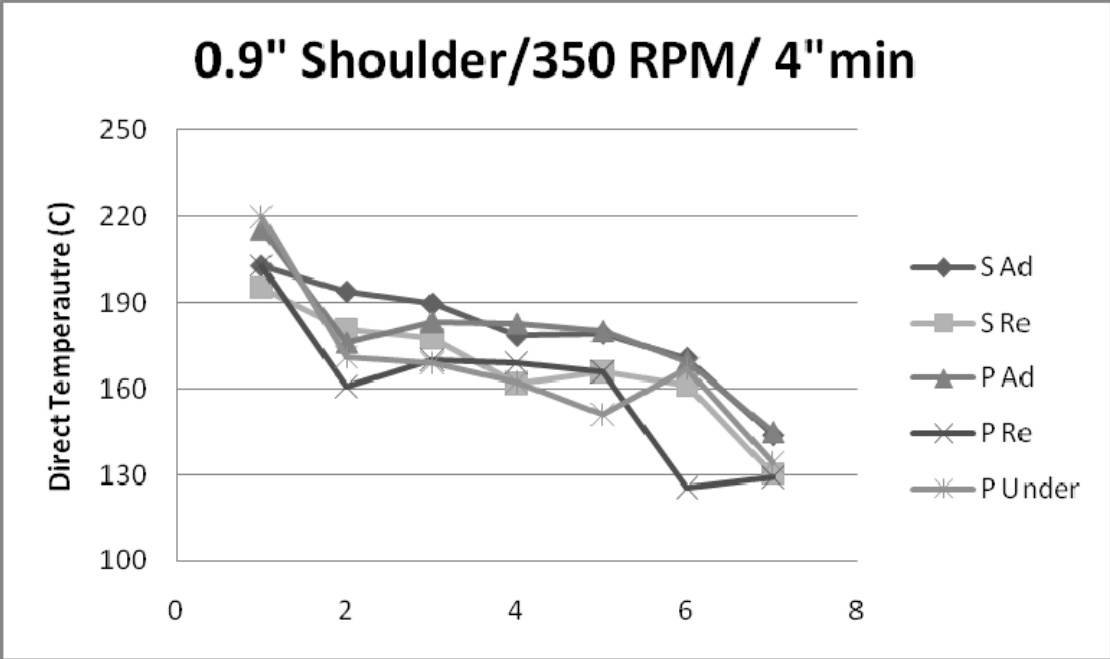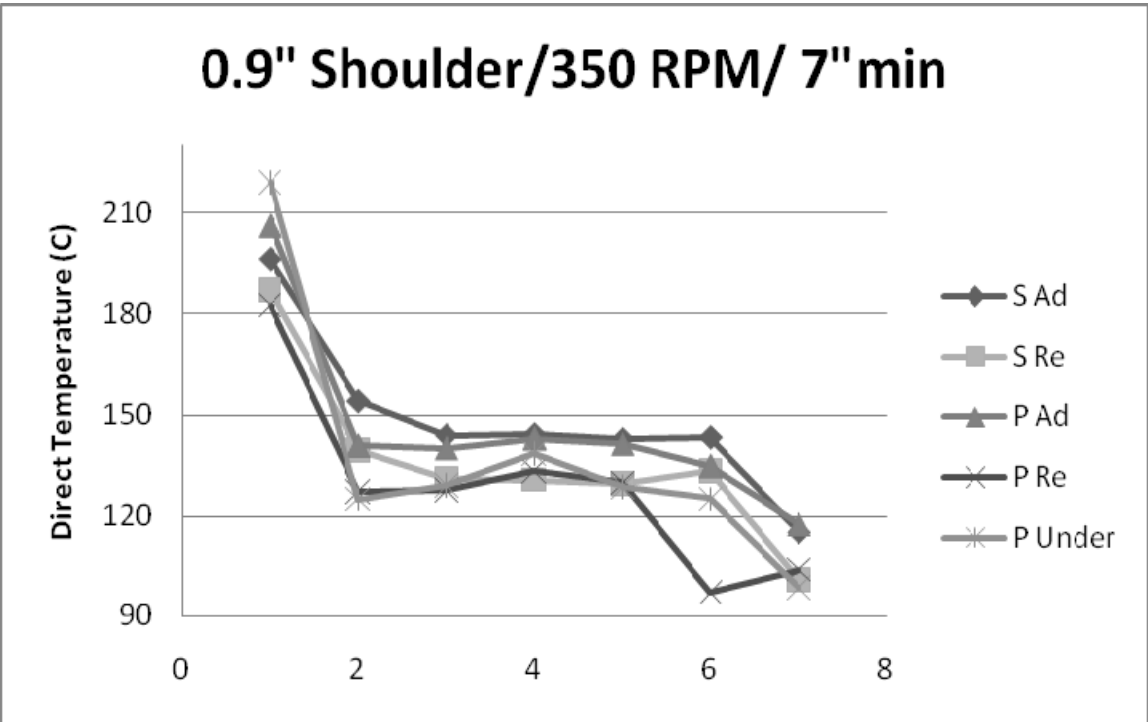Factor level combination 12: 350 RPM / 4 inch per min traverse / 0.5 inch shoulder

Entry Data:

| | Entry 1 | | Entry 2 | | Entry 1 | | Entry 2 | | Entry 1 | Entry 2 |
	S1	S2	S3	S4	P1	P2	P3	P4	U1	U2
RUN 1	332.8	349.8	316	329.7	338.14	349.8	299	320.2	366.5	324.4
RUN 2	333.8	345.4	318.1	328.6	325.74	349.6	301.6	322	379.9	332.5
RUN 3	350	352.5	332.5	334.2	335.9	359.7	317.6	319.3	375.6	339.3
RUN 4	327.4	353.1	317.9	330.9	340.77	358.7	303.4	320.5	369.9	322.6
RUN 5	332.1	344.6	320.2	330.6	349.96	352.5	303.6	323.8	379.5	328.7
RUN 6	333.7	344.8	318.4	327.4	336.36	348.1	301.7	324.8	364.8	332.3
RUN 7	321.6	343.5	319.4	322.3	341.88	373.4	301.8	314.1	372.8	325.5

Traverse Data:

| | Group 1 | | Group 2 | | Group 3 | | Group 4 | |
	S5	S6	S7	S8	S9	S10	S11	S12
RUN 1	301.2	324.6	304.1	317.3	310.66	320	309.5	317.4
RUN 2	308.7	325.6	303.1	319	308.9	319.6	307.8	316.5
RUN 3	326.5	330.4	313.2	318.7	310.57	326.4	306.4	327.1
RUN 4	306.1	323.6	304.6	320.6	312.68	322.8	302.4	319.5
RUN 5	309.9	326.1	306	320.2	308.46	318.6	303.4	320.4
RUN 6	310.5	331	306.2	322	291.05	312.6	292.6	313.9
RUN 7	305.3	316.2	300.5	313.9	309.67	322.6	308.2	311.8

| | Group 1 | | Group 2 | | Group 3 | | Group 4 | |
	P5	P6	P7	P8	P9	P10	P11	P12
RUN 1	305.8	325.3	308	321.5	311.18	327.3	278.7	323.8
RUN 2	309	326.8	306.6	324.2	308.72	318.2	277.9	322.2
RUN 3	324.2	335	321.4	328.7	320.87	327.9	280	339
RUN 4	309.6	325	308.4	323.4	311.59	319.9	275.8	323.1
RUN 5	311.7	328.1	310	325.8	308.95	319.1	276.7	326.6
RUN 6	307.7	322.7	315.8	321.9	312.21	323.6	264.1	323.3
RUN 7	308	318.2	306.9	317.2	310.78	323.8	275.9	319.6

(350 RPM / 4 inch per min traverse / 0.5 inch shoulder)

	Group 1	Group 2	Group 3	Group 4
	U3	U4	U5	U6
RUN 1	324.9	313.8	308.9	314.4
RUN 2	325.2	320.2	314.1	322
RUN 3	337.9	333.9	327	318.4
RUN 4	326.5	320.2	315.6	320.9
RUN 5	328.8	323.3	317.4	318.6
RUN 6	329.7	316.1	320.5	302.6
RUN 7	316.1	321.5	312.5	320.8

Exit Data

	Exit		Exit		Exit
	S13	S14	P13	P14	U7
RUN 1	287.9	303.5	290.2	305.9	301.04
RUN 2	290.9	299.3	292.8	305.3	303.85
RUN 3	303.1	307.4	309.5	323.3	303.99
RUN 4	284.7	301.4	287.8	302.5	300.52
RUN 5	287.1	306.6	291	307.7	300.6
RUN 6	279.3	296.5	287.9	301.4	289.08
RUN 7	290.2	303.3	293.6	300.6	299.24

(350 RPM / 4 inch per min traverse / 0.5 inch shoulder)

APPENDIX C:

Direct temperature plots: Average of the recorded peak temperatures of the 7 experiments for all factor level combinations.

Three different shoulders, with 2 different RPMs and 2 different feed rates were used in this experiment. That gives a total of 12 different factor level combinations. For each factor level combination, 7 experiments were done. For each experiment 7 sets of thermocouples (Entry 1, Entry 2, Group 1, Group 2, Group 3, Group 4 and Group 5) were used to record temperatures as discussed earlier in chapter 3. Recorded temperatures of all 7 experiments for 12 different parameters are given in Appendix A. Averages of the peak temperatures of the 7 experiments for all factor level combinations are given in this appendix.

In the plots shown below, except for point 1(Entry 1) which acts as entry point and point 7 (Group 5) which acts as exit point, temperatures at all other sets are more or less the same. Average of all advancing side and average of all retreating side temperatures in these 5 sets would give an appropriate value for advancing and retreating side temperatures for that given factor level combination.

0.5" Shoulder/350 RPM/4"min

0.7" Shoulder/350 RPM/ 4"min

164

0.9" Shoulder/350 RPM/ 4"min

0.5" Shoulder/350 RPM/ 7"min

0.7" Shoulder/350 RPM/ 7"min

0.9" Shoulder/350 RPM/ 7"min

0.5" Shoulder/450 RPM/ 4"min

0.7" Shoulder/450 RPM/ 4"min

0.9" Shoulder/450 RPM/ 4"min

0.5" Shoulder/450 RPM/ 4"min

0.7" Shoulder/450 RPM/ 7"min

0.9" Shoulder/450 RPM/7"min
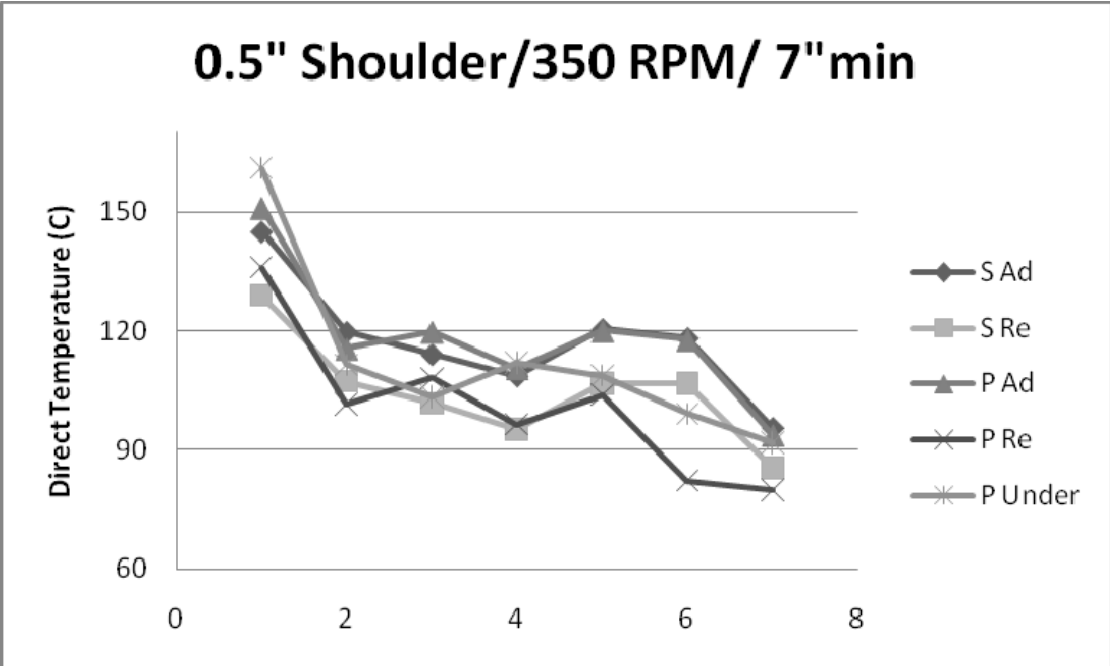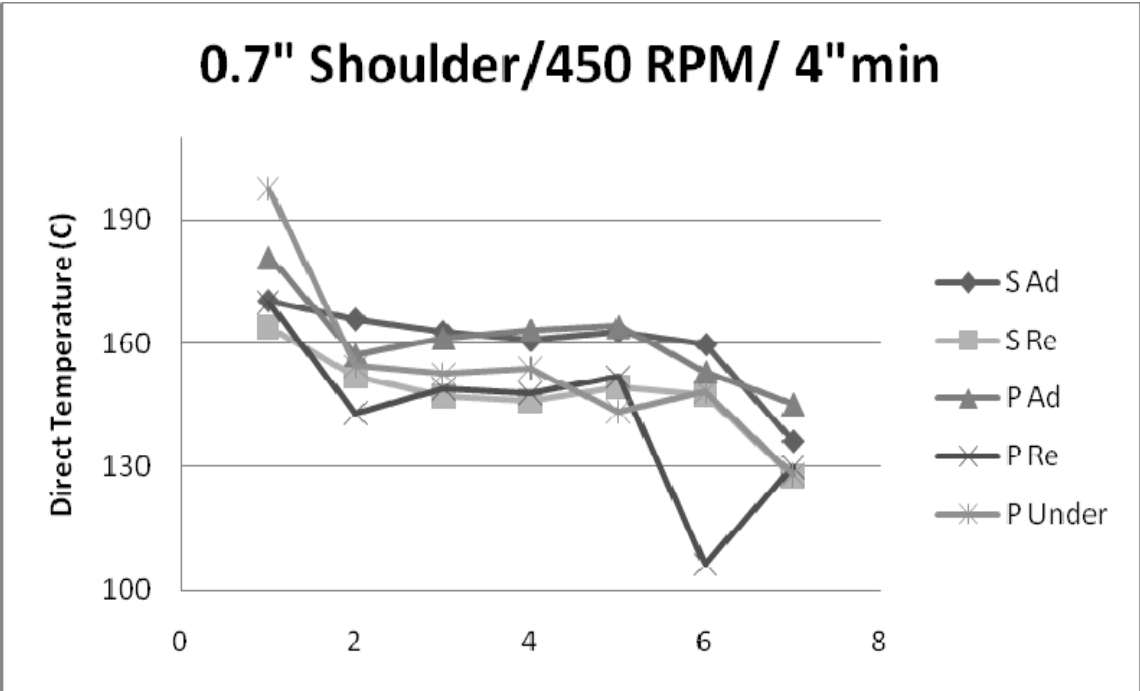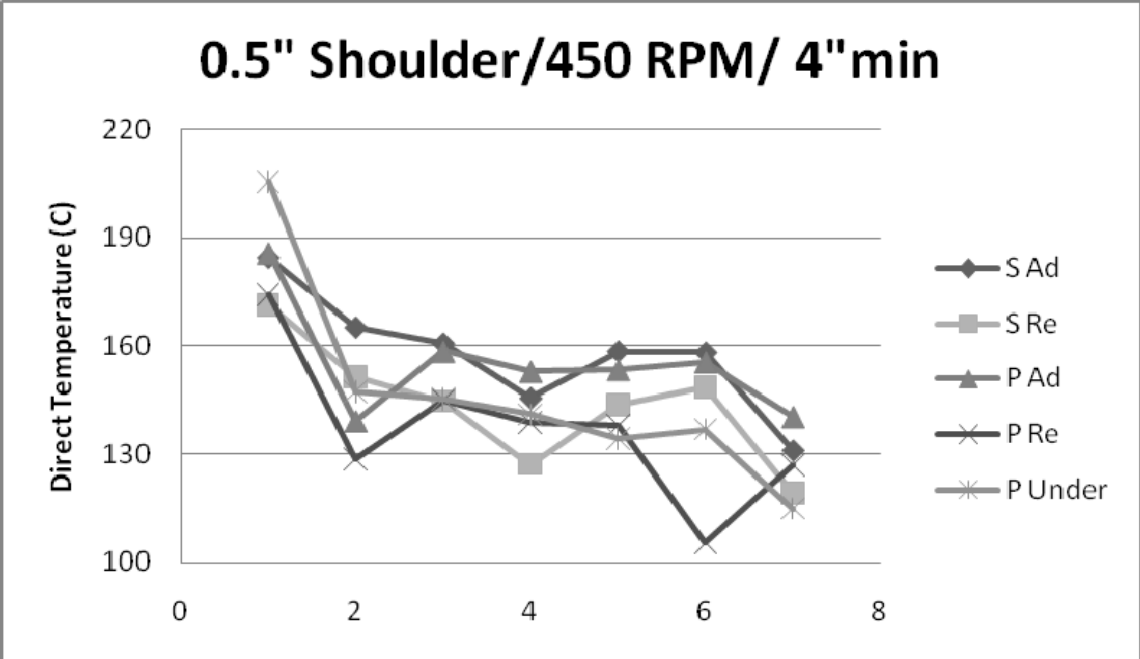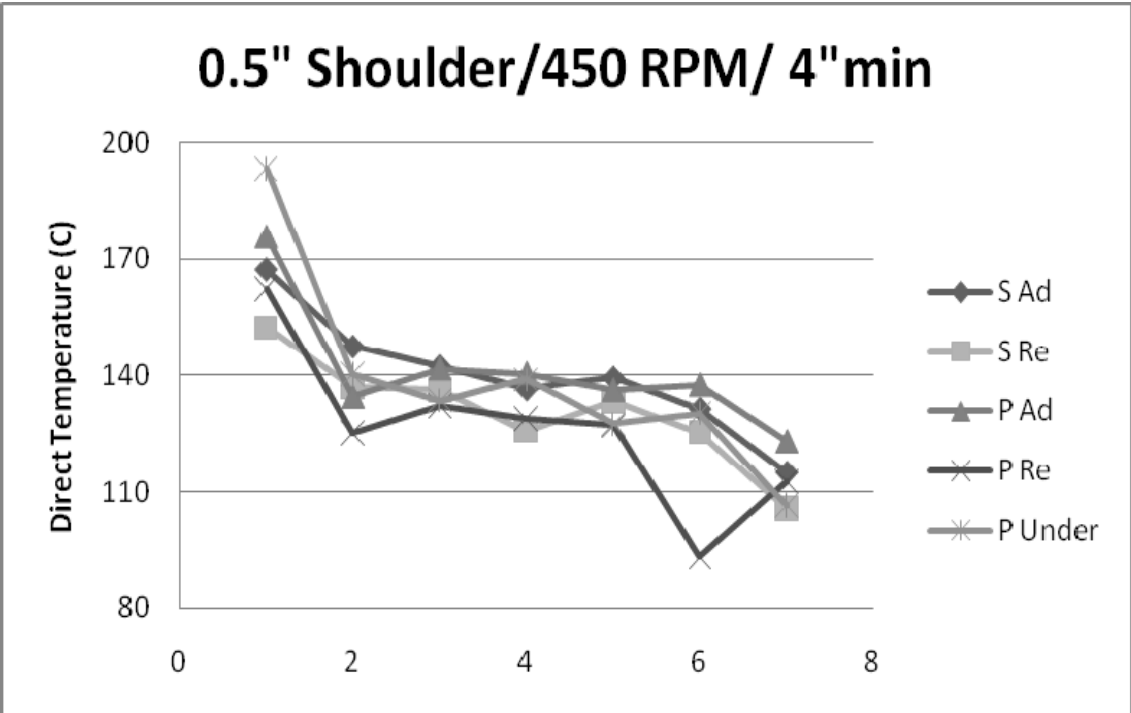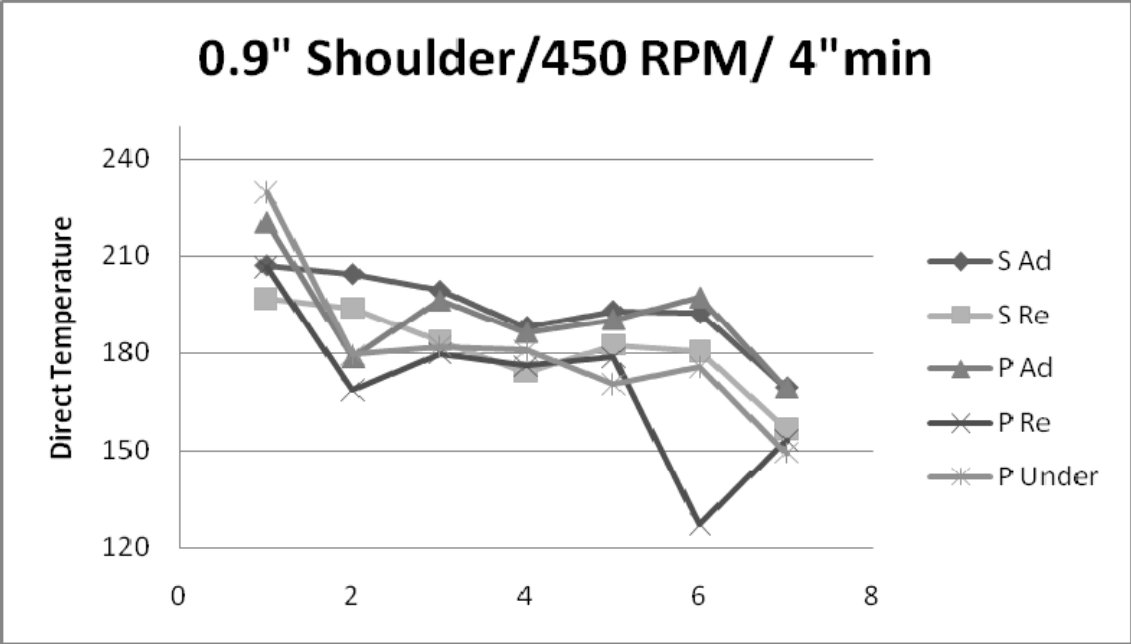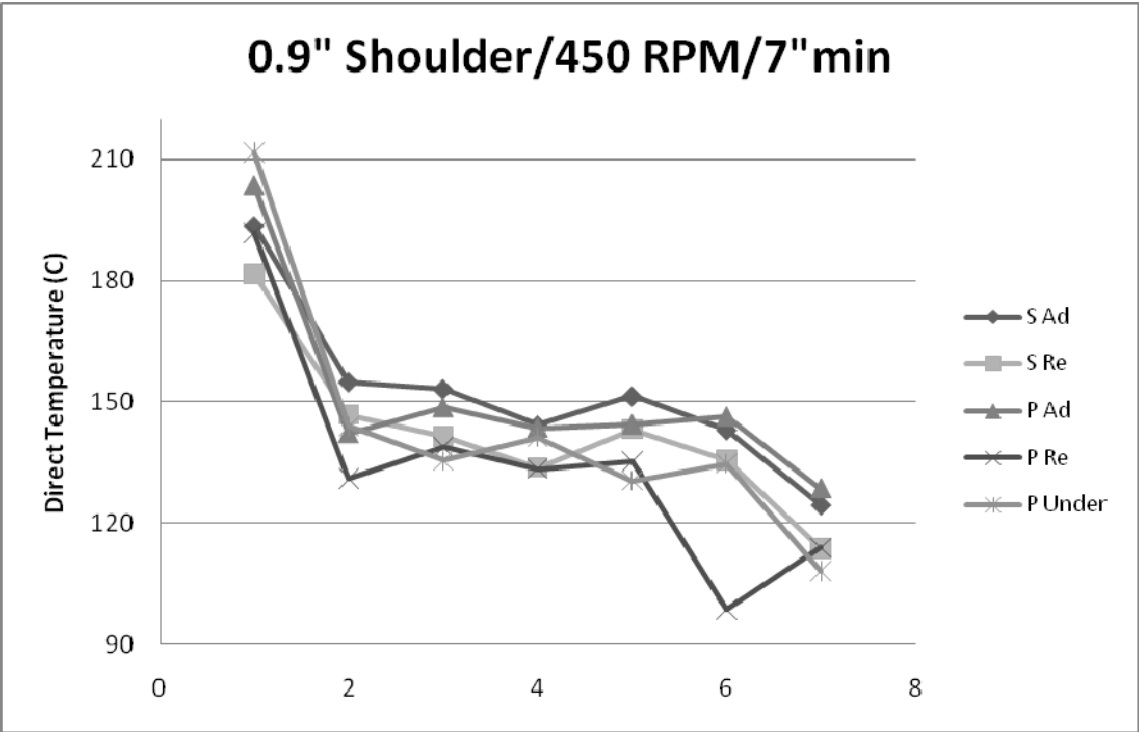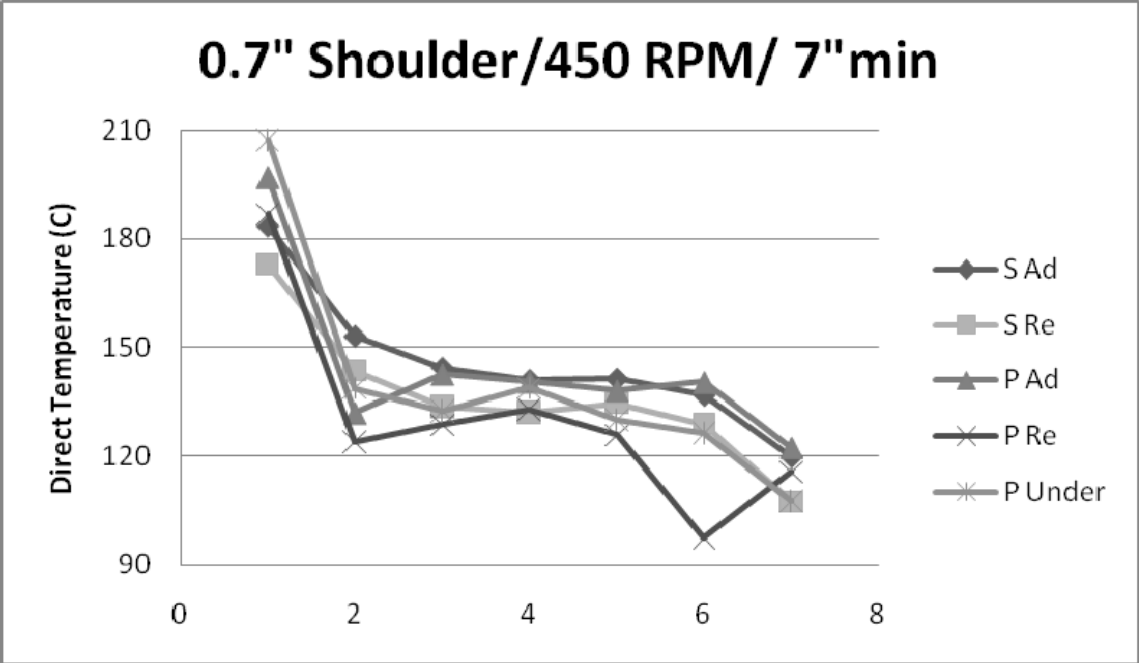
APPENDIX D:

Calculated temperature plots: Average of the calculated peak temperatures using thermodynamics equation of the 7 experiments for all factor level combinations.

Three different shoulders, with 2 different RPMs and 2 different feed rates were used in this experiment. That gives a total of 12 different factor level combinations. For each factor level combination, 7 experiments were done. For each experiment 7 sets of thermocouples (Entry 1, Entry 2, Group 1, Group 2, Group 3, Group 4 and Group 5) were used to record temperatures as discussed earlier in chapter 4. Recorded temperatures of all 7 experiments for 12 different parameters are given in Appendix A. One dimensional heat transfer equation was used to calculate the temperature at the tool tip from these recorded temperatures. The calculated temperatures are given in Appendix B. The calculated averages of the peak temperatures of the 7 experiments for all factor level combinations are given in this appendix.

In the plots which are going to follow , except for point 1(Entry 1) which acts as entry point and point 7 (Group 5) which acts as exit point, temperatures at all other sets are more or less the same. Average of all advancing side and average of all retreating side temperatures in these 5 sets would give an appropriate value for advancing and retreating side temperatures at the tool tip for that given factor level combination.

Calculated Temperature: 0.5" Shoulder/350 RPM/ 4"min
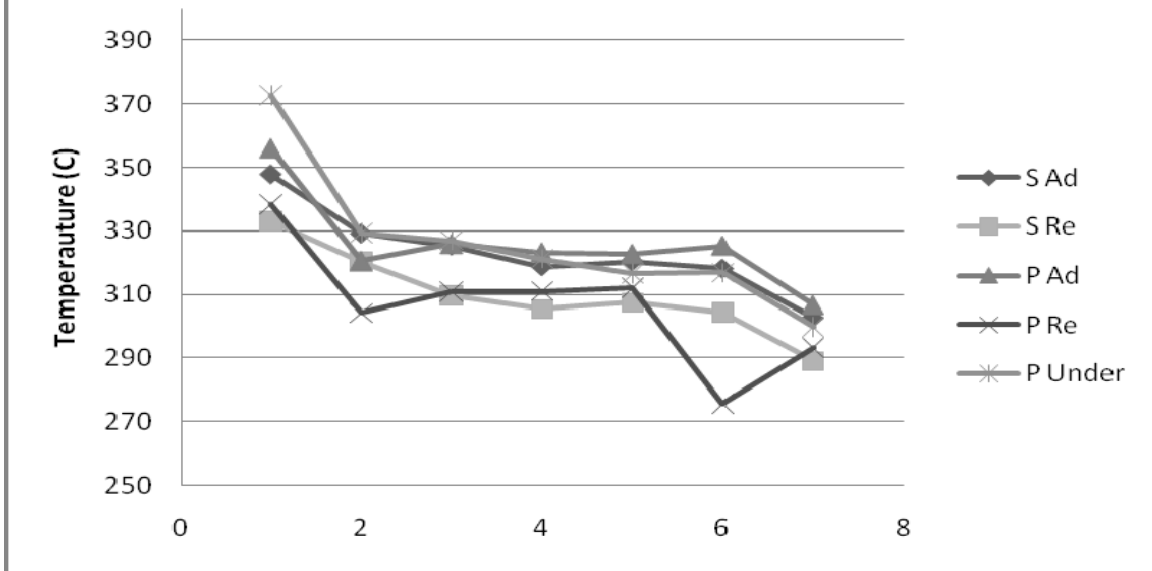
Calculated Temperature: 0.7" Shoulder/350 RPM/ 4"min

Calculated Temperature:
0.9" Shoulder/350 RPM/ 4"min



Calculated Temperature:
0.5" Shoulder/350 RPM/ 7"min

Calculated Temperature: 0.7" Shoulder/350 RPM/ 7"min

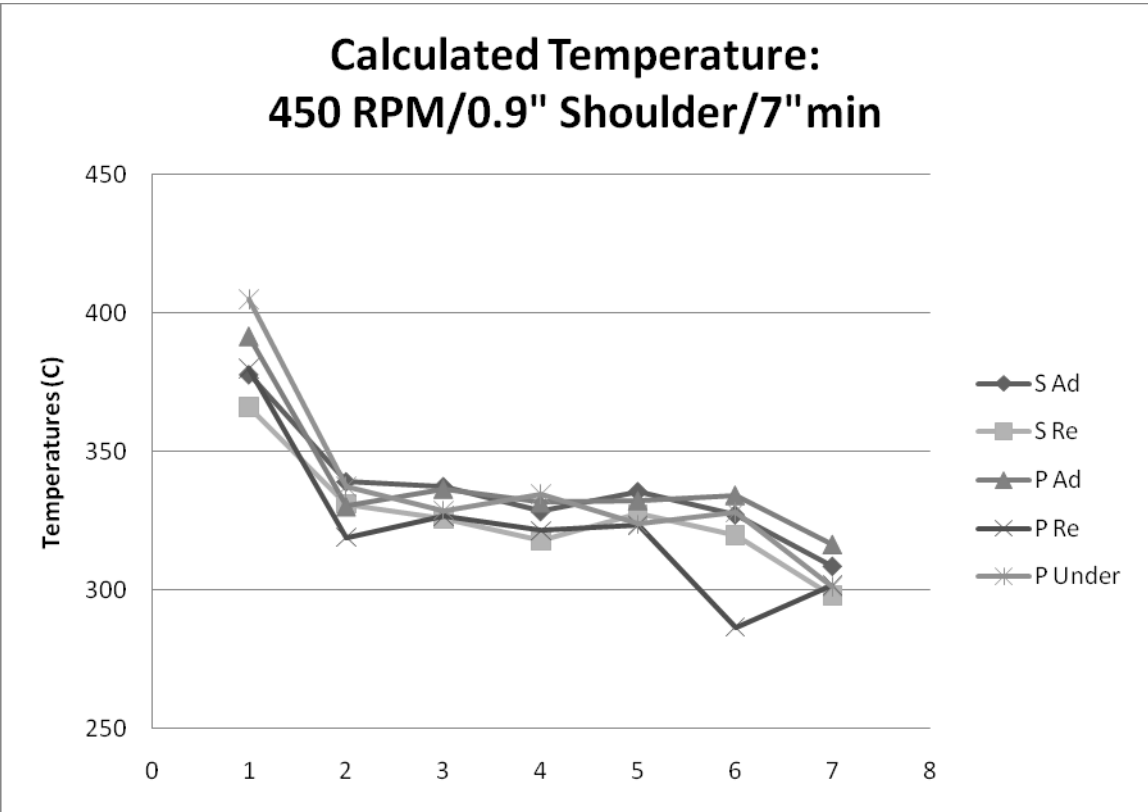**Calculated Temperature: 0.9" Shoulder/350 RPM/ 7"min**

173

Calculated Temperature:
0.5" Shoulder/450 RPM/ 4"min

Calculated Temperature:
0.7" Shoulder/450 RPM/ 4"min

174

Calculated Temperature: 0.9" Shoulder/450 RPM/ 4"min
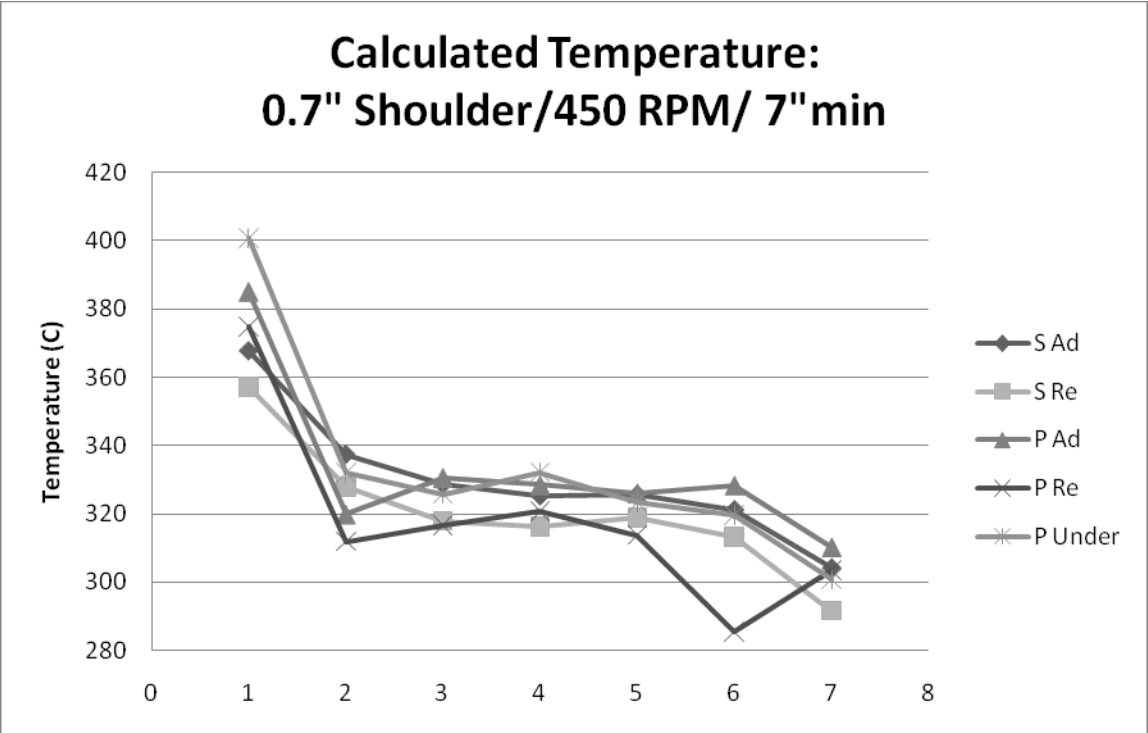

Calculated Temperature: 0.5" Shoulder/450 RPM/ 4"min
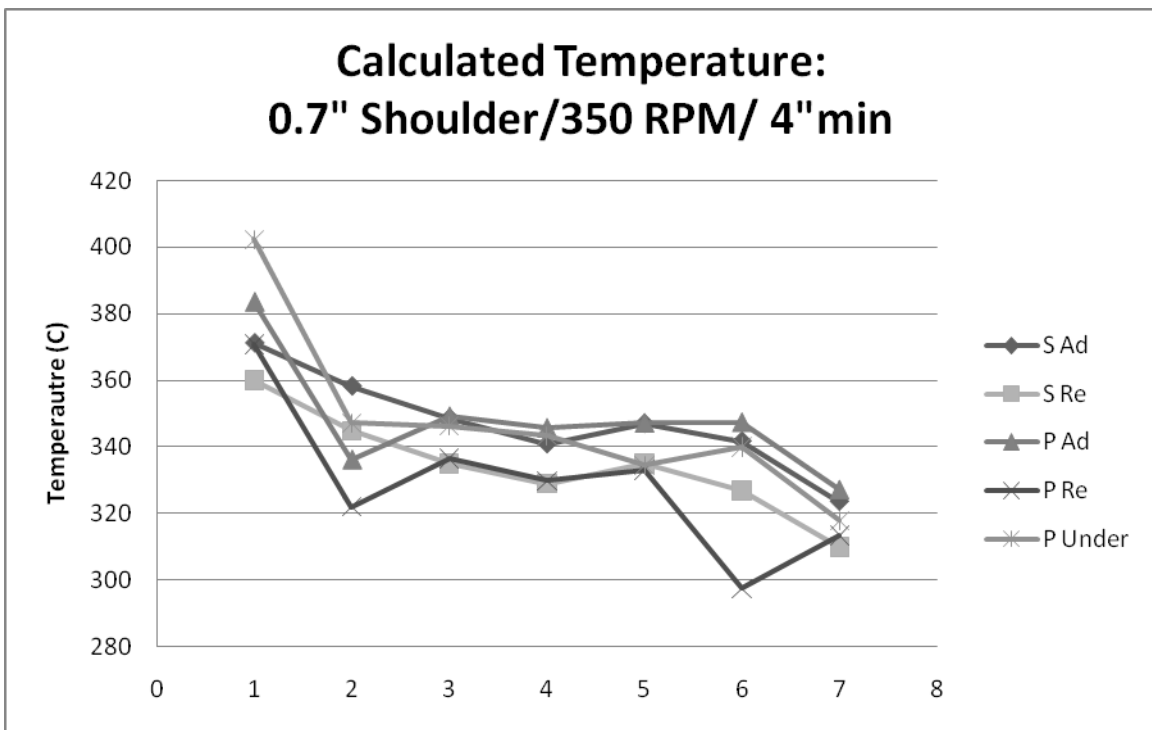
Calculated Temperature:
0.7" Shoulder/450 RPM/ 7"min
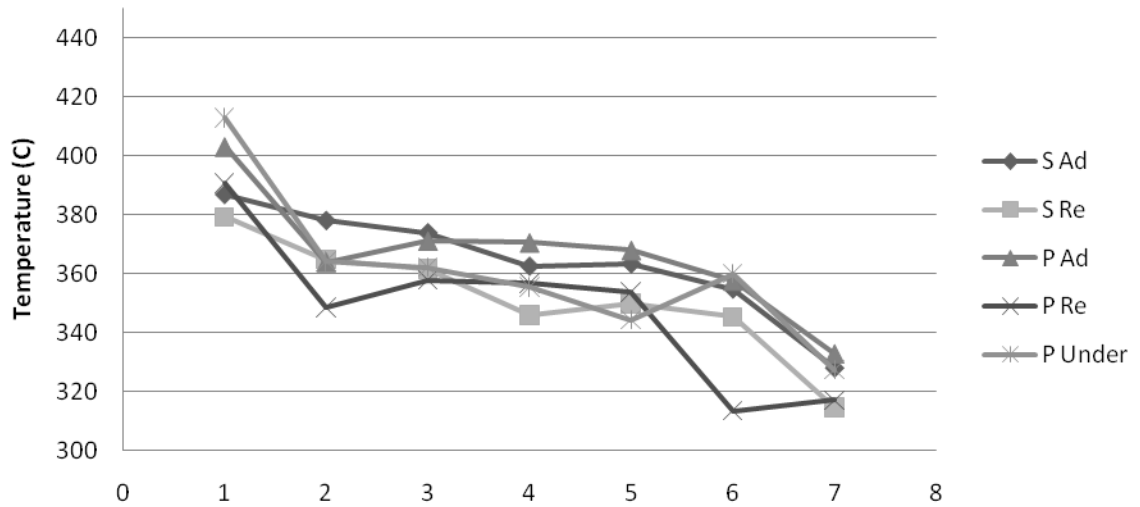
Calculated Temperature:
450 RPM/0.9" Shoulder/7"min
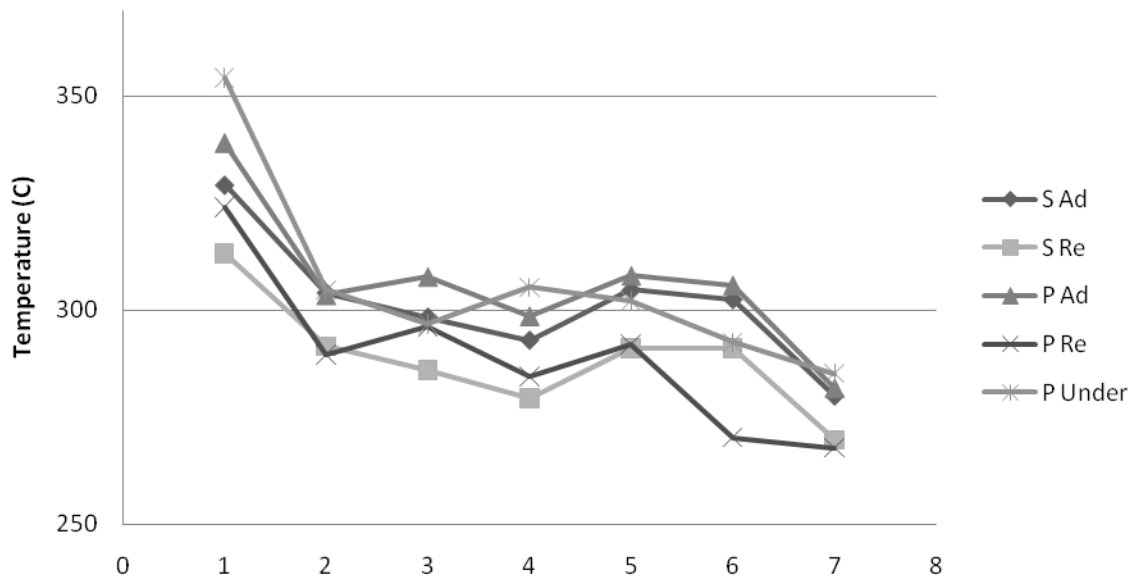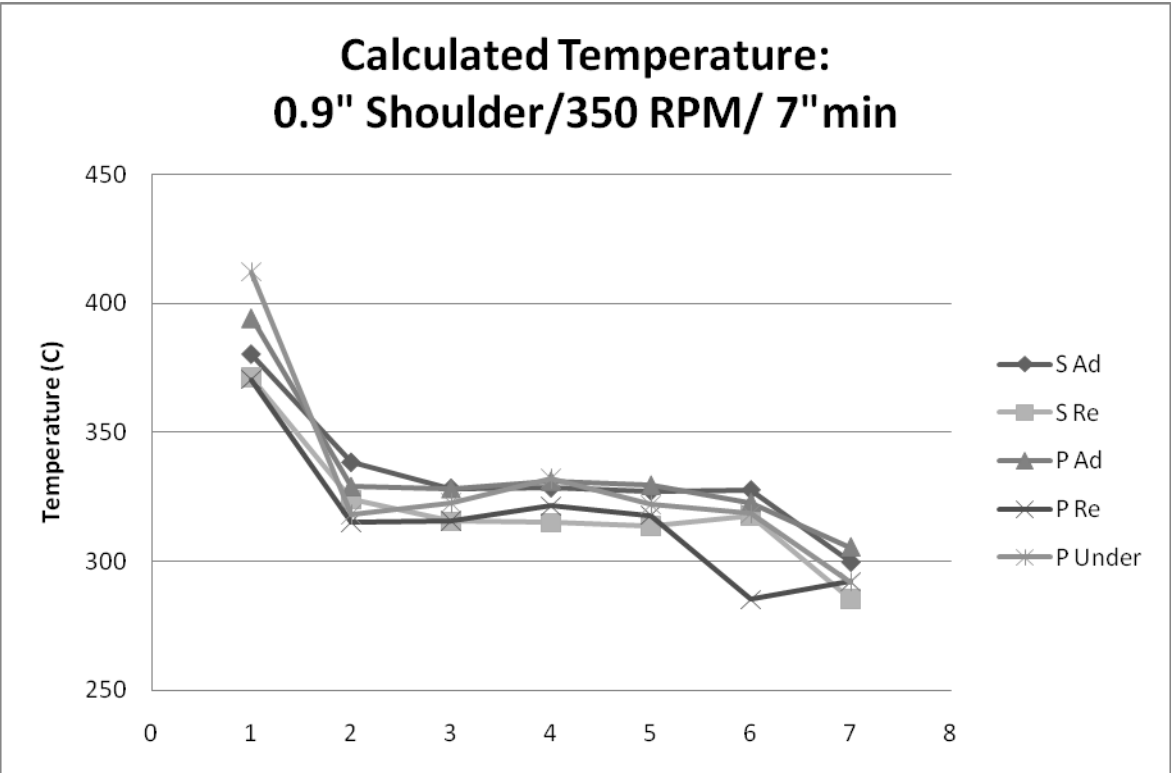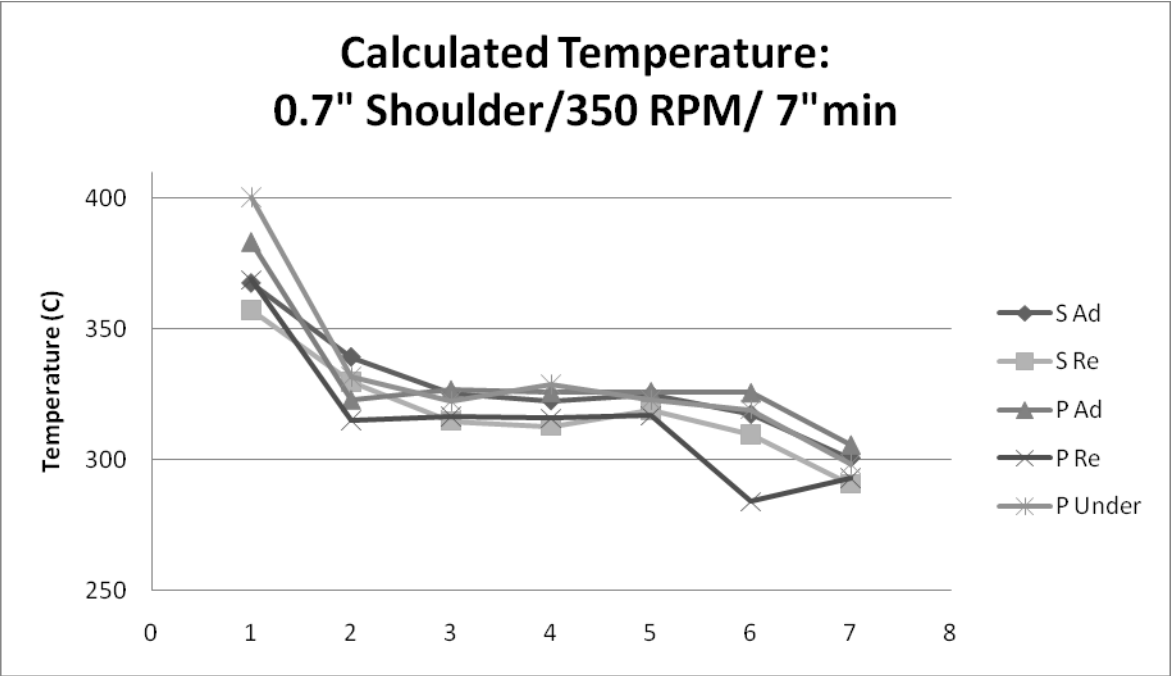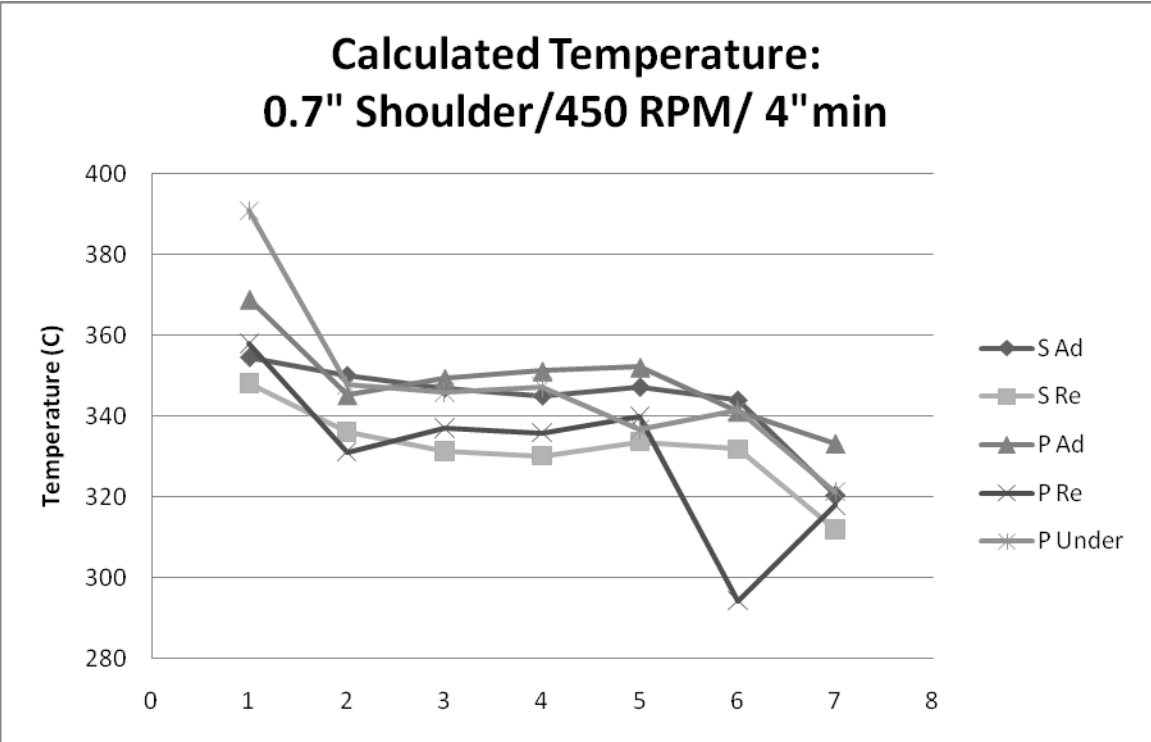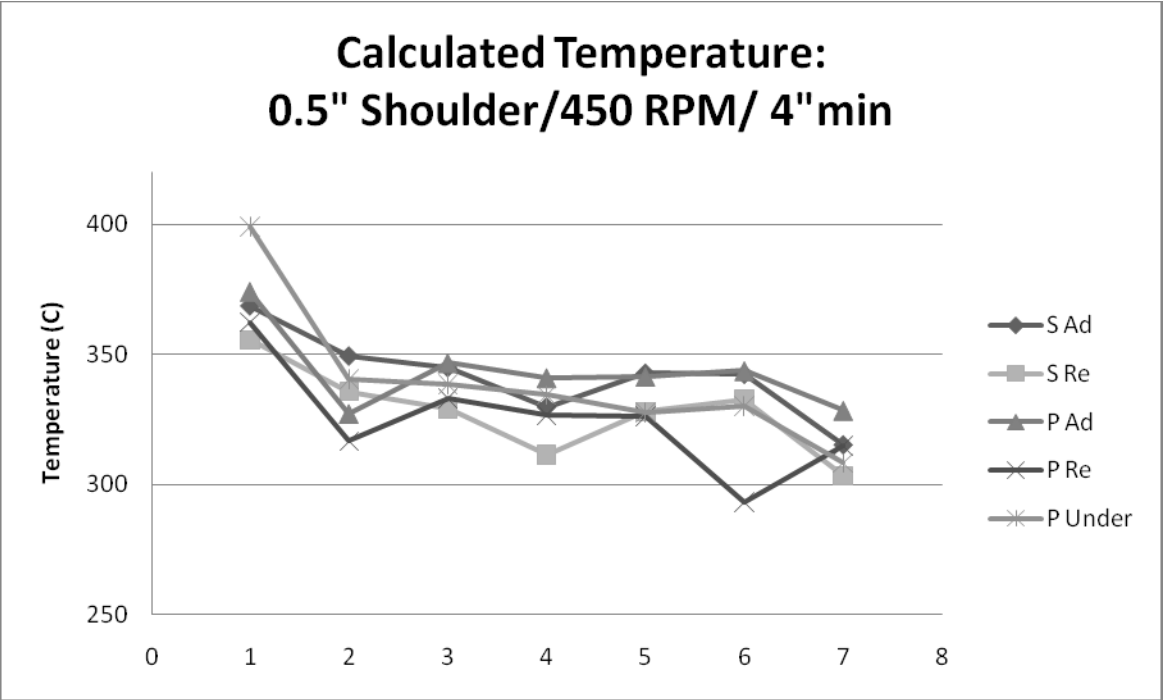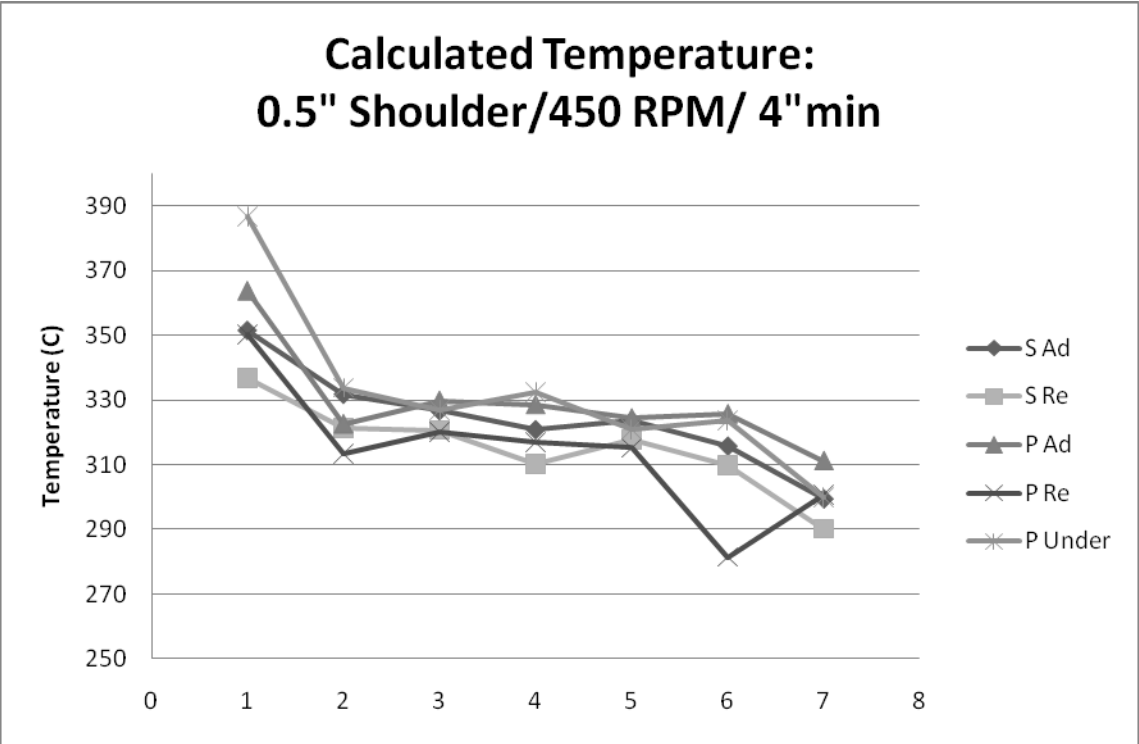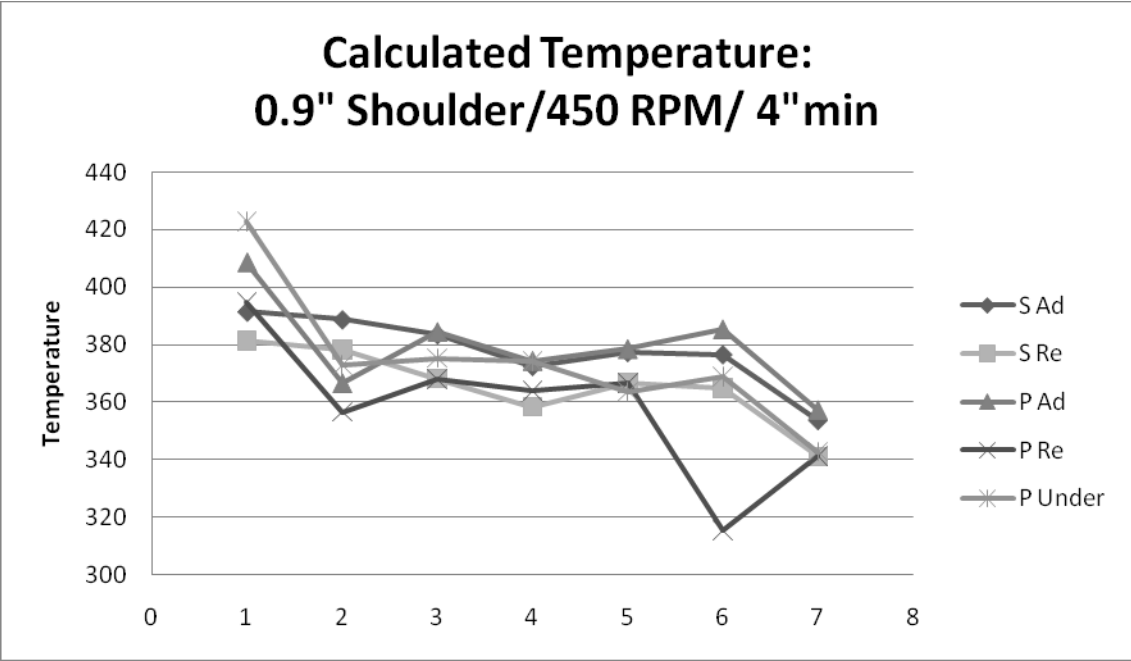
APPENDIX E:

Analysis of variance (ANOVA) is done for each responses involved in the experiment, to find the impact factors on the responses. In statistics, analysis of variance is a collection of statistical models, and their associated procedures, in which the observed variance is partitioned into components due to different explanatory variables. A summary of the largest impact factors are given in the results chapter. ANOVA tables for every response involved in this experiment are given in this appendix. STATEASE was the software used to do the analysis of variance. The responses involved with the experiment are,

Shoulder responses: S1, S2, S3… S14

Pin responses: P1, P2, P3… P14

Under the pin responses: U1, U2… U7

The ANOVA tables of every response that are to follow are the screen shots of the result obtained from STATEASE software. The most important value in the tables below is the F value. F value shows the significance of a factor on the response involved. The factor with the highest F-value has the strongest impact on the response.

Response   S1

ANOVA for selected factorial model

Analysis of variance table [Classical sum of squares - Type II]

Source	Sum of Squares	df	Mean Square	F Value	p-value Prob > F	
Model	30168.58	11	2742.60	123.00	< 0.0001	significant
A–RPM	153.19	1	153.19	6.87	0.0107	
B–Traverse	1814.66	1	1814.66	81.38	< 0.0001	
C–Shoulder	22219.52	2	11109.76	498.25	< 0.0001	
AB	1009.18	1	1009.18	45.26	< 0.0001	
AC	113.18	2	56.59	2.54	0.0861	
BC	1829.35	2	914.67	41.02	< 0.0001	
ABC	3029.50	2	1514.75	67.93	< 0.0001	
Pure Error	1605.43	72	22.30			
Cor Total	31774.01	83				

The Model F-value of 123.00 implies the model is significant. There is only
a 0.01% chance that a "Model F-Value" this large could occur due to noise.

Response   S2

ANOVA for selected factorial model

Analysis of variance table [Classical sum of squares - Type II]

Source	Sum of Squares	df	Mean Square	F Value	p-value Prob > F	
Model	24465.05	11	2224.10	97.47	< 0.0001	significant
A–RPM	140.82	1	140.82	6.17	0.0153	
B–Traverse	1253.56	1	1253.56	54.94	< 0.0001	
C–Shoulder	17028.63	2	8514.31	373.16	< 0.0001	
AB	660.15	1	660.15	28.93	< 0.0001	
AC	339.10	2	169.55	7.43	0.0012	
BC	1843.24	2	921.62	40.39	< 0.0001	
ABC	3199.55	2	1599.77	70.11	< 0.0001	
Pure Error	1642.83	72	22.82			
Cor Total	26107.88	83				

The Model F-value of 97.47 implies the model is significant. There is only
a 0.01% chance that a "Model F-Value" this large could occur due to noise.

Response   S3

ANOVA for selected factorial model

Analysis of variance table [Classical sum of squares - Type II]

Source	Sum of Squares	df	Mean Square	F Value	p-value Prob > F	
Model	37451.08	11	3404.64	168.07	< 0.0001	significant
A–RPM	9.69	1	9.69	0.48	0.4914	
B–Traverse	13976.24	1	13976.24	689.93	< 0.0001	
C–Shoulder	14621.65	2	7310.83	360.90	< 0.0001	
AB	1160.40	1	1160.40	57.28	< 0.0001	
AC	1284.70	2	642.35	31.71	< 0.0001	
BC	3855.66	2	1927.83	95.17	< 0.0001	
ABC	2542.74	2	1271.37	62.76	< 0.0001	
Pure Error	1458.53	72	20.26			
Cor Total	38909.61	83				

The Model F-value of 168.07 implies the model is significant. There is only
a 0.01% chance that a "Model F-Value" this large could occur due to noise.

Response   S4

ANOVA for selected factorial model

Analysis of variance table [Classical sum of squares - Type II]

Source	Sum of Squares	df	Mean Square	F Value	p-value Prob > F	
Model	38518.13	11	3501.65	108.33	< 0.0001	significant
A–RPM	19.29	1	19.29	0.60	0.4423	
B–Traverse	15618.39	1	15618.39	483.18	< 0.0001	
C–Shoulder	14835.67	2	7417.84	229.48	< 0.0001	
AB	1549.87	1	1549.87	47.95	< 0.0001	
AC	483.41	2	241.71	7.48	0.0011	
BC	3279.15	2	1639.58	50.72	< 0.0001	
ABC	2732.35	2	1366.17	42.26	< 0.0001	
Pure Error	2327.33	72	32.32			
Cor Total	40845.47	83				

The Model F-value of 108.33 implies the model is significant. There is only
a 0.01% chance that a "Model F-Value" this large could occur due to noise.

179

Response   S5

ANOVA for selected factorial model

Analysis of variance table [Classical sum of squares - Type II]

Source	Sum of Squares	df	Mean Square	F Value	p-value Prob > F	
Model	37490.98	11	3408.27	106.49	< 0.0001	significant
A–RPM	0.34	1	0.34	0.011	0.9185	
B–Traverse	13891.86	1	13891.86	434.04	< 0.0001	
C–Shoulder	13881.93	2	6940.96	216.86	< 0.0001	
AB	1091.51	1	1091.51	34.10	< 0.0001	
AC	913.25	2	456.62	14.27	< 0.0001	
BC	3628.71	2	1814.35	56.69	< 0.0001	
ABC	4083.38	2	2041.69	63.79	< 0.0001	
Pure Error	2304.45	72	32.01			
Cor Total	39795.43	83				

The Model F-value of 106.49 implies the model is significant. There is only
a 0.01% chance that a "Model F-Value" this large could occur due to noise.

Response   S6

ANOVA for selected factorial model

Analysis of variance table [Classical sum of squares - Type II]

Source	Sum of Squares	df	Mean Square	F Value	p-value Prob > F	
Model	40589.73	11	3689.98	130.24	< 0.0001	significant
A–RPM	86.07	1	86.07	3.04	0.0856	
B–Traverse	18622.07	1	18622.07	657.28	< 0.0001	
C–Shoulder	14398.19	2	7199.09	254.10	< 0.0001	
AB	1100.72	1	1100.72	38.85	< 0.0001	
AC	676.89	2	338.44	11.95	< 0.0001	
BC	2740.03	2	1370.01	48.36	< 0.0001	
ABC	2965.76	2	1482.88	52.34	< 0.0001	
Pure Error	2039.90	72	28.33			
Cor Total	42629.63	83				

The Model F-value of 130.24 implies the model is significant. There is only
a 0.01% chance that a "Model F-Value" this large could occur due to noise.

Response   S7

    ANOVA for selected factorial model

Analysis of variance table [Classical sum of squares - Type II]

Source	Sum of Squares	df	Mean Square	F Value	p-value Prob > F	
Model	31199.50	11	2836.32	106.29	< 0.0001	significant
A–RPM	12.78	1	12.78	0.48	0.4911	
B–Traverse	9677.03	1	9677.03	362.63	< 0.0001	
C–Shoulder	15343.24	2	7671.62	287.48	< 0.0001	
AB	1129.38	1	1129.38	42.32	< 0.0001	
AC	1504.68	2	752.34	28.19	< 0.0001	
BC	2132.14	2	1066.07	39.95	< 0.0001	
ABC	1400.24	2	700.12	26.24	< 0.0001	
Pure Error	1921.37	72	26.69			
Cor Total	33120.87	83				

The Model F-value of 106.29 implies the model is significant. There is only
a 0.01% chance that a "Model F-Value" this large could occur due to noise.

Response   S8

    ANOVA for selected factorial model

Analysis of variance table [Classical sum of squares - Type II]

Source	Sum of Squares	df	Mean Square	F Value	p-value Prob > F	
Model	33645.58	11	3058.69	104.95	< 0.0001	significant
A–RPM	6.334E-003	1	6.334E-003	2.173E-004	0.9883	
B–Traverse	13295.74	1	13295.74	456.21	< 0.0001	
C–Shoulder	14749.17	2	7374.58	253.04	< 0.0001	
AB	1466.54	1	1466.54	50.32	< 0.0001	
AC	756.70	2	378.35	12.98	< 0.0001	
BC	2031.47	2	1015.74	34.85	< 0.0001	
ABC	1345.95	2	672.98	23.09	< 0.0001	
Pure Error	2098.38	72	29.14			
Cor Total	35743.96	83				

The Model F-value of 104.95 implies the model is significant. There is only
a 0.01% chance that a "Model F-Value" this large could occur due to noise.

181

Response S9

ANOVA for selected factorial model

Analysis of variance table [Classical sum of squares - Type II]

Source	Sum of Squares	df	Mean Square	F Value	p-value Prob > F	
Model	29810.74	11	2710.07	92.42	< 0.0001	significant
A-RPM	309.01	1	309.01	10.54	0.0018	
B-Traverse	10273.27	1	10273.27	350.35	< 0.0001	
C-Shoulder	11361.75	2	5680.88	193.74	< 0.0001	
AB	1413.87	1	1413.87	48.22	< 0.0001	
AC	1382.02	2	691.01	23.57	< 0.0001	
BC	2579.24	2	1289.62	43.98	< 0.0001	
ABC	2491.58	2	1245.79	42.49	< 0.0001	
Pure Error	2111.23	72	29.32			
Cor Total	31921.96	83				

The Model F-value of 92.42 implies the model is significant. There is only a 0.01% chance that a "Model F-Value" this large could occur due to noise.

Response S10

ANOVA for selected factorial model

Analysis of variance table [Classical sum of squares - Type II]

Source	Sum of Squares	df	Mean Square	F Value	p-value Prob > F	
Model	31020.26	11	2820.02	107.26	< 0.0001	significant
A-RPM	420.97	1	420.97	16.01	0.0002	
B-Traverse	14244.82	1	14244.82	541.80	< 0.0001	
C-Shoulder	11007.03	2	5503.51	209.33	< 0.0001	
AB	1259.28	1	1259.28	47.90	< 0.0001	
AC	485.27	2	242.64	9.23	0.0003	
BC	1816.63	2	908.32	34.55	< 0.0001	
ABC	1786.26	2	893.13	33.97	< 0.0001	
Pure Error	1893.00	72	26.29			
Cor Total	32913.26	83				

The Model F-value of 107.26 implies the model is significant. There is only a 0.01% chance that a "Model F-Value" this large could occur due to noise.

Response   S11

ANOVA for selected factorial model

Analysis of variance table [Classical sum of squares - Type II]

Source	Sum of Squares	df	Mean Square	F Value	p-value Prob > F	
Model	30040.07	11	2730.92	121.37	< 0.0001	significant
A-RPM	942.35	1	942.35	41.88	< 0.0001	
B-Traverse	12290.21	1	12290.21	546.19	< 0.0001	
C-Shoulder	10638.99	2	5319.49	236.41	< 0.0001	
AB	2520.09	1	2520.09	112.00	< 0.0001	
AC	180.08	2	90.04	4.00	0.0225	
BC	1584.57	2	792.28	35.21	< 0.0001	
ABC	1883.79	2	941.89	41.86	< 0.0001	
Pure Error	1620.11	72	22.50			
Cor Total	31660.18	83				

The Model F-value of 121.37 implies the model is significant. There is only
a 0.01% chance that a "Model F-Value" this large could occur due to noise.

Response   S12

ANOVA for selected factorial model

Analysis of variance table [Classical sum of squares - Type II]

Source	Sum of Squares	df	Mean Square	F Value	p-value Prob > F	
Model	31892.25	11	2899.30	143.00	< 0.0001	significant
A-RPM	873.35	1	873.35	43.08	< 0.0001	
B-Traverse	16061.42	1	16061.42	792.19	< 0.0001	
C-Shoulder	10216.76	2	5108.38	251.96	< 0.0001	
AB	1974.84	1	1974.84	97.40	< 0.0001	
AC	213.62	2	106.81	5.27	0.0073	
BC	1192.34	2	596.17	29.40	< 0.0001	
ABC	1359.92	2	679.96	33.54	< 0.0001	
Pure Error	1459.78	72	20.27			
Cor Total	33352.03	83				

The Model F-value of 143.00 implies the model is significant. There is only
a 0.01% chance that a "Model F-Value" this large could occur due to noise.

183

Response   S13

ANOVA for selected factorial model

Analysis of variance table [Classical sum of squares - Type II]

Source	Sum of Squares	df	Mean Square	F Value	p-value Prob > F	
Model	25646.89	11	2331.54	90.24	< 0.0001	significant
A-RPM	762.77	1	762.77	29.52	< 0.0001	
B-Traverse	12208.57	1	12208.57	472.50	< 0.0001	
C-Shoulder	6647.46	2	3323.73	128.64	< 0.0001	
AB	1439.04	1	1439.04	55.69	< 0.0001	
AC	1983.09	2	991.54	38.37	< 0.0001	
BC	1596.83	2	798.41	30.90	< 0.0001	
ABC	1009.13	2	504.57	19.53	< 0.0001	
Pure Error	1860.36	72	25.84			
Cor Total	27507.25	83				

The Model F-value of 90.24 implies the model is significant. There is only
a 0.01% chance that a "Model F-Value" this large could occur due to noise.

Response   S14

ANOVA for selected factorial model

Analysis of variance table [Classical sum of squares - Type II]

Source	Sum of Squares	df	Mean Square	F Value	p-value Prob > F	
Model	26779.21	11	2434.47	100.66	< 0.0001	significant
A-RPM	470.92	1	470.92	19.47	< 0.0001	
B-Traverse	13316.94	1	13316.94	550.61	< 0.0001	
C-Shoulder	7545.43	2	3772.72	155.99	< 0.0001	
AB	1023.95	1	1023.95	42.34	< 0.0001	
AC	1725.56	2	862.78	35.67	< 0.0001	
BC	1366.48	2	683.24	28.25	< 0.0001	
ABC	1329.93	2	664.96	27.49	< 0.0001	
Pure Error	1741.39	72	24.19			
Cor Total	28520.60	83				

The Model F-value of 100.66 implies the model is significant. There is only
a 0.01% chance that a "Model F-Value" this large could occur due to noise.

Response   P1

  ANOVA for selected factorial model

Analysis of variance table [Classical sum of squares - Type II]

Source	Sum of Squares	df	Mean Square	F Value	p-value Prob > F	
Model	32127.52	11	2920.68	113.73	< 0.0001	significant
A-RPM	9.92	1	9.92	0.39	0.5362	
B-Traverse	1263.32	1	1263.32	49.19	< 0.0001	
C-Shoulder	22889.61	2	11444.81	445.67	< 0.0001	
AB	392.92	1	392.92	15.30	0.0002	
AC	388.28	2	194.14	7.56	0.0010	
BC	2490.73	2	1245.36	48.50	< 0.0001	
ABC	4692.74	2	2346.37	91.37	< 0.0001	
Pure Error	1848.96	72	25.68			
Cor Total	33976.48	83				

The Model F-value of 113.73 implies the model is significant. There is only a 0.01% chance that a "Model F-Value" this large could occur due to noise.

Response   P2

  ANOVA for selected factorial model

Analysis of variance table [Classical sum of squares - Type II]

Source	Sum of Squares	df	Mean Square	F Value	p-value Prob > F	
Model	30832.47	11	2802.95	74.66	< 0.0001	significant
A-RPM	175.48	1	175.48	4.67	0.0339	
B-Traverse	790.89	1	790.89	21.07	< 0.0001	
C-Shoulder	23799.41	2	11899.70	316.96	< 0.0001	
AB	701.65	1	701.65	18.69	< 0.0001	
AC	212.11	2	106.05	2.82	0.0659	
BC	2088.09	2	1044.04	27.81	< 0.0001	
ABC	3064.84	2	1532.42	40.82	< 0.0001	
Pure Error	2703.15	72	37.54			
Cor Total	33535.62	83				

The Model F-value of 74.66 implies the model is significant. There is only a 0.01% chance that a "Model F-Value" this large could occur due to noise.

185

Response P3

ANOVA for selected factorial model

Analysis of variance table [Classical sum of squares - Type II]

Source	Sum of Squares	df	Mean Square	F Value	p-value Prob > F	
Model	25431.93	11	2311.99	85.51	< 0.0001	significant
A–RPM	24.05	1	24.05	0.89	0.3488	
B–Traverse	7713.86	1	7713.86	285.29	< 0.0001	
C–Shoulder	11697.62	2	5848.81	216.31	< 0.0001	
AB	1633.01	1	1633.01	60.40	< 0.0001	
AC	506.67	2	253.33	9.37	0.0002	
BC	2871.35	2	1435.67	53.10	< 0.0001	
ABC	985.38	2	492.69	18.22	< 0.0001	
Pure Error	1946.78	72	27.04			
Cor Total	27378.71	83				

The Model F-value of 85.51 implies the model is significant. There is only a 0.01% chance that a "Model F-Value" this large could occur due to noise.

Response P4

ANOVA for selected factorial model

Analysis of variance table [Classical sum of squares - Type II]

Source	Sum of Squares	df	Mean Square	F Value	p-value Prob > F	
Model	25884.98	11	2353.18	113.59	< 0.0001	significant
A–RPM	3.13	1	3.13	0.15	0.6985	
B–Traverse	10145.66	1	10145.66	489.74	< 0.0001	
C–Shoulder	11744.56	2	5872.28	283.46	< 0.0001	
AB	897.42	1	897.42	43.32	< 0.0001	
AC	353.63	2	176.81	8.53	0.0005	
BC	2224.84	2	1112.42	53.70	< 0.0001	
ABC	515.74	2	257.87	12.45	< 0.0001	
Pure Error	1491.59	72	20.72			
Cor Total	27376.57	83				

The Model F-value of 113.59 implies the model is significant. There is only a 0.01% chance that a "Model F-Value" this large could occur due to noise.

186

Response   P5

ANOVA for selected factorial model

Analysis of variance table [Classical sum of squares - Type II]

Source	Sum of Squares	df	Mean Square	F Value	p-value Prob > F	
Model	31136.69	11	2830.61	132.78	< 0.0001	significant
A-RPM	239.58	1	239.58	11.24	0.0013	
B-Traverse	13371.17	1	13371.17	627.24	< 0.0001	
C–Shoulder	10244.81	2	5122.40	240.29	< 0.0001	
AB	1222.06	1	1222.06	57.33	< 0.0001	
AC	552.01	2	276.00	12.95	< 0.0001	
BC	2978.37	2	1489.19	69.86	< 0.0001	
ABC	2528.69	2	1264.35	59.31	< 0.0001	
Pure Error	1534.85	72	21.32			
Cor Total	32671.55	83				

The Model F-value of 132.78 implies the model is significant. There is only a 0.01% chance that a "Model F-Value" this large could occur due to noise.

Response   P6

ANOVA for selected factorial model

Analysis of variance table [Classical sum of squares - Type II]

Source	Sum of Squares	df	Mean Square	F Value	p-value Prob > F	
Model	34347.48	11	3122.50	130.65	< 0.0001	significant
A-RPM	350.03	1	350.03	14.65	0.0003	
B-Traverse	16250.55	1	16250.55	679.95	< 0.0001	
C–Shoulder	10703.13	2	5351.56	223.92	< 0.0001	
AB	1122.76	1	1122.76	46.98	< 0.0001	
AC	503.79	2	251.89	10.54	< 0.0001	
BC	3274.77	2	1637.38	68.51	< 0.0001	
ABC	2142.45	2	1071.23	44.82	< 0.0001	
Pure Error	1720.78	72	23.90			
Cor Total	36068.26	83				

The Model F-value of 130.65 implies the model is significant. There is only a 0.01% chance that a "Model F-Value" this large could occur due to noise.

187

Response   P7

ANOVA for selected factorial model

Analysis of variance table [Classical sum of squares - Type II]

Source	Sum of Squares	df	Mean Square	F Value	p-value Prob > F	
Model	32914.84	11	2992.26	149.09	< 0.0001	significant
A-RPM	1.10	1	1.10	0.055	0.8153	
B-Traverse	11975.93	1	11975.93	596.69	< 0.0001	
C-Shoulder	13549.61	2	6774.81	337.55	< 0.0001	
AB	1851.72	1	1851.72	92.26	< 0.0001	
AC	795.75	2	397.88	19.82	< 0.0001	
BC	2444.25	2	1222.12	60.89	< 0.0001	
ABC	2296.46	2	1148.23	57.21	< 0.0001	
Pure Error	1445.08	72	20.07			
Cor Total	34359.91	83				

The Model F-value of 149.09 implies the model is significant. There is only a 0.01% chance that a "Model F-Value" this large could occur due to noise.

Response   P8

ANOVA for selected factorial model

Analysis of variance table [Classical sum of squares - Type II]

Source	Sum of Squares	df	Mean Square	F Value	p-value Prob > F	
Model	33626.45	11	3056.95	110.24	< 0.0001	significant
A-RPM	0.043	1	0.043	1.536E-003	0.9688	
B-Traverse	15285.04	1	15285.04	551.20	< 0.0001	
C-Shoulder	11800.79	2	5900.40	212.78	< 0.0001	
AB	1686.64	1	1686.64	60.82	< 0.0001	
AC	407.60	2	203.80	7.35	0.0012	
BC	2123.47	2	1061.74	38.29	< 0.0001	
ABC	2322.88	2	1161.44	41.88	< 0.0001	
Pure Error	1996.60	72	27.73			
Cor Total	35623.06	83				

The Model F-value of 110.24 implies the model is significant. There is only a 0.01% chance that a "Model F-Value" this large could occur due to noise.

Response   P9

ANOVA for selected factorial model

Analysis of variance table [Classical sum of squares - Type II]

Source	Sum of Squares	df	Mean Square	F Value	p-value Prob > F	
Model	31083.85	11	2825.80	122.71	< 0.0001	significant
A-RPM	97.19	1	97.19	4.22	0.0436	
B-Traverse	13550.52	1	13550.52	588.43	< 0.0001	
C-Shoulder	11835.95	2	5917.97	256.99	< 0.0001	
AB	1737.76	1	1737.76	75.46	< 0.0001	
AC	666.45	2	333.23	14.47	< 0.0001	
BC	2235.07	2	1117.53	48.53	< 0.0001	
ABC	960.91	2	480.46	20.86	< 0.0001	
Pure Error	1658.04	72	23.03			
Cor Total	32741.89	83				

The Model F-value of 122.71 implies the model is significant. There is only a 0.01% chance that a "Model F-Value" this large could occur due to noise.

Response   P10

ANOVA for selected factorial model

Analysis of variance table [Classical sum of squares - Type II]

Source	Sum of Squares	df	Mean Square	F Value	p-value Prob > F	
Model	31716.27	11	2883.30	131.22	< 0.0001	significant
A-RPM	253.37	1	253.37	11.53	0.0011	
B-Traverse	15632.42	1	15632.42	711.44	< 0.0001	
C-Shoulder	10862.39	2	5431.19	247.18	< 0.0001	
AB	1316.76	1	1316.76	59.93	< 0.0001	
AC	116.21	2	58.10	2.64	0.0779	
BC	2562.36	2	1281.18	58.31	< 0.0001	
ABC	972.76	2	486.38	22.14	< 0.0001	
Pure Error	1582.06	72	21.97			
Cor Total	33298.33	83				

The Model F-value of 131.22 implies the model is significant. There is only a 0.01% chance that a "Model F-Value" this large could occur due to noise.

Response P11

ANOVA for selected factorial model

Analysis of variance table [Classical sum of squares - Type II]

Source	Sum of Squares	df	Mean Square	F Value	p-value Prob > F	
Model	14301.05	11	1300.10	62.09	< 0.0001	significant
A-RPM	40.28	1	40.28	1.92	0.1697	
B-Traverse	5441.30	1	5441.30	259.88	< 0.0001	
C-Shoulder	5606.65	2	2803.32	133.89	< 0.0001	
AB	353.08	1	353.08	16.86	0.0001	
AC	57.55	2	28.78	1.37	0.2596	
BC	1652.00	2	826.00	39.45	< 0.0001	
ABC	1150.19	2	575.10	27.47	< 0.0001	
Pure Error	1507.50	72	20.94			
Cor Total	15808.55	83				

The Model F-value of 62.09 implies the model is significant. There is only
a 0.01% chance that a "Model F-Value" this large could occur due to noise.

Response P12

ANOVA for selected factorial model

Analysis of variance table [Classical sum of squares - Type II]

Source	Sum of Squares	df	Mean Square	F Value	p-value Prob > F	
Model	32026.67	11	2911.52	54.56	< 0.0001	significant
A-RPM	682.95	1	682.95	12.80	0.0006	
B-Traverse	14537.92	1	14537.92	272.43	< 0.0001	
C-Shoulder	8720.60	2	4360.30	81.71	< 0.0001	
AB	1202.48	1	1202.48	22.53	< 0.0001	
AC	2037.45	2	1018.72	19.09	< 0.0001	
BC	2898.53	2	1449.26	27.16	< 0.0001	
ABC	1946.74	2	973.37	18.24	< 0.0001	
Pure Error	3842.16	72	53.36			
Cor Total	35868.83	83				

The Model F-value of 54.56 implies the model is significant. There is only
a 0.01% chance that a "Model F-Value" this large could occur due to noise.

Response P13

ANOVA for selected factorial model

Analysis of variance table [Classical sum of squares - Type II]

Source	Sum of Squares	df	Mean Square	F Value	p-value Prob > F	
Model	25649.34	11	2331.76	75.05	< 0.0001	significant
A-RPM	846.92	1	846.92	27.26	< 0.0001	
B-Traverse	11282.76	1	11282.76	363.12	< 0.0001	
C-Shoulder	5199.50	2	2599.75	83.67	< 0.0001	
AB	2315.40	1	2315.40	74.52	< 0.0001	
AC	1789.12	2	894.56	28.79	< 0.0001	
BC	883.17	2	441.59	14.21	< 0.0001	
ABC	3332.48	2	1666.24	53.63	< 0.0001	
Pure Error	2237.14	72	31.07			
Cor Total	27886.48	83				

The Model F-value of 75.05 implies the model is significant. There is only
a 0.01% chance that a "Model F-Value" this large could occur due to noise.

Response P14

ANOVA for selected factorial model

Analysis of variance table [Classical sum of squares - Type II]

Source	Sum of Squares	df	Mean Square	F Value	p-value Prob > F	
Model	28322.38	11	2574.76	92.00	< 0.0001	significant
A-RPM	884.31	1	884.31	31.60	< 0.0001	
B-Traverse	13970.22	1	13970.22	499.19	< 0.0001	
C-Shoulder	6209.10	2	3104.55	110.93	< 0.0001	
AB	2550.79	1	2550.79	91.15	< 0.0001	
AC	1636.74	2	818.37	29.24	< 0.0001	
BC	714.44	2	357.22	12.76	< 0.0001	
ABC	2356.77	2	1178.39	42.11	< 0.0001	
Pure Error	2014.99	72	27.99			
Cor Total	30337.37	83				

The Model F-value of 92.00 implies the model is significant. There is only
a 0.01% chance that a "Model F-Value" this large could occur due to noise.

191

Response U1

ANOVA for selected factorial model

Analysis of variance table [Classical sum of squares - Type II]

Source	Sum of Squares	df	Mean Square	F Value	p-value Prob > F	
Model	26790.33	11	2435.48	80.73	< 0.0001	significant
A-RPM	126.87	1	126.87	4.21	0.0439	
B-Traverse	1000.71	1	1000.71	33.17	< 0.0001	
C-Shoulder	17351.19	2	8675.59	287.57	< 0.0001	
AB	2396.56	1	2396.56	79.44	< 0.0001	
AC	174.14	2	87.07	2.89	0.0623	
BC	1379.90	2	689.95	22.87	< 0.0001	
ABC	4360.96	2	2180.48	72.28	< 0.0001	
Pure Error	2172.14	72	30.17			
Cor Total	28962.47	83				

The Model F-value of 80.73 implies the model is significant. There is only a 0.01% chance that a "Model F-Value" this large could occur due to noise.

Response U2

ANOVA for selected factorial model

Analysis of variance table [Classical sum of squares - Type II]

Source	Sum of Squares	df	Mean Square	F Value	p-value Prob > F	
Model	26214.86	11	2383.17	13.14	< 0.0001	significant
A-RPM	64.74	1	64.74	0.36	0.5520	
B-Traverse	12090.60	1	12090.60	66.69	< 0.0001	
C-Shoulder	6259.04	2	3129.52	17.26	< 0.0001	
AB	534.55	1	534.55	2.95	0.0903	
AC	1815.69	2	907.85	5.01	0.0092	
BC	2952.61	2	1476.30	8.14	0.0006	
ABC	2497.63	2	1248.81	6.89	0.0018	
Pure Error	13053.76	72	181.30			
Cor Total	39268.61	83				

The Model F-value of 13.14 implies the model is significant. There is only a 0.01% chance that a "Model F-Value" this large could occur due to noise.

192

Response   U3

ANOVA for selected factorial model

Analysis of variance table [Classical sum of squares - Type II]

Source	Sum of Squares	df	Mean Square	F Value	p-value Prob > F	
Model	32593.66	11	2963.06	53.08	< 0.0001	significant
A–RPM	8.16	1	8.16	0.15	0.7033	
B–Traverse	17322.92	1	17322.92	310.32	< 0.0001	
C–Shoulder	8632.31	2	4316.16	77.32	< 0.0001	
AB	1176.38	1	1176.38	21.07	< 0.0001	
AC	1268.13	2	634.06	11.36	< 0.0001	
BC	2198.72	2	1099.36	19.69	< 0.0001	
ABC	1987.03	2	993.52	17.80	< 0.0001	
Pure Error	4019.26	72	55.82			
Cor Total	36612.92	83				

The Model F-value of 53.08 implies the model is significant. There is only
a 0.01% chance that a "Model F-Value" this large could occur due to noise.

Response   U4

ANOVA for selected factorial model

Analysis of variance table [Classical sum of squares - Type II]

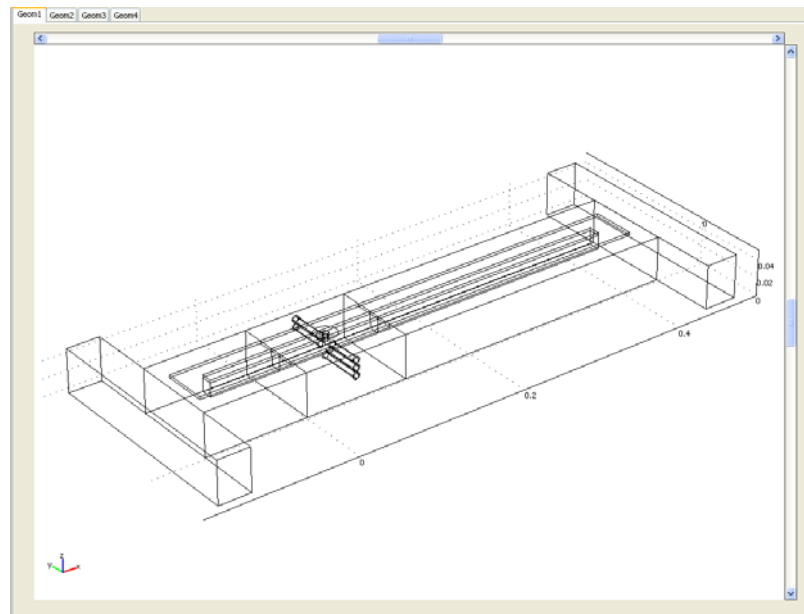| Source	Sum of Squares	df	Mean Square	F Value	p-value Prob > F	
Model	22826.62	11	2075.15	45.07	< 0.0001	significant
A–RPM	122.21	1	122.21	2.65	0.1076	
B–Traverse	7119.77	1	7119.77	154.64	< 0.0001	
C–Shoulder	9304.03	2	4652.02	101.04	< 0.0001	
AB	1887.08	1	1887.08	40.99	< 0.0001	
AC	1090.80	2	545.40	11.85	< 0.0001	
BC	1919.04	2	959.52	20.84	< 0.0001	
ABC	1383.68	2	691.84	15.03	< 0.0001	
Pure Error	3314.84	72	46.04			
Cor Total	26141.47	83				

The Model F-value of 45.07 implies the model is significant. There is only
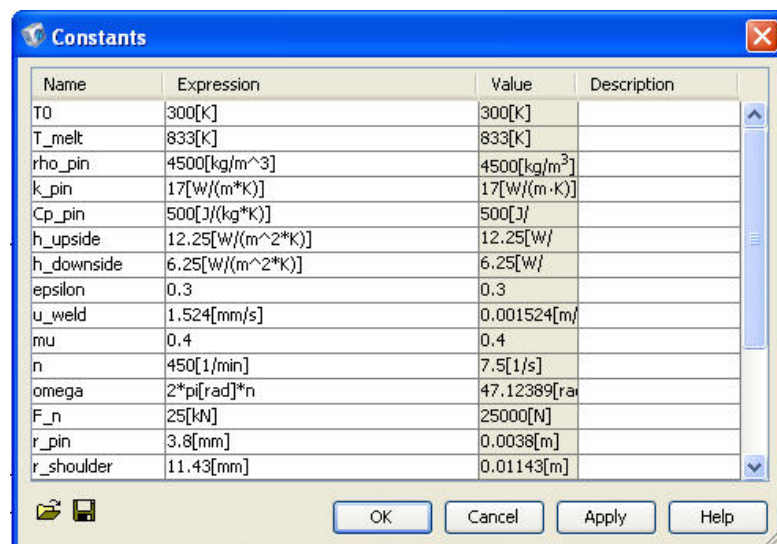a 0.01% chance that a "Model F-Value" this large could occur due to noise.

193

Response U5

ANOVA for selected factorial model

Analysis of variance table [Classical sum of squares - Type II]

Source	Sum of Squares	df	Mean Square	F Value	p-value Prob > F	
Model	18323.81	11	1665.80	36.71	< 0.0001	significant
A–RPM	152.62	1	152.62	3.36	0.0708	
B–Traverse	6873.93	1	6873.93	151.49	< 0.0001	
C–Shoulder	6610.60	2	3305.30	72.84	< 0.0001	
AB	1420.71	1	1420.71	31.31	< 0.0001	
AC	757.50	2	378.75	8.35	0.0005	
BC	1829.32	2	914.66	20.16	< 0.0001	
ABC	679.14	2	339.57	7.48	0.0011	
Pure Error	3266.99	72	45.37			
Cor Total	21590.80	83				

The Model F-value of 36.71 implies the model is significant. There is only
a 0.01% chance that a "Model F-Value" this large could occur due to noise.

Response U6

ANOVA for selected factorial model

Analysis of variance table [Classical sum of squares - Type II]

Source	Sum of Squares	df	Mean Square	F Value	p-value Prob > F	
Model	32473.82	11	2952.17	63.66	< 0.0001	significant
A–RPM	4.54	1	4.54	0.098	0.7553	
B–Traverse	14230.71	1	14230.71	306.89	< 0.0001	
C–Shoulder	11034.67	2	5517.33	118.98	< 0.0001	
AB	1188.74	1	1188.74	25.64	< 0.0001	
AC	1156.42	2	578.21	12.47	< 0.0001	
BC	2558.95	2	1279.47	27.59	< 0.0001	
ABC	2299.80	2	1149.90	24.80	< 0.0001	
Pure Error	3338.71	72	46.37			
Cor Total	35812.53	83				

The Model F-value of 63.66 implies the model is significant. There is only
a 0.01% chance that a "Model F-Value" this large could occur due to noise.

Response U7

ANOVA for selected factorial model

Analysis of variance table [Classical sum of squares - Type II]

Source	Sum of Squares	df	Mean Square	F Value	p-value Prob > F	
Model	20667.24	11	1878.84	44.35	< 0.0001	significant
A-RPM	352.51	1	352.51	8.32	0.0052	
B-Traverse	11372.59	1	11372.59	268.47	< 0.0001	
C-Shoulder	4457.09	2	2228.54	52.61	< 0.0001	
AB	520.55	1	520.55	12.29	0.0008	
AC	835.14	2	417.57	9.86	0.0002	
BC	2646.25	2	1323.12	31.23	< 0.0001	
ABC	483.11	2	241.56	5.70	0.0050	
Pure Error	3050.00	72	42.36			
Cor Total	23717.24	83				

The Model F-value of 63.66 implies the model is significant. There is only a 0.01% chance that a "Model F-Value" this large could occur due to noise.

195

APPENDIX F:

Simulation Screen Shots:

Step 1: Model

Simple drawing options were used to create the model with the actual dimensions of the

instrument. The instrument is modeled in such a way that the slot for the aluminum stock already

bears the material.

Step 2: Constants

Constants should be assigned and the values of the constants are to be declared.

Step 3: Boundary expressions

Boundary expressions are the heat equations that apply to the surface of the material that is been

used. This physically allows the user to select the surface where the equation is to be applied.
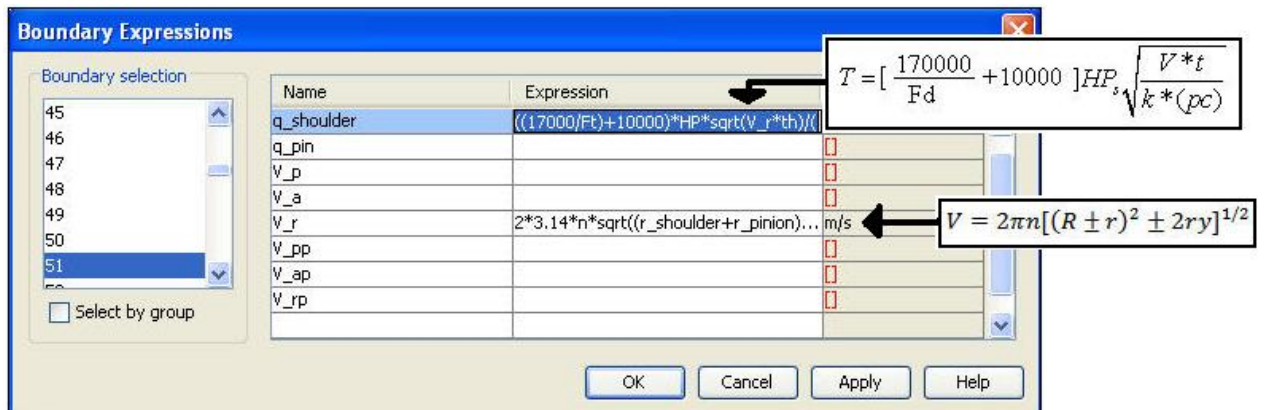
Step 4: Subdomain settings
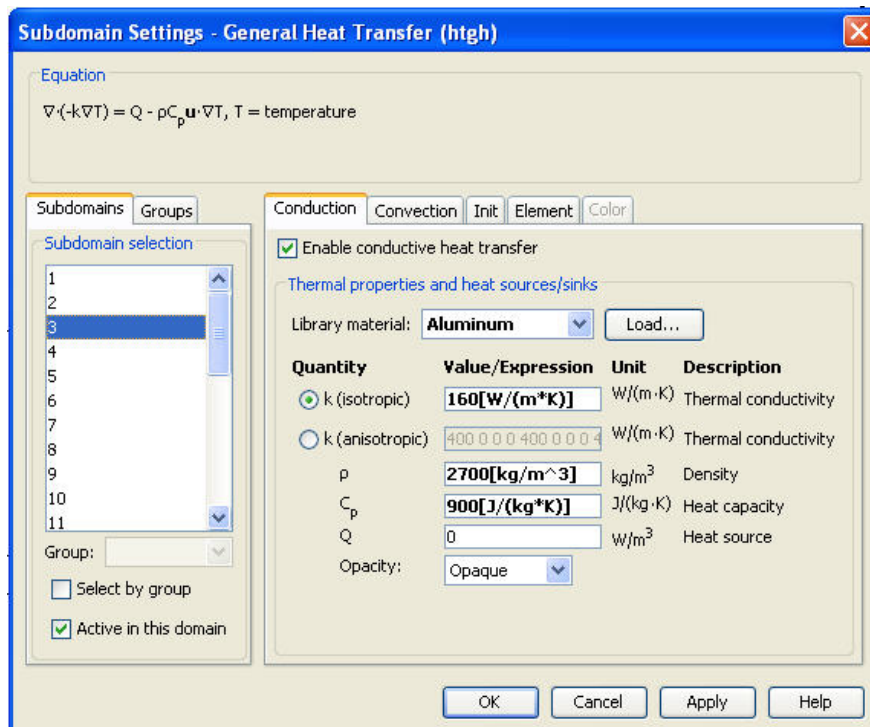
Subdomain settings allows the user to select the material that is been used in the model. Multiple

materials can be selected and their thermal properties are entered here.

Step 5: Boundary Settings

Boundary settings allow the user to apply the boundary expression to the surface that is selected. In the below figure, for the 51st boundary, the heat equation used is q_shoulder. The expression q_shoulder is already defined in boundary expression.
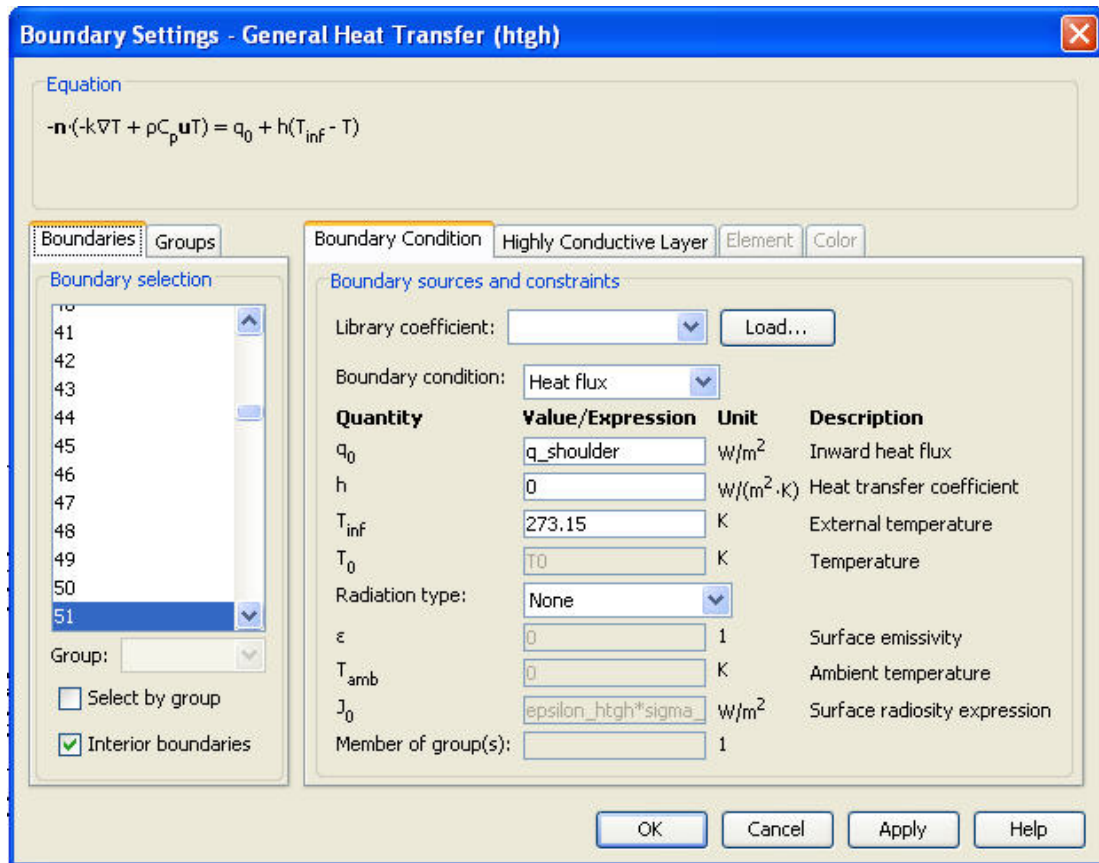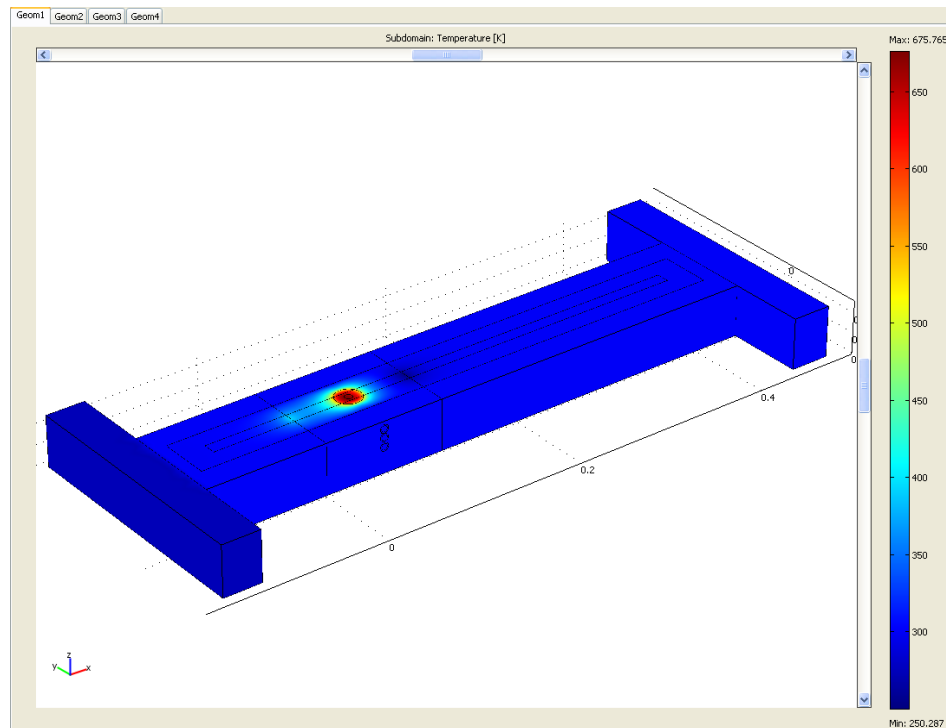

Step 6: Meshing

As discussed in Chapter 9 (Simulation of the process), Normal mesh is chosen for the process.

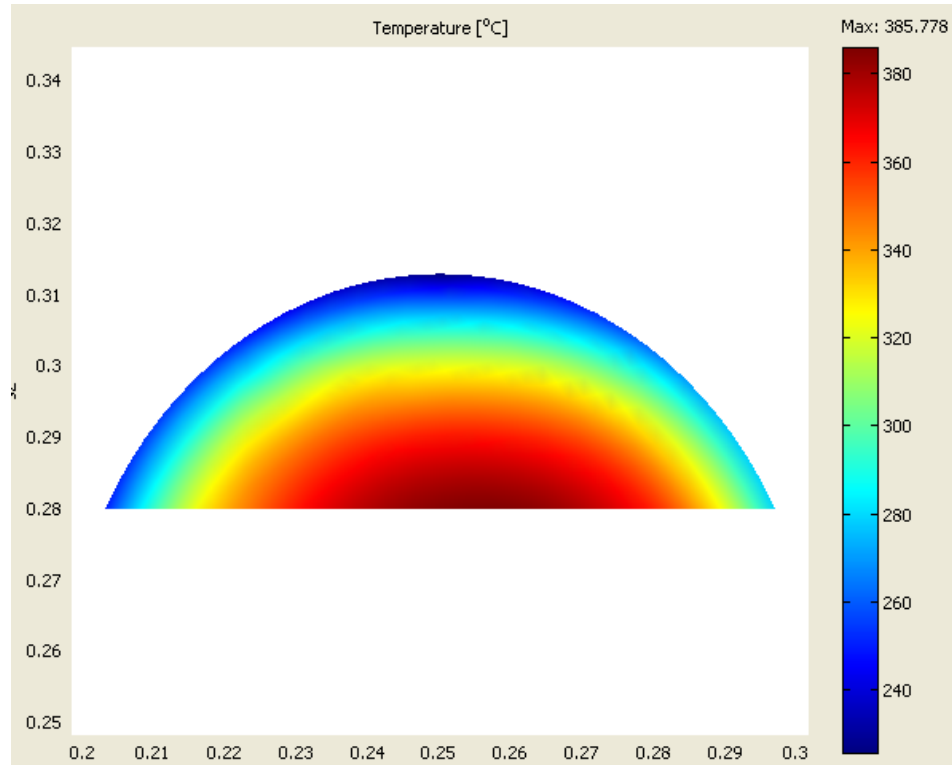The mesh details and the number of elements are given in Chapter 9.
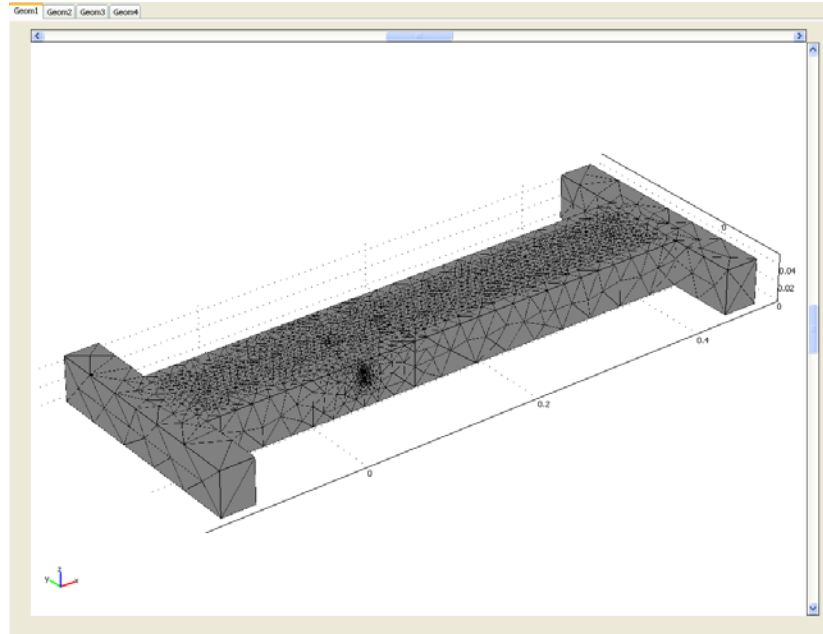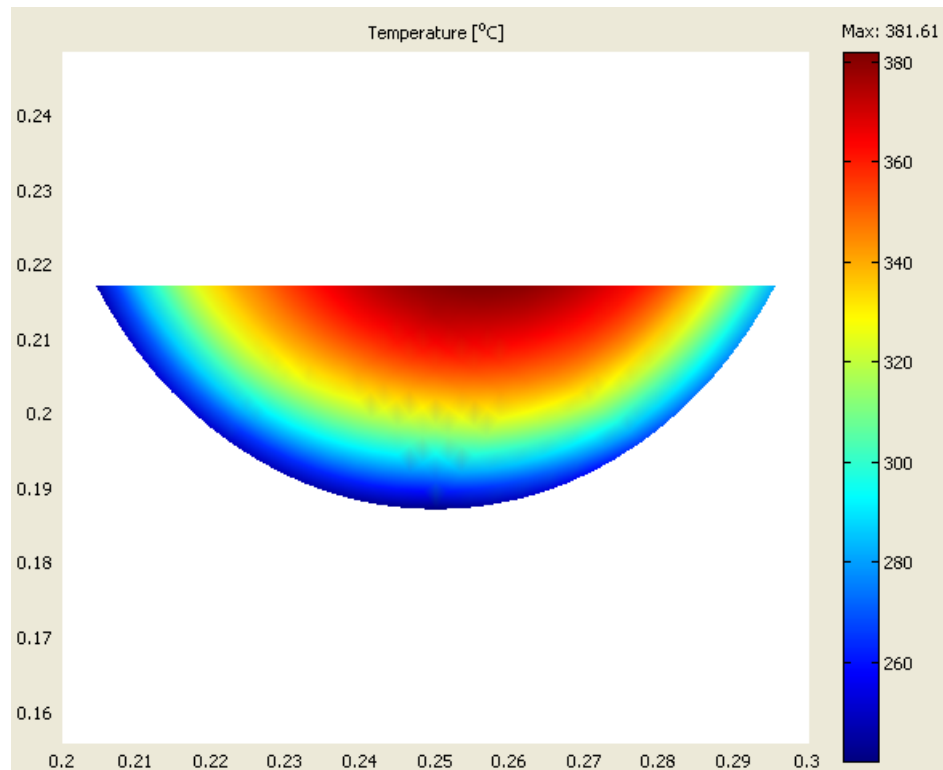
Step 7: Solving

The applied equation is solved with the model designed to get a heat distribution along the model.
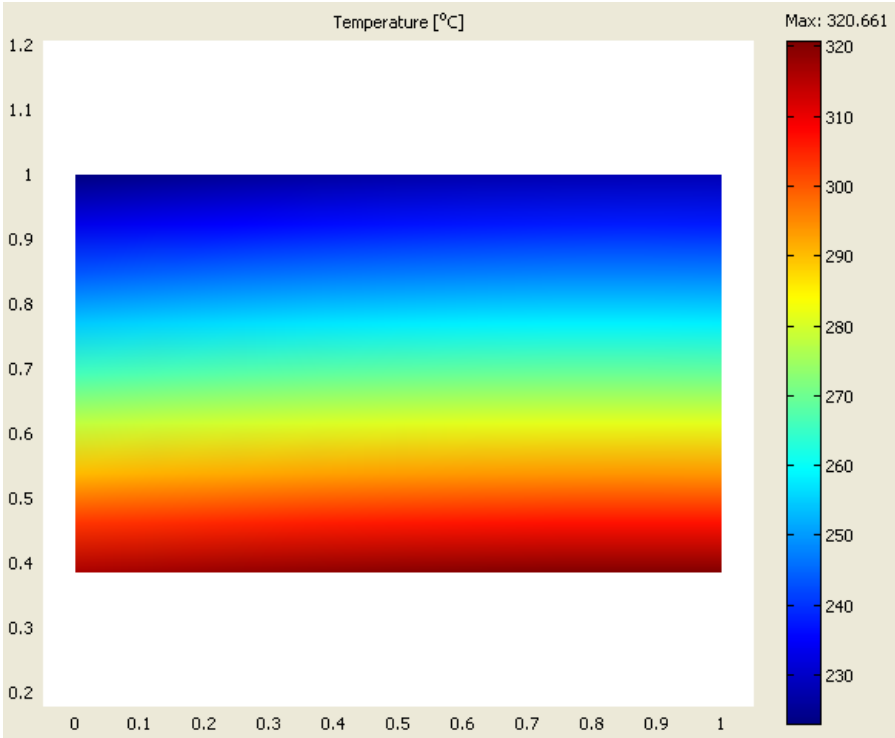

199

Results: Advancing side shoulder temperature: Peak temperature = 385.7C

Retreating side shoulder temperature: Peak temperature = 381.6 C

Advancing side pin temperature: Peak temperature = 320.6

Retreating side pin temperature: Peak temperature = 315.3 C